

Nano Revolution  
for the Future

# MANA RESEARCH DIGEST 2018

International Center for  
Materials Nanoarchitectonics (WPI-MANA)  
National Institute for Materials Science (NIMS)



# Preface

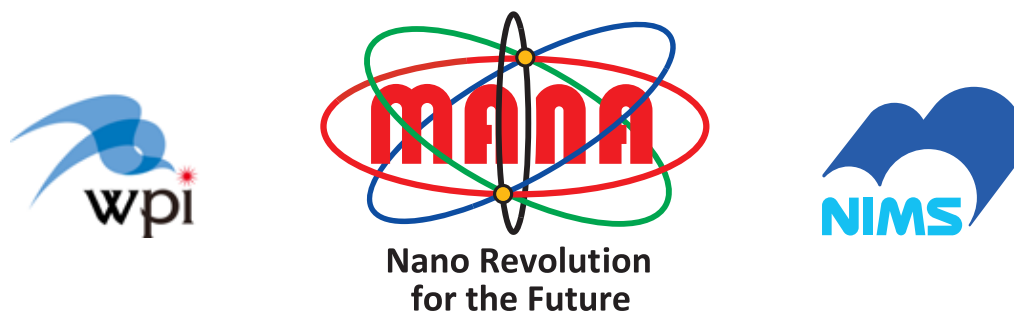
**Takayoshi Sasaki**  
MANA Director  
NIMS



The International Center for Materials Nanoarchitectonics (MANA) was established at NIMS in 2007 in the framework of the World Premier International Research Center Initiative (WPI), which is sponsored by Japan's Ministry of Education, Culture, Sports, Science and Technology (MEXT). After the end of the 10 year WPI funding in March 2017, MANA is positioned as one of seven research centers in NIMS and as a WPI academy member, engaging in bottom-up type fundamental research.

Founded on the concept of nanoarchitectonics, we are proud that today, MANA has grown into a world-class research center that produces much ground-breaking research in the fields of nanotechnology and material science and attracts global attention. MANA has been called one of Japan's best research institutes not only for its research output, but also for its efforts to internationalize and establish effective programs for training young researchers. MANA will generally continue to maintain and develop the present direction of research on nano- and mesoarchitectonics that is performed in three research fields (Nano-Materials, Nano-Systems and Nano-Theory) with Independent Scientists as additional workforce.

On behalf of all the researchers of MANA, I hope that the research activities described in this booklet will be a strong inspiration for your work in the future.



# MANA Research Digest 2018

Principal Investigators (photos)	6-7
Researchers of Research Groups (photos)	8-12
Other Researchers (photos)	13

## NANO-MATERIALS FIELD (10 Research Groups)

Introduction of Nano-Materials Field	14
<b>Thermal Energy Materials Group</b>	
<b>Takao MORI</b> (Field Coordinator, Principal Investigator, Group Leader) Development of Thermal Energy Materials	15
<b>Soft Chemistry Group</b>	
<b>Takayoshi SASAKI</b> (MANA Director, Principal Investigator, Group Leader) Inorganic Nanosheets	16
<b>Supramolecules Group</b>	
<b>Katsuhiko ARIGA</b> (Principal Investigator, Group Leader) Supramolecular Materials	17
<b>Junichi TAKEYA</b> (Principal Investigator, The University of Tokyo) Semiconductor Devices of Organic Nano-Sheet Crystals	18
<b>Nanostructured Semiconducting Materials Group</b>	
<b>Naoki FUKATA</b> (Principal Investigator, Group Leader) Next-Generation Semiconductor Nanodevices	19
<b>Nanotubes Group</b>	
<b>Dmitri GOLBERG</b> (Principal Investigator, Group Leader) Nanomaterial Properties Uncovered Under <i>in situ</i> TEM	20
<b>Mesoscale Materials Chemistry Group</b>	
<b>Yusuke YAMAUCHI</b> (Principal Investigator, Group Leader) Tailored Design of Two Dimensional Nanoporous Carbon Materials	21
<b>Photocatalytic Materials Group</b>	
<b>Jinhua YE</b> (Principal Investigator, Group Leader) Hybrid Artificial Photosynthetic System	22

<b>Functional Nanomaterials Group</b>	
<b>Renzhi MA</b> (Associate PI, Group Leader)	23
Multifunctional Nanomaterials	
<b>Nano Electronics Device Materials Group</b>	
<b>Takahiro NAGATA</b> (Group Leader)	24
Nano Electrics and Related Materials	
<b>Frontier Molecules Group</b>	
<b>Takashi NAKANISHI</b> (Group Leader)	25
Exotic and Functional Molecular Materials	
<b>Gero DECHER</b> (Satellite PI, University of Strasbourg, CNRS, France)	26
Nanoscale Multimaterials with Complex Anisotropies	
<b>Thomas E. MALLOUK</b> (Satellite PI, Pennsylvania State University, USA)	27
Acoustic Propulsion of Autonomous Micromotors	
<b>Zhong Lin WANG</b> (Satellite PI, Georgia Tech, USA)	28
Ultrathin Piezotronic Transistors with 2 nm Channel Lengths	
<b>Jan LABUTA</b> (Independent Scientist)	29
Multi-Responsive Porphyrin/Polymer Systems for Sensing Applications	
<b>Liwen SANG</b> (Independent Scientist)	30
Semiconductor Nano-Interface Engineering for Power Device Application	
<b>Daiki UMEYAMA</b> (Independent Scientist)	31
Molecular Expansion of Layered Perovskites for Exotic Properties	

## NANO-SYSTEMS FIELD (11 Research Groups)

Introduction of Nano-Systems Field	32
<b>Nanoionic Devices Group</b>	
<b>Kazuya TERABE</b> (Field Coordinator, Principal Investigator, Group Leader)	33
Creation of Decision-Making Ionics Devices	
<b>Nano Functionality Integration Group</b>	
<b>Tomonobu NAKAYAMA</b> (MANA Deputy Director, Administrative Director, Principal Investigator, Group Leader)	34
Integration of Nano Functionality	

<b>Quantum Device Engineering Group</b>	
<b>Yutaka WAKAYAMA</b> (MANA Deputy Director, Group Leader)	35
Multi-Level Logic Circuits with Organic FET	
<b>Nano-System Theoretical Physics Group</b>	
<b>Xiao HU</b> (Principal Investigator, Group Leader)	36
Topological Photonic States in Honeycomb Structures	
<b>Photonics Nano-Engineering Group</b>	
<b>Tadaaki NAGAO</b> (Principal Investigator, Group Leader)	37
Materials and Devices for Nano-Scale Photo-Energy Transducers	
<b>Nano Frontier Superconducting Materials Group</b>	
<b>Yoshihiko TAKANO</b> (Principal Investigator, Group Leader)	38
Data-Driven Approach for Discovery of New Pressure-Induced Superconductors	
<b>Thin Film Electronics Group</b>	
<b>Kazuhiro TSUKAGOSHI</b> (Principal Investigator, Group Leader)	39
Pronounced Photogating Effect in Atomically Thin WSe <sub>2</sub> with a Self-Limiting Surface Oxide Layer	
<b>Medical Soft Matter Group</b>	
<b>Kohsaku KAWAKAMI</b> (Group Leader)	40
Non-Equilibrium Dynamics of Pharmaceutical Glass	
<b>Mechanobiology Group</b>	
<b>Jun NAKANISHI</b> (Group Leader)	41
Materials for Cellular Mechanobiology	
<b>Surface Quantum Phase Materials Group</b>	
<b>Takashi UCHIHASHI</b> (Group Leader)	42
Tunable 2D Superconducting Heterostructures with Organic Molecules	
<b>Nanomechanical Sensing Group</b>	
<b>Genki YOSHIKAWA</b> (Group Leader)	43
Nanomechanical Sensing towards Mobile Olfaction	
<b>James K. GIMZEWSKI</b> (Satellite PI, CNSI, UCLA, USA)	44
MANA Brain: Neuromorphic Atomic Switch Networks	
<b>Christian JOACHIM</b> (Satellite PI, CEMES, CNRS, France)	45
Surface Atomic Scale Logic Gate	

<b>Françoise M. WINNIK</b> (Satellite PI, University of Helsinki, Finland) Nanoarchitectonics-Driven Functional Nanoparticles and Interfaces	46
<b>Hisatoshi KOBAYASHI</b> (Managing Researcher) Materials for Functional Nanomedicine	47
<b>Gaku IMAMURA</b> (Independent Scientist) Data Analysis Methods for Sensor Systems	48
<b>Takako KONOIKE</b> (Independent Scientist) Magnetic Susceptibility in Organic Dirac Fermion System	49
<b>Akihiro OKAMOTO</b> (Independent Scientist) Microbial Transmembrane Nano Electric Conduit	50

## NANO-THEORY FIELD (3 Research Groups)

Introduction of Nano-Theory Field	51
<b>First-Principles Simulation Group</b>	
<b>Tsuyoshi MIYAZAKI</b> (Field Coordinator, Principal Investigator, Group Leader) Theoretical Study of Nano-Scale Materials using Large-Scale DFT and Machine Learning Techniques	52
<b>Computational Nanoscience Group</b>	
<b>Masao ARAI</b> (Group Leader) Theoretical Studies of Low Dimensional System	53
<b>Emergent Materials Property Theory Group</b>	
<b>Akihiro TANAKA</b> (Group Leader) Theoretical Quest for Emergent Materials Function	54
<b>Yoshitaka TATEYAMA</b> (Principal Investigator) Nano-System Computational Science	55
<b>David BOWLER</b> (Satellite PI, University College London, UK) Development and Application of O(N) DFT, and Studies of Strain and Doping on Nanomaterials	56

# Principal Investigators

<p><b>NANO- MATERIALS FIELD</b></p>	<p>Field Coordinator</p>  <p><b>Takao MORI</b> NIMS Principal Investigator Group Leader</p>	 <p><b>Takayoshi SASAKI</b> NIMS MANA Director Principal Investigator Group Leader</p>	 <p><b>Katsuhiko ARIGA</b> NIMS Principal Investigator Group Leader</p>	
	 <p><b>Naoki FUKATA</b> NIMS Principal Investigator Group Leader</p>	 <p><b>Dmitri GOLBERG</b> QUT, Australia<sup>1</sup> Principal Investigator Group Leader</p>	 <p><b>Yusuke YAMAUCHI</b> UQ, Australia<sup>1</sup> Principal Investigator Group Leader</p>	 <p><b>Jinhua YE</b> NIMS Principal Investigator Group Leader</p>
	 <p><b>Junichi TAKEYA</b> The University of Tokyo<sup>1</sup> Principal Investigator</p>	 <p><b>Gero DECHER</b> University of Strasbourg, CNRS, France Satellite PI</p>	 <p><b>Thomas E. MALLOUK</b> The Pennsylvania State University, USA Satellite PI</p>	 <p><b>Zhong Lin WANG</b> Georgia Tech, USA Satellite PI</p>

<sup>1</sup> Cross Appointment with NIMS.

**NANO-  
SYSTEMS  
FIELD**

Field Coordinator



**Kazuya  
TERABE**  
NIMS  
Principal Investigator  
Group Leader



**Tomonobu  
NAKAYAMA**  
NIMS  
MANA Deputy Director  
Administrative Director  
Principal Investigator  
Group Leader



**Xiao  
HU**  
NIMS  
Principal Investigator  
Group Leader



**Tadaaki  
NAGAO**  
NIMS  
Principal Investigator  
Group Leader



**Yoshihiko  
TAKANO**  
NIMS  
Principal Investigator  
Group Leader



**Kazuhito  
TSUKAGOSHI**  
NIMS  
Principal Investigator  
Group Leader



**James K.  
GIMZEWSKI**  
UCLA, USA  
Satellite PI



**Christian  
JOACHIM**  
CEMES, CNRS  
France  
Satellite PI



**Françoise M.  
WINNIK**  
University of Helsinki,  
Finland  
Satellite PI

**NANO-  
THEORY  
FIELD**

Field Coordinator



**Tsuyoshi  
MIYAZAKI**  
NIMS  
Principal Investigator  
Group Leader



**Yoshitaka  
TATEYAMA**  
NIMS  
Principal Investigator



**David  
BOWLER**  
UCL, UK  
Satellite PI

# Researchers of Research Groups

NANO-  
MATERIALS  
FIELD  
(10 groups)

## Thermal Energy Materials Group



**Takao Mori**  
Group Leader



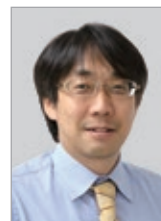
**Takashi Aizawa**  
Chief Researcher



**Yuichi Michiue**  
Chief Researcher



**Naohito Tsujii**  
Principal Researcher



**Isao Ohkubo**  
Senior Researcher

## Soft Chemistry Group



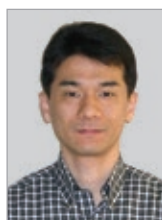
**Takayoshi Sasaki**  
Group Leader



**Naoto Shirahata**  
Associate PI



**Yasuo Ebina**  
Principal Researcher



**Nobuyuki Sakai**  
Senior Researcher



**Satoshi Tominaka**  
Senior Researcher



**Minoru Osada**  
Visiting Researcher<sup>1</sup>

## Supramolecules Group



**Katsuhiko Ariga**  
Group Leader



**Junichi Takeya**  
Principal Investigator<sup>2</sup>



**Jonathan P. Hill**  
Chief Researcher



**Lok Kumar Shrestha**  
Principal Researcher

## Nanostructured Semiconducting Materials Group



**Naoki Fukata**  
Group Leader



**Wipakorn Jevasuwan**  
Senior Researcher



**Ryo Matsumura**  
Researcher

<sup>1</sup> Cross Appointment with Nagoya University.

<sup>2</sup> Cross Appointment with The University of Tokyo.

### Nanotubes Group



**Dmitri Golberg**  
Group Leader



**Masanori Mitome**  
Chief Researcher



**Naoyuki Kawamoto**  
Senior Researcher

### Mesoscale Materials Chemistry Group



**Yusuke Yamauchi**  
Group Leader



**Joel Henzie**  
Senior Researcher



**Yusuke Ide**  
Senior Researcher

### Photocatalytic Materials Group



**Jinhua Ye**  
Group Leader



**Mitsutake Oshikiri**  
Principal Researcher



**Tetsuya Kako**  
Senior Researcher

### Functional Nanomaterials Group



**Renzhi Ma**  
Group Leader



**Takaaki Taniguchi**  
Senior Researcher



**Daiming Tang**  
Researcher

### Nano Electronics Device Materials Group



**Takahiro Nagata**  
Group Leader



**Michiko Yoshitake**  
Chief Researcher



**Shinjiro Yagyū**  
Principal Researcher



**Yoshiyuki Yamashita**  
Principal Researcher



**Jun Chen**  
Senior Researcher

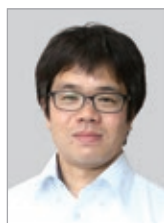
### Frontier Molecules Group



**Takashi Nakanishi**  
Group Leader



**Kentaro Tashiro**  
Principal Researcher



**Shinsuke Ishihara**  
Senior Researcher



**Kazuhiko Nagura**  
Researcher

**NANO-  
SYSTEMS  
FIELD  
(11 groups)**

**Nanoionic Devices Group**



**Kazuya  
Terabe**  
Group  
Leader



**Yuji  
Okawa**  
Chief  
Researcher



**Makoto  
Sakurai**  
Principal  
Researcher



**Tohru  
Tsuruoka**  
Principal  
Researcher



**Takashi  
Tsuchiya**  
Senior  
Researcher

**Nano Functionality Integration Group**



**Tomonobu  
Nakayama**  
Group  
Leader



**Shigeki  
Kawai**  
Principal  
Researcher



**Takeo  
Minari**  
Principal  
Researcher



**Yoshitaka  
Shingaya**  
Senior  
Researcher

**Quantum Device Engineering Group**



**Yutaka  
Wakayama**  
Group  
Leader



**Shu  
Nakaharai**  
Principal  
Researcher



**Ryoma  
Hayakawa**  
Senior  
Researcher

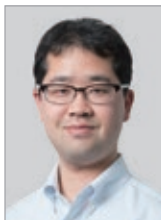


**Satoshi  
Moriyama**  
Senior  
Researcher

**Nano-System Theoretical Physics Group**



**Xiao  
Hu**  
Group  
Leader



**Toshikaze  
Kariyado**  
Researcher

**Photonics Nano-Engineering Group**



**Tadaaki  
Nagao**  
Group  
Leader



**Satoshi  
Ishii**  
Senior  
Researcher

## Nano Frontier Superconducting Materials Group



**Yoshihiko  
Takano**  
Group  
Leader



**Hiroyuki  
Takeya**  
Chief  
Researcher

## Thin Film Electronics Group



**Kazuhito  
Tsukagoshi**  
Group  
Leader



**Toshihide  
Nabatame**  
Chief  
Researcher



**Seiichi  
Kato**  
Senior  
Researcher

## Medical Soft Matter Group



**Kohsaku  
Kawakami**  
Group  
Leader



**Chiho  
Kataoka**  
Senior  
Researcher



**Yoko  
Shirai**  
Principal  
Engineer

## Mechanobiology Group



**Jun  
Nakanishi**  
Group  
Leader



**Mitsuhiro  
Ebara**  
Associate  
PI



**Takeshi  
Ueki**  
Senior  
Researcher



**Chiaki  
Yoshikawa**  
Senior  
Researcher

## Surface Quantum Phase Materials Group



**Takashi  
Uchihashi**  
Group  
Leader



**Ryuichi  
Arafune**  
Senior  
Researcher



**Katsumi  
Nagaoka**  
Senior  
Researcher



**Takashi  
Yamaguchi**  
Senior  
Researcher

## Nanomechanical Sensing Group



**Genki  
Yoshikawa**  
Group  
Leader



**Kota  
Shiba**  
Senior  
Researcher

**NANO-  
THEORY  
FIELD  
(3 groups)**

**First-Principles Simulation Group**



**Tsuyoshi  
Miyazaki**  
Group  
Leader



**Ayako  
Nakata**  
Senior  
Researcher



**Jun  
Nara**  
Senior  
Researcher



**Ryo  
Tamura**  
Senior  
Researcher

**Computational Nanoscience Group**



**Masao  
Arai**  
Group  
Leader



**Takahisa  
Ohno**  
Senior Scientist  
with Special  
Missions



**Wataru  
Hayami**  
Principal  
Researcher



**Junichi  
Inoue**  
Principal  
Researcher



**Kazuaki  
Kobayashi**  
Principal  
Researcher



**Shigeru  
Suehara**  
Principal  
Researcher

**Emergent Materials Property Theory Group**



**Junya  
Shimizu**  
Principal  
Engineer



**Akihiro  
Tanaka**  
Group  
Leader



**Yoshihiko  
Nonomura**  
Principal  
Researcher



**Igor  
Solovyev**  
Principal  
Researcher

**Managing  
Researcher**



**Hisatoshi  
Kobayashi**

**Independent  
Scientists**



**Gaku  
Imamura**



**Takako  
Konoike**



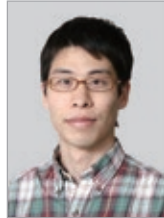
**Jan  
Labuta**



**Akihiro  
Okamoto**



**Liwen  
Sang**



**Daiki  
Umeyama**



**Koichiro  
Uto**  
(from Nov 2018)



**Michio  
Matsumoto**  
(from Dec 2018)

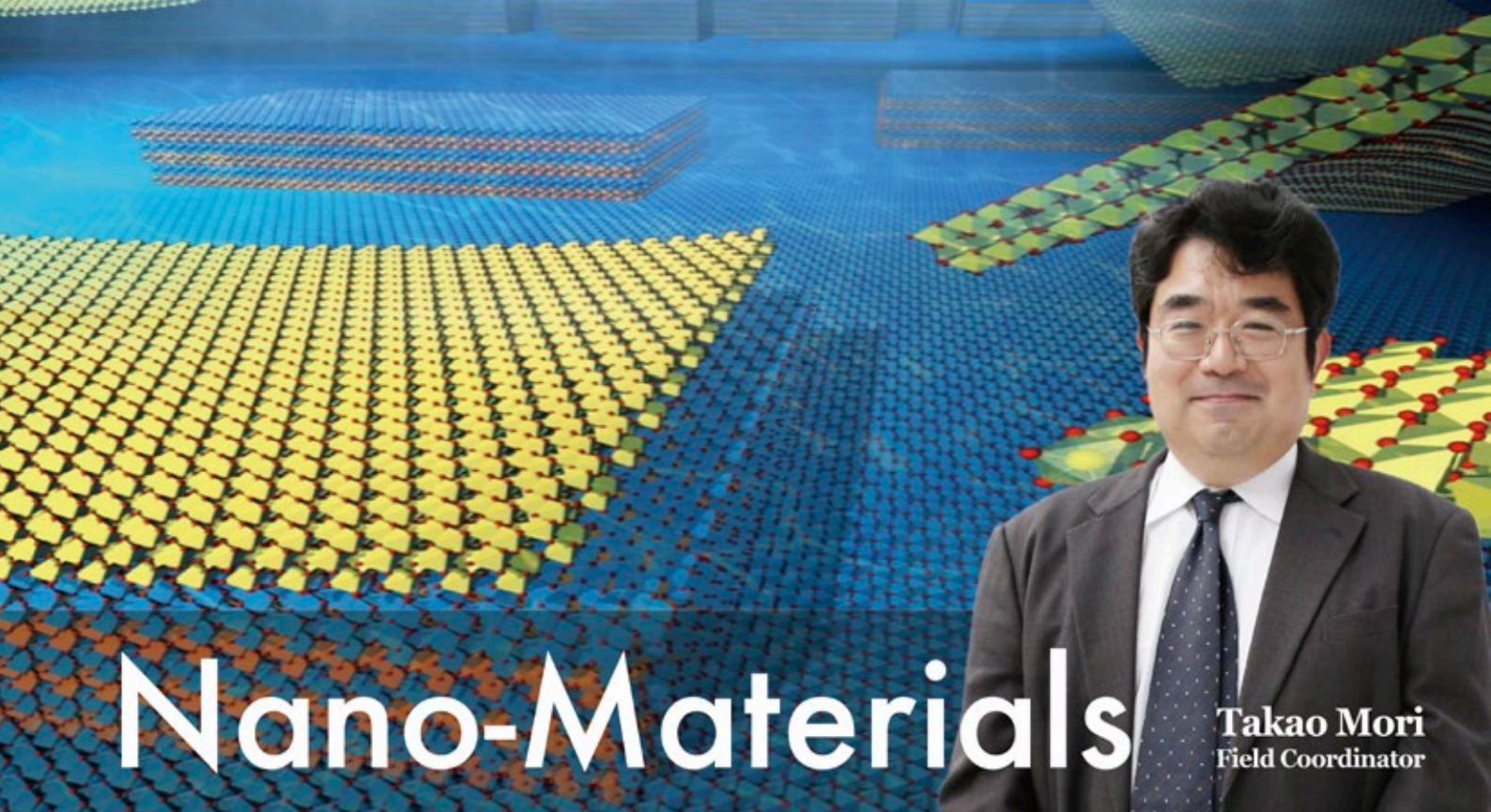
**ICYS  
WPI-MANA  
Researchers**



**Takuya  
Iwasaki**



**Thiyagu  
Subramani**



# Nano-Materials

Takao Mori  
Field Coordinator

## 10 Research Groups

- Thermal Energy Materials Group
- Soft Chemistry Group
- Supermolecules Group
- Nanostructured Semiconducting Materials Group
- Nanotubes Group
- Mesoscale Materials Chemistry Group
- Photocatalytic Materials Group
- Functional Nanomaterials Group
- Nano Electronics Device Materials Group
- Frontier Molecules Group

## **Creating new materials and eliciting novel functions by sophisticated control of compositions and structures at the nano level**

Making full use of MANA's advanced chemical synthesis technologies, beginning with soft chemistry, supermolecular chemistry and template synthesis, we are researching the creation of new nanomaterials such as nanotubes, nanowires, and nanosheets. Based on a wide range of material systems, spanning both organic and inorganic materials, we aim to discover novel physical properties and phenomena arising from size and shape in the nanometer range. MANA also develops and owns cutting-edge characterization facilities, including an integrated system of the transmission electron microscope with the scanning probe microscope, and is actively using these instruments for in-situ analysis of individual nanomaterials. In addition, we are promoting chemical nano- and mesoarchitectonics, in which these nanomaterials are precisely arranged, integrated and hybridized in the nano-to-meso range. By constructing artificial nanostructured materials in a designed manner, our aim is to create new materials that will exhibit advanced, innovative functions, and contribute to progress in a wide range of technological fields, including electronics, energy and the environment.

## Development of Thermal Energy Materials

## Principal Investigator

(Field Coordinator, Group Leader)

## Takao MORI

Takashi Aizawa (Chief Researcher), Yuichi Michiue (Chief Researcher), Naohito Tsujii (Principal Researcher), Isao Ohkubo (Senior Researcher)



## 1. Outline of Research

Approximately two thirds of primary energy (fossil fuels, etc.) being consumed in the world, sadly turns out to be unutilized, with much of the waste being heat. It is imperative to develop better thermal management (insulators, thermal dissipation, etc.) materials. The direct conversion of waste heat to electricity is also a large incentive to find viable thermoelectric (TE) materials, and we are developing novel enhancement principles to functionalize abundant and safe element materials.<sup>1-5)</sup>

## 2. Research Activities

## (1) Novel concepts for TE enhancement.

We recently clarified the importance of the interaction of the charge carrier and magnetic moment to enhance thermoelectric power factor.<sup>6,7)</sup> The robust feature of this principle is that it is not magnon-derived and therefore is not dependent on ordering, and the enhancement has been shown to be effective at relatively high temperatures. This work has attracted some attention, and attempts to magnetically dope thermoelectric materials appear to be increasing throughout the world.

As a striking new development, we have shown by experiments on an electron-doped Heusler alloy, that spin fluctuation can enhance thermoelectric power factor.<sup>8)</sup> This was previously theoretically predicted,<sup>9)</sup> but in this work we have actually shown that it can lead to large thermoelectric power factors.<sup>8)</sup>

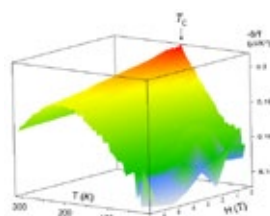


Fig. 1. Thermoelectric enhancement through spin fluctuation.<sup>8)</sup>

## (2) Nanostructuring to enhance TE.

We have previously shown by controlled nanostructuring that we could enhance the thermoelectric performance of a leading thermoelectric material, skutterudites by 100%, leading to a high  $ZT \sim 1.6$  at high temperatures.<sup>10)</sup> This year we have two different approaches leading to striking results.

A) Energy filtering. The first is utilization of the energy filtering effect first proposed by Shakouri et al.<sup>11)</sup> We have synthesized p-type  $\text{Bi}_{0.5}\text{Sb}_{1.5}\text{Te}_3$  nanocomposited by  $\text{Sb}_2\text{O}_3$  nanoparticles successfully mainly dispersed in the grain boundaries. As a result, we achieved an enhancement of  $ZT$  to 1.51 at 350 K, and importantly  $ZT > 1.0$  over a relatively wide range of temperature up to 450 K.<sup>12)</sup> Although the aforementioned pores are stable due to their intrinsic nature, nanostructured effects in general sometimes tend to not be stable over long periods of time. Although it is not usually

done, we have notably carried out characterizations over 24 months to test the stability. As a result, there was some slight degradation, but overall, our nanocomposite samples were found to exhibit excellent thermal and chemical stability over this 24 month period (Fig. 2).<sup>12)</sup>

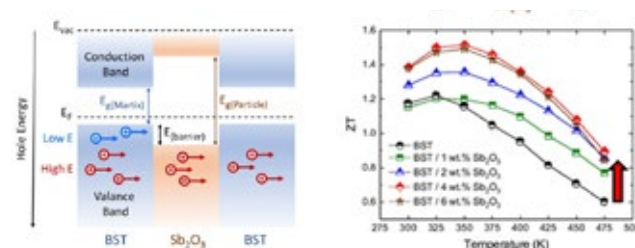


Fig. 2. Energy filtering enhanced thermoelectric materials with relatively high stability over 24 month period.<sup>12)</sup>

B) Nanomicrocomposites to selectively lower thermal conductivity. As a byproduct of the magnetic doping experiments, Fe was found to form secondary phases in  $\text{CuGaTe}_2$ , creating a composite material. As a result of selective phonon scattering,  $ZT$  was enhanced to 0.92.<sup>13)</sup> Regarding nanocomposite advanced measurements, the Nanotube Gr. developed a novel TEM thermal probe.<sup>14)</sup>

## (3) International collaborations to enhance thermoelectric materials.

We have actively moved forward cooperations on thermoelectric materials with research groups in Germany,<sup>15)</sup> Canada,<sup>16)</sup> Portugal,<sup>17)</sup> Australia, Austria, US, etc. resulting in notable results. Domestic cooperations with AIST,<sup>18)</sup> RIKEN,<sup>19)</sup> etc. were also fruitful.

## References

- 1) T. Mori, S. Priya, *MRS Bulletin* **43**, 176 (2018).
- 2) T. Mori, in *Advanced Thermoelectrics: Materials, Contacts, Devices, and Systems*, (Taylor and Francis, London, 2018) 393.
- 3) I. Petsagkourakis et al., *Sci. Tech. Adv. Mater.* **19**, 836 (2018).
- 4) T. Mori, *Small* **13**, 1702013 (2017).
- 5) "Thermoelectric Nanomaterials", ed. K. Koumoto, T. Mori, Springer Series in Materials Science (Springer, Heidelberg, 2013) pp.1-373.
- 6) F. Ahmed et al., *J. Mat. Chem. A* **5**, 7545 (2017).
- 7) H. Takaki et al., *Materials Today Phys.* **3**, 85 (2017).
- 8) N. Tsujii et al., *Sci. Adv.* (2019), in press.
- 9) T. Okabe, *J. Phys. Condens. Matter* **22**, 115604 (2010).
- 10) A.U. Khan et al., *Nano Energy* **31**, 152 (2017).
- 11) A. Shakouri, *Annu. Rev. Mater. Res.* **41**, 399 (2011).
- 12) A. Pakdel et al., *J. Mater. Chem. A* **6**, 21341 (2018).
- 13) F. Ahmed et al., *J. Materiomics* **4**, 221 (2018).
- 14) N. Kawamoto et al., *Nano Energy* **52**, 323 (2018).
- 15) K. Rasim et al., *Angew. Chem. Int. Ed.* **57**, 6130 (2018).
- 16) L.R. Macario et al., *ACS Appl. Mater. Interfaces* **10**, 40585 (2018).
- 17) M. Piotrowski et al., *J. Phys. Chem. C* **122**, 48 (2018).
- 18) D. Song et al., *J. Mat. Chem. C* **6**, 12260 (2018).
- 19) P. He et al., *ACS Appl. Mater. Interfaces* (2019), in press. Front cover.



## Inorganic Nanosheets

### Principal Investigator

(MANA Director, Group Leader)

**Naoto Shirahata** (Associate PI), **Yasuo Ebina** (Principal Researcher),  
**Nobuyuki Sakai** (Senior Researcher), **Satoshi Tominaka** (Senior Researcher)

### Takayoshi SASAKI

## 1. Outline of Research

We aim at synthesizing 2D inorganic nanosheets as a unique class of nanoscale materials by delaminating various layered compounds through soft-chemical processes. Particular attention is paid to fine control of their composition and structure via doping and substitution of constituent elements, expecting new or enhanced properties.

We develop a new nanofabrication process for precisely organizing functional nanosheets into multilayer or superlattice assemblies through solution-based processes (Fig. 1). Based on the exotic approach with the nanosheets (soft-chemical materials nanoarchitectonics), we establish the tailoring ability and controllability over nanostructures with a precision down to 1 nm, which is comparable to that in lattice engineering utilizing modern vapor-phase deposition techniques.

In the second stage, we take challenges to develop innovative nanostructured materials and nanodevices through nanoscale assembly of nanosheets and a range of foreign species (organic modules, metal complexes, clusters...). Particularly we attempt to realize new or sophisticated functions by cooperative interaction between nanosheets themselves or between nanosheets and other functional modules.

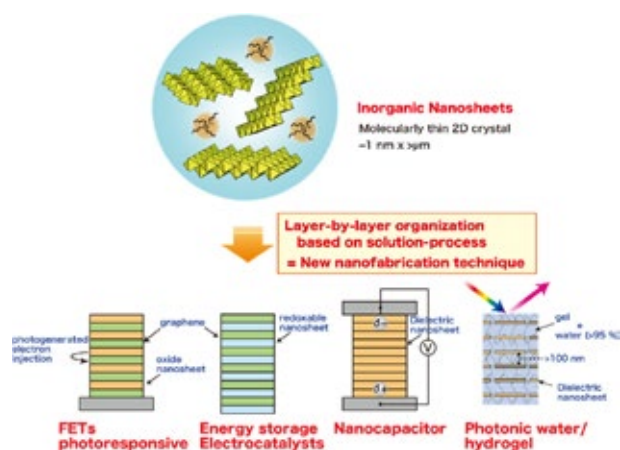


Fig. 1. Conceptual explanation of the research plan.

## 2. Research Activities

### (1) Controlled Co doping into 2D Mn oxide nanosheet.<sup>1)</sup>

We successfully synthesized Co-substituted MnO<sub>2</sub> nanosheets with a composition of Mn<sub>1-x</sub>Co<sub>x</sub>O<sub>2</sub> ( $x = 0.2-0.5$ ) by exfoliating the protonated form of Na<sub>0.6</sub>Mn<sub>1-x</sub>Co<sub>x</sub>O<sub>2</sub>. Protonation and exfoliation can be achieved with preserving the chemical composition and structure of the host layers of

the starting material (Fig. 2a). The optical absorption peak of the obtained Mn<sub>1-x</sub>Co<sub>x</sub>O<sub>2</sub> nanosheets was continuously blue shifted as the Co content increased, showing the homogeneous distribution of the Co ions into the MnO<sub>2</sub> lattice (Fig. 2b). The Mn<sub>1-x</sub>Co<sub>x</sub>O<sub>2</sub> nanosheets showed electrochemical redox reactions with improved cycle performance compared to MnO<sub>2</sub> nanosheets and high capacitance of 700–1000 F g<sup>-1</sup> (Fig. 2c), making them favorable for applications such as energy-storage devices.

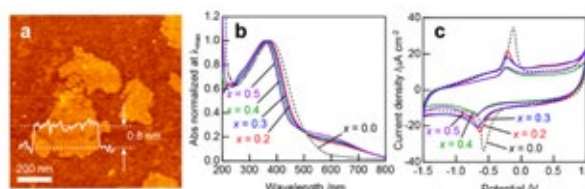


Fig. 2. a: AFM image of Mn<sub>1-x</sub>Co<sub>x</sub>O<sub>2</sub> ( $x = 0.2$ ) nanosheets. b: Optical absorption spectra of Mn<sub>1-x</sub>Co<sub>x</sub>O<sub>2</sub> nanosheet suspensions. c: Cyclic voltammograms of Mn<sub>1-x</sub>Co<sub>x</sub>O<sub>2</sub> nanosheets.

### (2) Fabrication of superlattice materials of manganese oxide nanosheets and graphene.<sup>2)</sup>

We have successfully combined MnO<sub>2</sub> nanosheets and reduced graphene oxide (rGO) into a superlattice-like assembly via facile solution process. (Fig. 3a). Polycation was added into the suspension of rGO to turn its surface charge positive and then mixed with the suspension of MnO<sub>2</sub> nanosheets, which brought about immediate flocculation. The obtained superlattice material was found to show a very large capacity based on so-called conversion reaction with excellent cycling stability (Fig. 3b), which can be ascribed to the superlattice structure where MnO<sub>2</sub> nanosheets as an active material are isolated from each other by the carbon network of rGO to suppress significant morphology change in repeated charge/discharge processes.

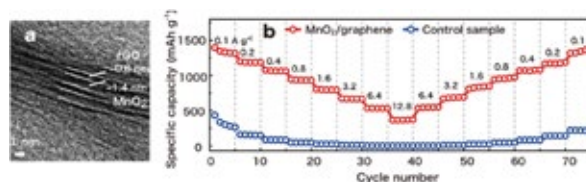


Fig. 3. a: TEM image of MnO<sub>2</sub>/rGO superlattice composite. b: Rate performance: red: MnO<sub>2</sub>/graphene superlattice, blue: the control sample (randomly restacked MnO<sub>2</sub>/graphene composite).

## References

- 1) N. Sakai, K. Fukuda, R. Ma, T. Sasaki, *Chem. Mater.* **30**, 1517 (2018).
- 2) P. Xiong, R. Ma, N. Sakai, T. Sasaki, *ACS Nano* **12**, 1768 (2018).

Supramolecular Materials

Principal Investigator

Katsuhiko ARIGA

(Group Leader)

Jonathan P. Hill (Chief Researcher), Lok Kumar Shrestha (Principal Researcher), Junichi Takeya (Invited Researcher)



1. Outline of Research

Functional materials have been wisely constructed via bottom-up approaches as seen in preparation of molecular and nano patterns, complexes, and nanomaterials organized nano- and microstructures, and function materials. We are working in exploratory research for innovative materials and sensing systems based on supramolecular concept.<sup>1-6)</sup>

2. Research Activities

Carbon nanosheets, thin materials consisting of only carbon, have many useful properties, including energy-storage and catalytic functionality. The large-scale production of carbon nanosheets, however, has been challenging. Our group has discovered a relatively simple method for the fabrication of large carbon nanosheets on the basis of collaboration with Itami group of Nagoya University (Fig. 1).

The fabrication process started from a solution of specially designed organic molecules, CPPhen provided by Kenichiro Itami at the Nagoya University, in chloroform. CPPhen molecules have an ellipsoidal shape and consist of several hexagonal benzene rings, typical precursors for graphitic (i.e., layered carbon) networks. The solution was put dropwise onto an air–water interface undergoing vortex flow (the type of motion observed when stirring a liquid in a glass). The centrifugal rotation helped to spread the CPPhen molecules uniformly on the air–water interface. After stopping stirring, the chloroform was left to evaporate, and the resulting self-assembled thin film was put on a substrate. The final step was to ‘carbonize’ the on-substrate film by heating and exposure to nitrogen gas flow.

Importantly, the produced film, having a thickness of about 10 nanometer, indeed showed uniform two-dimensional morphology. Mori and colleagues also noted that the sheets were highly porous, pore sizes were about 20 to 30 nanometer.

The researchers attribute the success of their approach to the role of the intermolecular interactions between the CPPhen molecules; applying the same procedure to molecules containing elements of the CPPhen structure did not lead to the formation of planar carbon sheets.

The scientists also explored the synthesis of nitrogen-doped carbon sheets with their carbonization method. Mixing CPPhen with pyridine, a nitrogen-containing compound, before dripping it onto the vortex air–water interface, resulted in sheets with high nitrogen content —

Mori and colleagues assume the pyridine molecules were trapped within the CPPhen molecules or between them during carbonization. The electrical conductivity of the nitrogen-doped carbon sheets was significantly higher than that of the undoped ones, which is promising for applications. Indeed, the scientists conclude that this “would allow the utilization of nitrogen-doped carbon nanosheets as highly efficient catalysts for oxygen-reduction reactions for high-performance fuel cells.”

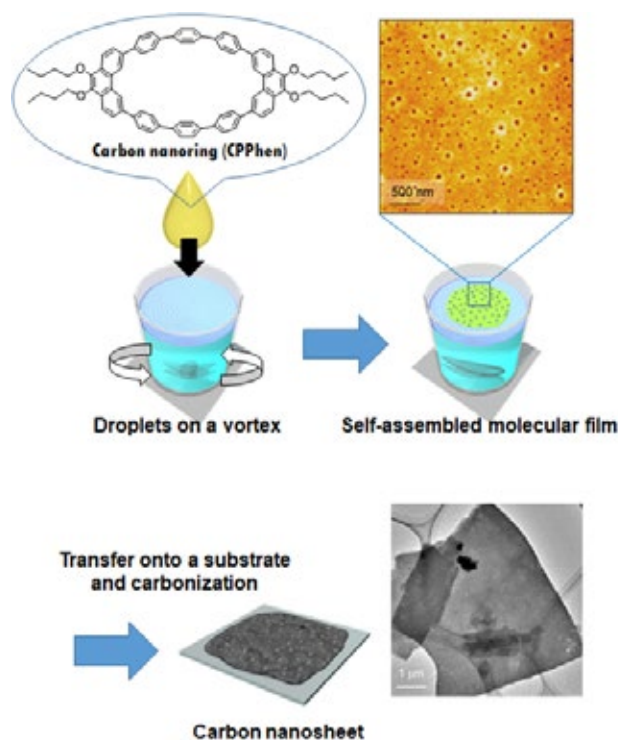


Fig. 1. Synthesis of carbon nanosheets from CPPhen molecules.

References

- 1) T. Mori, H. Tanaka, A. Dalui, N. Mitoma, K. Suzuki, M. Matsumoto, N. Aggarwal, A. Patnaik, S. Acharya, L. K. Shrestha, H. Sakamoto, K. Itami, K. Ariga, *Angew. Chem. Int. Ed.* **57**, 9679 (2018).
- 2) M. Li, S. Kang, J. Du, J. Zhang, J. Wang, K. Ariga, *Angew. Chem. Int. Ed.* **57**, 4936 (2018).
- 3) K. Ariga, S. Watanabe, T. Mori, J. Takeya, *NPG Asia Mater.* **10**, 90 (2018).
- 4) K. Ariga, D.T. Leong, T. Mori, *Adv. Funct. Mater.* **28**, 1702905 (2018).
- 5) P. Bairi, T. Tsuruoka, S. Acharya, Q. Ji, J. P. Hill, K. Ariga, Y. Yamauchi, L. K. Shrestha, *Mater. Horizons* **5**, 285 (2018).
- 6) W.A. Webre, H.B. Gobeze, S. Shao, P.A. Karr, K. Ariga, J.P. Hill, F. D’Souza, *Chem. Commun.* **54**, 1351 (2018).



## Semiconductor Devices of Organic Nano-Sheet Crystals

**Principal Investigator**  
(The University of Tokyo, Japan)  
Cross Appointment with NIMS

**Junichi TAKEYA**

## 1. Outline of Research

It is known that periodically arrayed two-dimensional sheets of molecules can generate diverse functions of cell-biology, regulating communication between inner outer circumstances. Self-assembling nature of the molecules, soft dynamics and large area-to-volume ratio are substantial in such functionalization. In our recent studies of elongated  $\pi$ -conjugated semiconducting molecules, we found that soft nano-sheet single crystal films are self-organized to the size of more than inches and that the electronic device performance is maximized. Moreover, it turned out that the structurally well-defined soft electronic material is highly useful to immediately translate mechanical stimulation to electronic signal, demonstrating a giant strain gauge coefficient exceeding 20.

## 2. Research Activities

### (1) Self-organization of Organic Nano-sheet Crystals.<sup>1,2)</sup>

Fig. 1 shows an example of the semiconducting molecules which grows to wafer-scale molecular layer crystals. The molecules of alkylated dinaphthobenzodithiophene ( $C_n$ -DNBDT) are first dissolved in organic solvents and are gradually crystallized during evaporation of the solvents at bottom surface of a blade in our home-made equipment with sliding substrate<sup>1)</sup> (Fig. 1b). By properly adjusting temperature and speed of the crystal growth, it is found that a-few-monolayer crystal films are reproducibly grown to the size over inches.<sup>2)</sup>

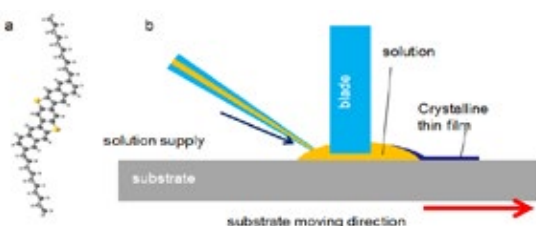


Fig. 1. Molecular structure of  $C_n$ -DNBDT (a) and the method of crystallization (b).

### (2) Devices of Organic Nano-sheet Crystals.<sup>3)</sup>

Bi-layers of the self-organized  $C_n$ -DNBDT nano-sheets are grown directly on multilayer substrates of field-effect transistors, presenting outstanding charge transporting property (Fig. 2). The carrier mobility exceeds  $20 \text{ cm}^2/\text{Vs}$  in the transistor channel and the most efficient carrier injection is realized from the top electrodes through the ultrathin film. Therefore, the devices show the fastest response ever realized with molecular semiconductors.<sup>3)</sup> With our recent development of high-mobility p- and n-type semiconductor molecules, the result opens the way to printed low-cost CMOS circuits on plastic films. Such organic CMOS

technology is highly expected for low-power operation of digital data in battery-less IoT sensors.

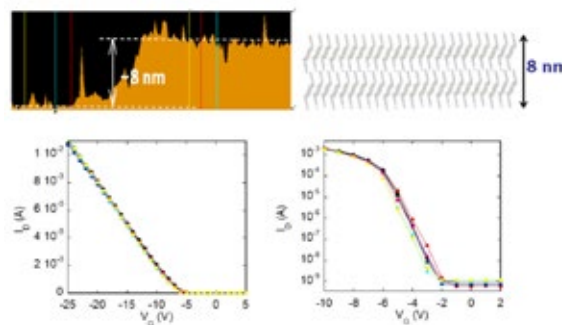


Fig. 2. Bi-molecular-layer  $C_n$ -DNBDT semiconductor films and their transistor performances.

### (3) Flexible Mechano-electronics.<sup>3,4)</sup>

We grew a bi-layer single-crystal film of  $C_n$ -DNBDT on a plastic substrate and an acceptor layer is deposited at the top of the nano-sheet crystal film. It turned out that the bi-layer film is efficiently doped with delocalized high-mobility holes because of the minimized thickness of the semiconducting crystal films with negligible defects (Fig. 3). At maximum, 3% strain is uniaxially applied without any damage to the sample so that room-temperature mobility increased by the factor of 1.7.<sup>4)</sup> Analysis using X-ray diffraction (XRD) measurements and density functional theory (DFT) calculations reveal the origin to be the suppression of the thermal fluctuation of the individual molecules, which is consistent with temperature dependent measurements.<sup>5)</sup>

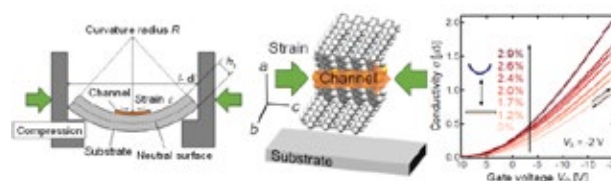


Fig. 3. Giant strain effect in doped nano-sheet organic crystals.

## References

- 1) C. Mitsui, T. Okamoto, M. Yamagishi, J. Tsurumi, K. Yoshimoto, K. Nakahara, J. Soeda, Y. Hirose, H. Sato, A. Yamano, T. Uemoura, J. Takeya, *Adv. Mater.* **26**, 4546 (2014).
- 2) J. Soeda, T. Uemura, T. Okamoto, C. Mitsui, M. Yamagishi, J. Takeya, *Appl. Phys. Exp.* **6**, 076503 (2013).
- 3) A. Yamamura, S. Watanabe, M. Uno, M. Mitani, C. Mitsui, J. Tsurumi, N. Isahaya, Y. Kanaoka, T. Okamoto, J. Takeya, *Sci. Adv.* **4**, eaao5758 (2018).
- 4) T. Kubo, R. Häusermann, J. Tsurumi, J. Soeda, Y. Okada, Y. Yamashita, N. Akamatsu, A. Shishido, C. Mitsui, T. Okamoto, S. Yanagisawa, H. Matsui, *Nature Comm.* **7**, 11156 (2016).
- 5) J. Tsurumi, H. Matsui, T. Kubo, R. Häusermann, C. Mitsui, T. Okamoto, S. Watanabe, *Nature Phys.* **13**, 994 (2017).

## Next-Generation Semiconductor Nanodevices

**Principal Investigator**  
(Group Leader)

**Naoki FUKATA**

**Wipakorn Jevasuwan** (Senior Researcher), **Ryo Matsumura** (Researcher)



### 1. Outline of Research

Considerable work has been done regarding one-dimensional semiconducting nanowires (NWs).<sup>1)</sup> Silicon (Si) and germanium (Ge) NWs have attracted particular attention due to their compatibility with current Si complementary metal-oxide semiconductor (Si CMOS) integrated circuit technology and their better scalability. These NWs have potential for use in the channel, source and drain regions of MOS field-effect transistors (FETs). However, the problem of retardation of carrier mobility caused by impurity scattering must be solved if impurity atoms are doped into the channel region. Core-shell NWs using Si and Ge appear to have major potential for suppression of impurity scattering. A radial heterojunction design separates the carrier transport pathway from the impurity-doped regions. This structure is similar to that in high electron mobility transistors (HEMTs).

To realize the enhancement of carrier mobility in core-shell NWs, doping sites and the electrical activity of impurity atoms need to be controlled. We have established and reported characterization methods of impurity atoms in SiNWs, GeNWs, and their core-shell NWs.<sup>2)</sup> The accumulation of hole gas by forming Ge/Si core shell NWs has been investigated using this technique.<sup>2)</sup> In this study, we report our clear verification about the hole gas accumulation from B-doped p-Si core regions to undoped i-Ge shell regions in p-Si/i-Ge core-shell NWs which is the opposite structure of the previous i-Ge/p-Si core-shell NWs.

### 2. Research Activities

#### (1) Formation of Si/Ge core-shell NWs.

p-Si/i-Ge core-shell NWs were grown by two step growth using chemical vapor deposition (CVD) (Fig. 1). Gold nanocolloid particles were used as seeds for vapor-liquid-solid (VLS) growth of p-SiNWs. The total pressure was set at 8 Torr by mixing with N<sub>2</sub> gas. The axial growth of p-SiNWs were grown using SiH<sub>4</sub> gas with a flux of 19 sccm

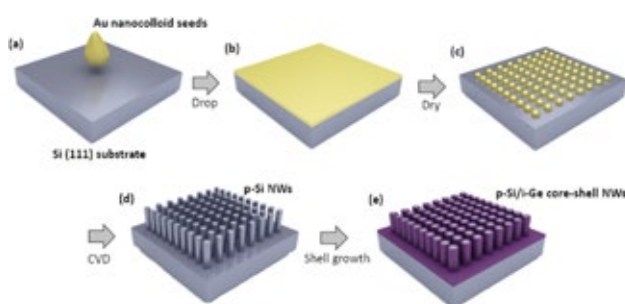


**Fig. 1. Schematic of p-Si/i-Ge core-shell NW CVD growth process:** (a)-(c) deposition of colloidal Au catalyst seeds on the Si (111) substrate; (d) formation of p-Si core NWs by SiH<sub>4</sub> gas flux; (e) final p-Si/i-Ge core-shell NWs.

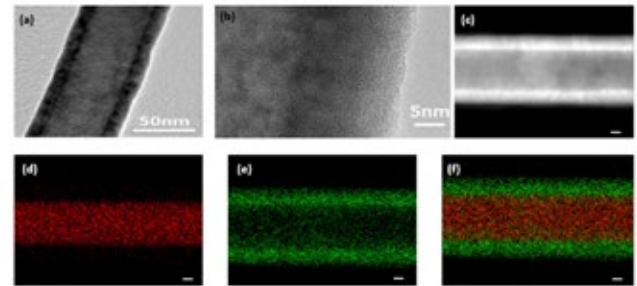


**Fig. 2. (a) Low and (b) high resolution TEM images of p-Si/i-Ge core-shell NW with the shell growth time of 60 sec.** The scale bar of (a) and (b) are 50 nm and 5 nm, respectively. (c) STEM image and (d)-(f) EDX mapping with the scale bars of 10 nm. The red color and green color represent Si and Ge, respectively.

and B<sub>2</sub>H<sub>6</sub> (1 % in H<sub>2</sub>) gas with various fluxes of 0 ~ 0.5 sccm at 600 °C for 15 min and the subsequent radial growth of the i-Ge shell layer was achieved at 500 °C using 10 sccm of GeH<sub>4</sub> (100%) to form the i-Ge/p-Si core-shell NWs. The representative TEM, STEM and EDX images are shown in Fig. 2.

#### (2) Demonstration of hole gas accumulation in Ge shell.<sup>3)</sup>

To demonstrate the hole accumulation into the i-Ge shell in p-Si/i-Ge core-shell NWs, we summarized the Raman data observed for various samples with different structures in Fig. 3. The Ge optical phonon peak observed for i-GeNWs showed a slightly downshift compared to bulk Ge, which is due to the phonon confinement. The Ge optical phonon peak observed for i-Si/i-Ge and p-Si/i-Ge core-shell NWs upshifts compared to i-GeNWs due to the compressive stress from the i-SiNWs and p-SiNWs. The Ge optical phonon peak slightly shifted lower when Si NWs were doped with B. This result clearly demonstrate the hole gas accumulation in the i-Ge shell layer.<sup>3)</sup>

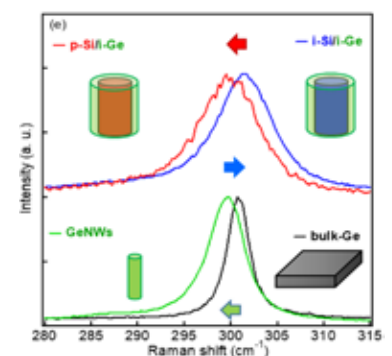


**Fig. 3. Ge optical phonon peaks observed for bulk Ge, i-Ge NWs, i-Si/i-Ge core-shell NWs, and p-Si/i-Ge core-shell NWs.**

### References

- 1) N. Fukata, *Adv. Mater.* **21**, 2829 (2009).
- 2) N. Fukata, M. Yu, W. Jevasuwan, T. Takei, Y. Bando, W. Wu, Z. L. Wang, *ACS Nano* **9**, 12182 (2015).
- 3) X. Zhang, W. Jevasuwan, K.C. Pradel, T. Subramani, T. Takei, N. Fukata, *Nanoscale*, in press.



## Nanomaterial Properties Uncovered Under *in situ* TEM

**Principal Investigator**  
(Group Leader)

**Dmitri GOLBERG**

Cross Appointment with Queensland University of Technology, Australia  
**Masanori Mitome** (Chief Researcher), **Naoyuki Kawamoto** (Senior Researcher)

### 1. Outline of Research

Functional properties of nanomaterials under a full control of their morphology, crystallography, atomic structure, defect networks and spatially-resolved chemical compositions are unambiguously determined using nanoscale manipulations and probing in a high-resolution transmission electron microscope (HRTEM) under ultimately high spatial, energy and temporal resolutions. Clear structure-property relationship is obtained which is a “Holy Grail” of the Materials Science. Our research opens up a wide horizon for practical implementations of diverse advanced nanoscale materials in structural nanocomposites, nanoelectronic, optoelectronic and photovoltaic fields, ion-batteries and quantum computers.

### 2. Research Activities

(1) *Mechanical, electrical and crystallographic property dynamics of strained Ge/Si core-shell nanowires.*

We simultaneously investigated the crystallography changes, and electrical and mechanical behaviors of Ge/Si core-shell nanowires under bending and tensile deformation in TEM (Fig. 1).<sup>1)</sup> The Young's modulus was measured to be ~191 GPa, and a tensile strength was 3-8 GPa. The core-shell Ge/Si nanowires could be elastically bent to very high limits. Using high-resolution imaging, we confirmed that under high bending strain, Si shells had irregularly changed to the amorphous state, whereas Ge cores kept single crystal status with a local lattice strain on the compressed side. The nanowires revealed cyclically changed electrical properties and mechanical robustness. *In situ* taken electron diffraction patterns paired with theoretical simulations

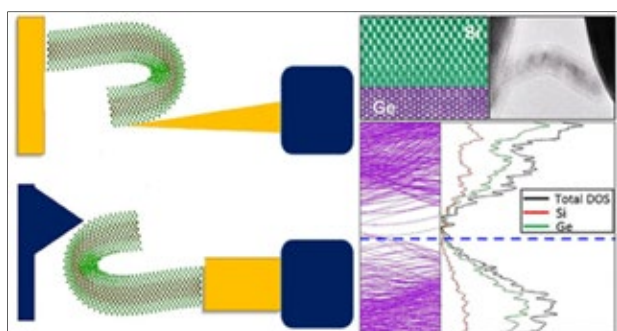


Fig. 1. Experimental schemes for electrical (upper left) and mechanical probing (lower left) of a core-shell Ge/Si nanowire, HRTEM image of the Ge/Si interface and low-magnification image of an experimentally bent in TEM nanowire (upper right), and total and partial density of states of a bent nanowire calculated using DFT method (lower right).

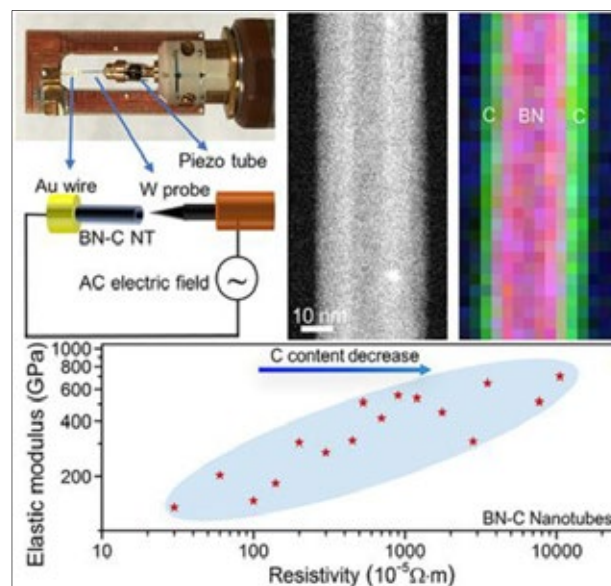


Fig. 2. A scheme for initiating resonance modes in a cantilevered core-shell BN/C nanotube (upper left), spatially-resolved chemical maps from an individual C-coated BN nanotube (upper right), and dependence of the Young's modulus and electrical resistivity of BN/C nanotubes as a function of the coated carbon content on a BN nanotube core.

imply that non-equilibrium phases of amorphous Si and  $\beta$ -Sn Ge appearing during the deformations may explain the observed mechanical robustness and varying conductivities under deformations.

(2) *Tunable mechanical and electrical properties of core-shell BN/C nanotubes.*

Graphitic C-coated BN nanotubes (BN-C NTs) were synthesized and their mechanical and electrical properties were in parallel measured using *in situ* HRTEM (Fig. 2).<sup>2)</sup> As a function of the coated carbon content, the elastic modulus obtained from the second order harmonic resonance of heterostructured nanotubes was tuned from ~140 GPa to ~700 GPa, and their electrical resistivity was adjusted within three orders of magnitude from ~0.16  $\Omega\cdot\text{m}$  to  $\sim 2.5 \times 10^{-4} \Omega\cdot\text{m}$ . This work opens the way for making custom-designed heterostructures for the requirements of any specific application.

### References

- 1) C. Zhang, D.G. Kvashnin, L. Bourgeois, J.F.S. Fernando, K. Firestein, P.B. Sorokin, N. Fukata, D. Golberg, *Nano Lett.* **18**, 7238 (2018).
- 2) X. Zhou, F.C. Hsia, D.M. Tang, O. Cretu, C. Zhang, M. Mitome, Y. Bando, T. Sasaki, D. Golberg, *Phys. Stat. Sol. RRL* 1800576 (2018).

## Tailored Design of Two Dimensional Nanoporous Carbon Materials

**Principal Investigator**  
(Group Leader)

**Yusuke YAMAUCHI**

Cross Appointment with The University of Queensland, Australia  
**Joel Henzie** (Senior Researcher), **Yusuke Ide** (Senior Researcher)



### 1. Outline of Research

Layered materials represent a multiple and largely unexploited source of two-dimensional (2D) systems with unusual physical properties, outstanding electrical properties and, most importantly, ultrahigh exposed surface area, which are important for energy storage, catalysis, and sensing applications. Among them, carbon materials, with 2D or pseudo-2D morphologies, are of particular interest for the applications such as catalysis, water/gas purification, or energy conversion/storage, owing to their intrinsic advantages of large specific surface area, excellent electrical conductivity, chemical inertness and low cost. However, the applications of 2D-structured carbon materials are mostly hampered by the severe aggregation, especially after processing into a compressed electrode, that cause the limitations of ion accessibility, diffusion and mass transportation.

To address the aforementioned issues, many efforts have been devoted to construct 2D carbon materials with designed structures to increase the ion-accessible surface area and to improve the ion transport efficiency. The commonly used methods include preparing crumpled nanosheets or incorporating small dimensional nanoparticles within the nanosheets, which can generate interlayer space when being packed together; however, the curved interlayer spacer and the randomly distributed interlayer spacers will lead to a complex and even blocked pathway for ion diffusion, limiting the ion-accessible surface area. Consequently, it is still a great challenge to design appropriate carbon nanostructure which could provide efficient ion diffusion routes when being packed together.

In this report, we report ordered mesoporous carbon nanosheets (OMCNS) with high graphitization degree, by the confinement polymerization of resol-F127 micelles in the interlayer space of montmorillonite (MONT) followed by calcination and acid washing.<sup>1-4)</sup> The combination of abundant in-plane pores, which would facilitate more accessible surface and easier ion transport path, and high graphitization degree, which would promote electron transfer, enables the OMCNS to achieve excellent electrochemical performance as electrode materials for electric double layer capacitors (EDLC) in ionic liquid electrolyte.

### 2. Research Activities

A schematic illustration of the preparation process is shown in Fig. 1. MONT is a typical layered clay mineral. To achieve better dispersion, resol and MONT are firstly

dispersed into ethanol separately. Upon mixing the two solutions, the resol oligomers and F127 unimers are intercalated into the interlayer space of MONT, driven by the hydrogen bonding between the OH group of the resol oligomers/F127 and terminating oxygen present on the MONT (Fig. 1a). By vacuum evaporation at room temperature following thermal polymerization, the F127 micelles@Resol are assembled in the interlayer space of MONT, and then transformed into tightly arranged ordered micelles (Fig. 1b). The OMCNS are obtained after carbonization followed by acid washing to remove MONT (Fig. 1c-d).

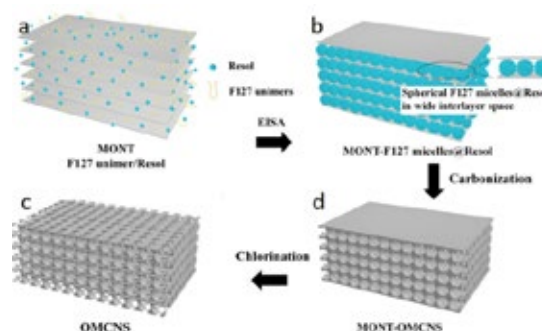


**Fig. 1.** Schematic illustration of the preparation process for OMCNS.

The transmission electron microscopy (TEM) image of OMCNS show large domains of highly ordered hexagonal mesostructure (space group of  $p6mm$ ). The pore size is  $\sim 5$  nm and pore wall are  $\sim 6$  nm. Notably, the high-resolution TEM (HRTEM) image demonstrates that, the OMCNS show highly crystallized graphite fringes with an obvious curvature. It is well-known that the resol source usually gives non-graphitized carbon even after calcination at high temperature. Interestingly, in this approach, it is proved that the limited 2D confined space of MONT favors the formation of  $sp^2$  C-C, leading to highly graphitized carbon. This is due to the confinement effect of MONT which promotes the formation of C-C in the sample plane. The high graphitization degree is crucial for improving the conductivity of OMCNS.

### References

- 1) V. Malgras, J. Henzie, T. Takei, Y. Yamauchi, *Angew. Chem. Int. Ed.* **57**, 8881 (2018).
- 2) Z.L. Wang, K. Sun, J. Henzie, X.F. Hao, C.L. Li, T. Takei, Y.M. Kang, Y. Yamauchi, *Angew. Chem. Int. Ed.* **57**, 5848 (2018).
- 3) J. Wang, Y.L. Xu, B. Ding, Z. Chang, X.G. Zhang, Y. Yamauchi, K.C.W. Wu, *Angew. Chem. Int. Ed.* **57**, 2894 (2018).
- 4) B. Jiang, Y. Guo, J.H. Kim, A.E. Whitten, K. Wood, K. Kani, A.E. Rowan, J. Henzie, Y. Yamauchi, *J. Am. Chem. Soc.* **140**, 12434 (2018).



## Hybrid Artificial Photosynthetic System

**Principal Investigator**  
(Group Leader)

**Jinhua YE**

**Mitsutake Oshikiri** (Principal Researcher), **Tetsuya Kako** (Senior Researcher)

### 1. Outline of Research

We are conducting research and development of novel photocatalytic materials for a more efficient utilization of solar energy, as well as application of these materials for degradation of hazardous organics, solar hydrogen production and CO<sub>2</sub> conversion to useful hydrocarbon fuels. Our research approaches mainly include composition- and morphology-controlled fabrication of nanometals, organic/inorganic semiconductor materials and integration of those materials for advanced utilization of sunlight and efficient conversion to chemical energy. Also, through conducting fusion researches between theoretical calculations and in-situ measurements, we are elucidating reaction mechanisms in order to provide crucial design guidelines for new material development, and lead to the discovery of new principles and functions. For more details, we are conducting (Fig. 1):

- 1) Design and fabrication of new semiconductors which can utilize solar energy sufficiently by energy band structure engineering, with the help of theoretical calculation basing on the first principle theory.
- 2) Nanoarchitectonics of the photosynthetic system by not only fabrication of nano particles using various soft chemical method, but also assembling of nano-metal/nano-oxide hybridized system to achieve efficient transportation and separation of electron-hole charge carriers.
- 3) Mechanism study by experimental and theoretical approaches, to establish guidelines for development of higher efficient system.

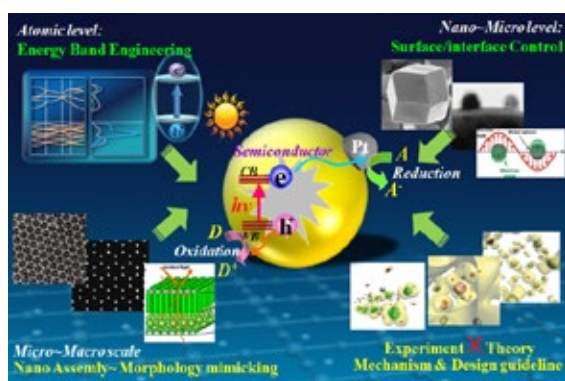


Fig. 1. Outline of research in photocatalytic materials group.

### 2. Research Activities

- (1) Integrating *g*-C<sub>3</sub>N<sub>4</sub> nanosheet with B–H bonding decorated Metal–Organic Framework for CO<sub>2</sub> activation and Photoreduction.<sup>1)</sup>

We realized the integration of a carbon nitride nanosheet and zeolite-like porous boron imidazolate framework with B–H bonding in high density, thus giving rise to the composite BIF-20@*g*-C<sub>3</sub>N<sub>4</sub> nanosheet with high CO<sub>2</sub> photoreduction activity (Fig. 2). The first-principles

simulations and energy transfer investigation demonstrate that the existence of B–H bonding can not only trap photoexcited electrons and effectively avoid the recombination of charge carriers but also activate the adsorbed CO<sub>2</sub>, achieving a photocatalytic CO<sub>2</sub> reduction activity much higher than that of the bare *g*-C<sub>3</sub>N<sub>4</sub> nanosheet and ZIF-8@*g*-C<sub>3</sub>N<sub>4</sub> nanosheet. This integration strategy will be applicable to a broad range of catalytic applications, particularly to those that require solar harvesting and gaseous compatibility.

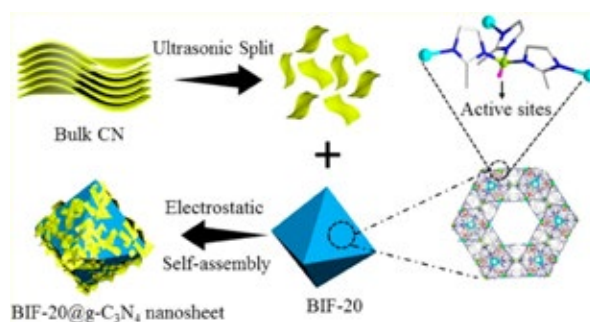


Fig. 2. Schematic description of the preparation of the BIF-20@*g*-C<sub>3</sub>N<sub>4</sub> nanosheet photocatalyst.<sup>1)</sup>

- (2) Visible-light-mediated methane activation over Rh/TiO<sub>2</sub> catalysts.<sup>2)</sup>

We found that visible light illuminated TiO<sub>2</sub> supported Rh nanoparticles could significantly enhance methane (CH<sub>4</sub>) activation in steam methane reforming at mild operating temperature (below 300 °C), with a ~50% decrease in apparent activation energy compared to that of pure thermal process. Femtosecond transient absorption spectroscopy and DFT calculations show an ultrafast separation of hot carriers at the Rh-TiO<sub>2</sub> interface, resulting in the formation of electron-deficient state of Rh<sup>δ+</sup> at surface for the successive CH<sub>4</sub> activation (Fig. 3).

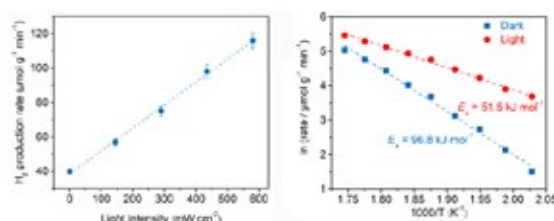


Fig. 3. Left: Dependence of H<sub>2</sub> production rate of Rh/TiO<sub>2</sub> at 260 °C on light intensity. Right: Arrhenius plots for H<sub>2</sub> production rate under dark and visible light conditions of Rh/TiO<sub>2</sub> catalysts.<sup>2)</sup>

### References

- 1) G. Xu, H. Zhang, J. Wei, H. Zhang, X. Wu, Y. Li, C. Li, J. Zhang, J. Ye, *ACS Nano* **12**, 5333 (2018).
- 2) H. Song, X. Meng, Z.J. Wang, Z. Wang, H. Chen, Y. Weng, F. Ichihara, M. Oshikiri, T. Kako, J. Ye, *ACS Catal.* **8**, 7556 (2018).

Multifunctional Nanomaterials



**Associate Principal Investigator Renzhi MA**  
(Group Leader)

**Takaaki Taniguchi** (Senior Researcher), **Daiming Tang** (Researcher)  
X. Li (Postdoc), X. Lu (Postdoc), L. Nurdiwijayanto (Postdoc), H. Xue (Postdoc),  
Y. He (Graduate Student), M. Bai (Graduate Student), H. Gong (Graduate Student),  
W. Li (Graduate Student)

**1. Outline of Research**

We work on the design and synthesis of different kinds of functional nanomaterials, particularly focusing on single-layer nanosheets (Fig. 1). Various layered compounds including metal oxides, hydroxides and dichalcogenides, as well as graphite oxide are exfoliated under suitable conditions, yielding molecularly thin nanosheets. An ultimate 2D anisotropic feature and quantum effect of the nanosheets can radically increase accessible surface area, offer short ion and electron diffusion paths, and thus induce emergent physicochemical properties. Furthermore, we strive to construct artificial nanocomposites by rationally assembling the nanomaterials as building blocks. We aim to create advanced multifunctional composites and devices that were difficult to realize with existing materials and technologies. Through the so-called nanoarchitectonic strategy, it is expected to bring new possibilities to a wide range of application fields, such as next-generation secondary batteries and supercapacitors that far exceed the current performance, non-precious electrocatalysts that show the highest efficiency, as well as superionic transport/separation membranes and solid electrolytes, etc.

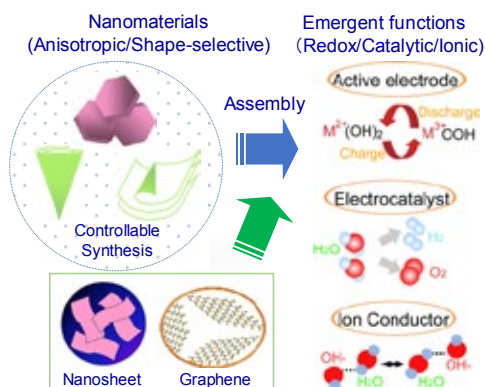


**Fig. 1. The strategy for developing multifunctional nanomaterials.**

**2. Research Activities**

(1) *Nanomaterials with unique coordination configuration functioning as highly efficient electrocatalyst.*<sup>1)</sup>

Coordinationally asymmetric or unsaturated metal centers may serve as accessible active sites and allow strong interaction with incoming guests in catalysis, sensing and separation applications. We have succeeded in synthesizing nanoribbons of  $\text{NaCo}_4(\text{PO}_4)_3$ , in which all Co atoms were in very rare 5 coordination environments. The nanoribbons were characterized with high efficiency for oxygen evolution reaction (OER) in neutral electrolyte, which remarkably outperformed congeneric phosphates such as  $\text{Na}_2\text{CoP}_2\text{O}_7$  with 4-coordinations and even comparable to benchmarking  $\text{RuO}_2$  nanoparticles (Fig. 2). The study validates a great

potential in exploiting nanostructures with coordinatively unsaturated metal centers for energy storage and conversion applications.

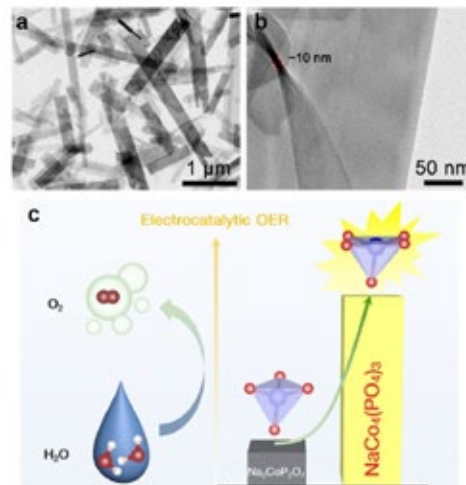


**Fig. 2. (a,b) TEM images of  $\text{NaCo}_4(\text{PO}_4)_3$  nanoribbons. (c) The 5-coordinated nanoribbons show higher OER performance.**

(2) *Superionic properties of single-layer nanosheets.*<sup>2)</sup>

Despite both proton ( $\text{H}^+$ ) and hydroxide ions ( $\text{OH}^-$ ) exhibit anomalously high mobilities in aqueous solutions,  $\text{OH}^-$  conduction in solid electrolytes is considerably lower than that of  $\text{H}^+$ , impeding a paradigm shift to many renewable energy applications in alkaline environments (Fig. 3). We revealed that the mobility/diffusivity of hydroxide ions in single-layer nanosheets can reach an unprecedented high level of  $10^{-1} \text{ S cm}^{-1}$  even at moderate relative humidity (RH) and temperature *via* direct measurements on individual nanosheets of layered double hydroxides (LDHs). This work provides important insights into the origin and mechanism of  $\text{OH}^-$  conduction in 2D nanosheets, which might inspire the creation of superionic membrane/electrolytes using these nanomaterials.

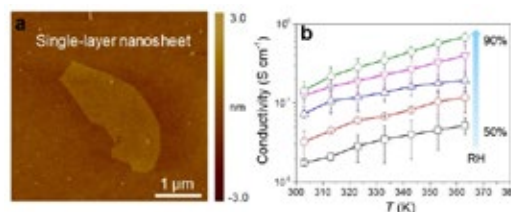


**Fig. 3. (a) AFM image of single-layer LDH nanosheet and (b) Measured  $\text{OH}^-$  conductivities at 50-90% RH.**

**References**

- 1) H. Wan, R. Ma, X. H. Liu, J. Pan, H. Wang, S. Q. Liang, G. Z. Qiu, T. Sasaki, *ACS Energy Lett.* **3**, 1254 (2018).
- 2) P.Z. Sun, R. Ma, T. Sasaki, *Chem. Sci.* **9**, 33 (2018).



## Nano Electrics and Related Materials

Group Leader

Takahiro NAGATA

Michiko Yoshitake (Chief Researcher), Shinjiro Yagyu (Principal Researcher),  
Yoshiyuki Yamashita (Principal Researcher), Jun Chen (Senior Researcher)

## 1. Outline of Research

We have proposed fluorides as a new dielectric gate insulator for the nitride semiconductor based MIS (metal-insulator-semiconductor) structure. High-frequency switchable high-power compact electronic devices that can function under high temperature harsh conditions are indispensable for aviation and automotive systems, smart power transmission, and some domestic applications. A variety of wide-band gap semiconductor, such as SiC and GaN, based high-power active devices have been developed over the years and are currently in advanced manufacturing stage.<sup>1,2)</sup> However, there is an issue of interface states due to the formation of oxides using the oxide based insulator, such as SiO<sub>2</sub> and Al<sub>2</sub>O<sub>3</sub>. To overcome this issue, we have proposed the direct growth of fluorides such as LaF<sub>3</sub> on the semiconductors as the high-k insulator. LaF<sub>3</sub> is used as optical materials such as the reflection coating already. LaF<sub>3</sub> also has wide bandgap (~9 eV) and high dielectric constant (> 40) properties,<sup>3,4)</sup> which should be suitable for the gate insulator, and expected to eliminate the interface oxidation of semiconductors. We demonstrated the possibility of the fluoride gate insulator on GaN.

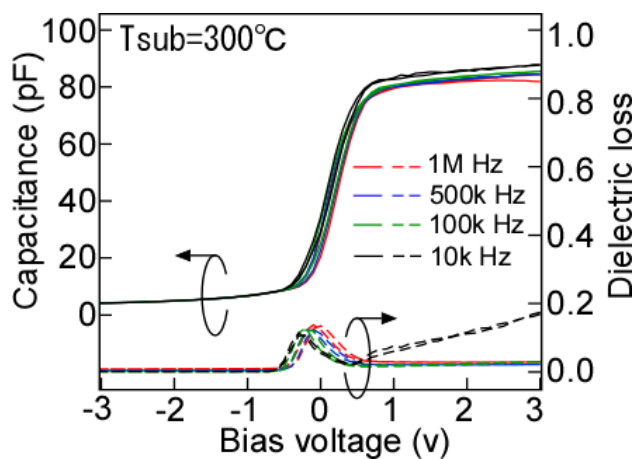


Fig. 1. C-V properties of LaF<sub>3</sub>/GaN stack structure.

## 2. Research Activities

The LaF<sub>3</sub> MIS structure was formed on a GaN freestanding single crystal by ultrahigh vacuum-thermal evaporation method. Capacitance-voltage properties indicated the electron accumulation at the LaF<sub>3</sub> layer (positive bias voltage) with the dielectric constant of 22 and small hysteresis curves, as shown in Fig. 1. TEM observation revealed no oxidized interface layer. By combining the

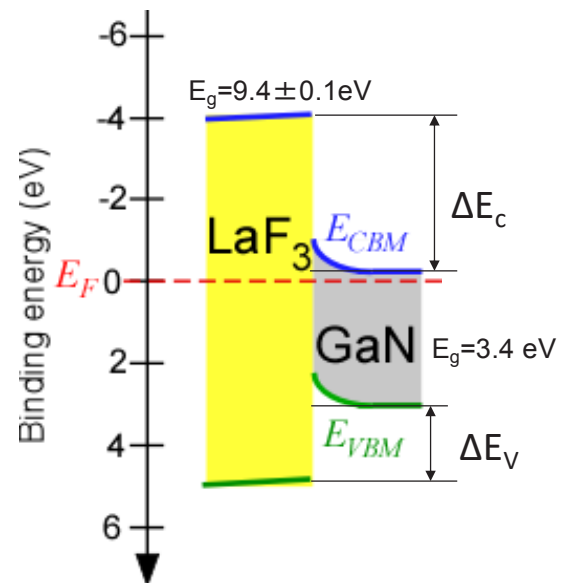


Fig. 2. A schematic illustration of the band diagram of the LaF<sub>3</sub>/GaN stack structure.  $E_F$ : Fermi level,  $E_{CBM}$ : conduction band minimum,  $E_{VBm}$ : valence band maximum,  $E_g$ : band gap.

conventional XPS and hard x-ray photoelectron spectroscopy, we revealed the band alignment between LaF<sub>3</sub> and GaN, as shown in Fig. 2. For LaF<sub>3</sub>, the band gap was estimated as 9.4 eV by the loss spectra of F1s core level. By combining the reported band gaps for GaN (3.39 eV), the band alignment between LaF<sub>3</sub> and GaN was estimated to be  $\Delta E_c$  (difference in the conduction band) =  $4.2 \pm 0.1$  eV. This value is much larger than those of other oxide-based gate insulators such as Al<sub>2</sub>O<sub>3</sub> [ $\Delta E_c = 2.0 \sim 2.5$  eV],<sup>5)</sup> meaning that LaF<sub>3</sub> has the potential to provide a lower leakage current and higher breakdown voltage than oxide-based gate insulators. Although an issue remains concerning the low resistivity of LaF<sub>3</sub> for high-power compact electronic device applications, it is a candidate high-k material for a nitride semiconductor-based MIS structure.

We also demonstrated the MIS operation of CeF<sub>3</sub>/Ge MIS structure, and showed the potential of fluorides for the electronics application.

## References

- 1) H. Morkoç, S. Strite, G.B. Gao, M.E. Lin, B. Sverdlov, M. Burns, *J. Appl. Phys.* **76**, 1363 (1994).
- 2) T. Kachi, *Jpn. J. Appl. Phys.* **53**, 100210 (2014).
- 3) H.D. Wiemhöfer, S. Harke, U. Vohrer, *Solid State Ion.* **40/41**, 433 (1990).
- 4) J.C. Krupa, M. Queffelec, *J. Alloy. Comp.* **250**, 287 (1997).
- 5) Z. Yatabe, J.T. Asubar, T. Hashizume, *J. Phys. D: Appl. Phys.* **49**, 393001 (2016).

## Exotic and Functional Molecular Materials

## Group Leader

Takashi NAKANISHI

Kentaro Tashiro (Principal Researcher), Shinsuke Ishihara (Senior Researcher), Kazuhiko Nagura (Researcher)



## 1. Outline of Research

From this annual year, a new permanent researcher, Dr. Kazuhiko Nagura, has joined to the Frontier Molecules Group (FMG) from the ICYS-Sengen program. As the third year of FMG established, we are working on synthesis of unique and frontier molecules possessing advanced functions and uncommon phenomena towards applications in sensor, actuator as well as bio-medical usage. Our research contains original molecular design strategy, synthesis, self-assembly, molecular recognition and hybridization with inorganic or bio-nanomaterials. We are aiming at development of world-top-level functional molecular systems/materials with our original molecules.<sup>1-4)</sup> In this annual year, we have achieved rather sophisticated molecular systems than our last two years.

## 2. Research Activities

(1) Supercooling of functional alkyl- $\pi$  molecular liquids.

Metastable states of soft matters are extensively used in designing stimuli-responsive materials. However, the non-steady properties may obstruct consistent performance. An approach to eradicate the indistinguishable metastable supercooled state of functional molecular liquids (FMLs), which remains as a liquid for weeks or months before crystallizing, has been developed via rational molecular design.<sup>1)</sup> The phases (solid, kinetically stable liquid, and supercooled liquid) of a model FML, branched alkyl chain-substituted 9,10-diphenylanthracene (DPA), are found to be governed by subtle alterations of the molecular structure (alkyl-DPA ratio and bulkiness of the DPA unit). We thus outline molecular design principles to avoid supercooled FML formation. Moreover, we demonstrate a practical technique to rapidly discriminate supercooled FMLs by accelerating their crystallization in differential scanning calorimetry heating via pre-annealing or relatively slow scanning.

## (2) NMR chiral sensing using simple achiral molecules.

The use of chiral auxiliaries, which derivatize enantiomers to diastereomers, is an established technique for NMR spectroscopic analysis of chirality and enantiomeric excess (*ee*). In contrast, we reported that some small achiral molecules (e.g. benzylamine) exhibit *ee*-dependent splitting of <sup>1</sup>H NMR signals at room temperature based on acid/base interactions with chiral analytes, especially when either a chiral or prochiral acid contains a phenoxy group at the  $\alpha$ -position of the carboxylic acid.<sup>2)</sup> This finding inspires novel design of achiral molecules available for NMR chiral sensing.

## (3) Science of Molecular and Supramolecular Sequences.

A synthetic molecular sequence of Arg-Pt-Arg-Ru exhibited unique binding behavior to natural molecular sequences such as GSH and ct-DNA, indicating the huge potential of the "Science of Molecular Sequences" developed through the fusion of synthetic and natural

molecular sequences (Fig. 1). On the other hand, a supramolecular homo-sequence of a Pt complex switches its photochemical reactivity by varying the mode of metal-metal interaction, allowing the stabilization/activation of a monomer coupled with its supramolecular polymerization/de-polymerization.<sup>3)</sup>

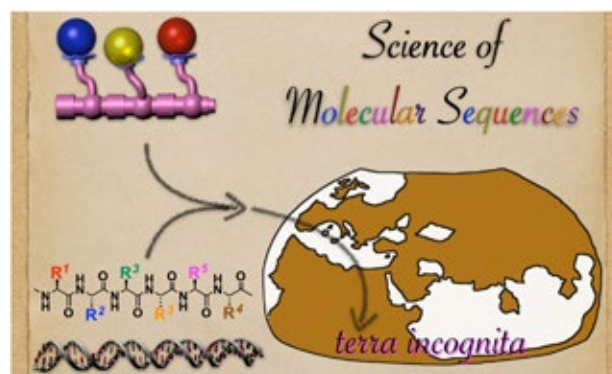


Fig. 1. Fusion of synthetic and natural molecular sequences that will lead researchers to a frontier as similar to the unexplored area in the Ptolemy's map (see <https://doi.org/10.1002/cbic.201800252>).

## (4) Control of Macromolecular Motion.

Precise control of molecular motion in the synthetic macromolecules has great potentials to create functional materials like proteins exhibiting sophisticated functions even under thermal fluctuation. However, their countless conformers with rotatable bonds make it challenging. We revealed that the bow-shaped macromolecule with rigid  $\pi$ -conjugated arc and flexible alkyl string shows thermally activated bow-like motion (Fig. 2). The thermal *anti*- to *gauche* conformational changes in alkyl string bend a  $\pi$ -conjugated arc moiety. Consequently, this system shows significant thermochromism in the solution state.<sup>4)</sup>

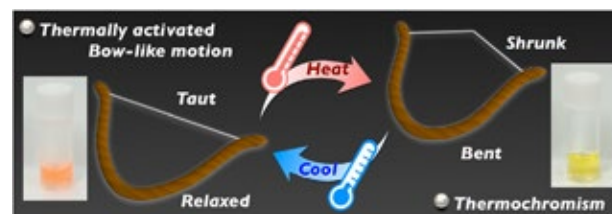


Fig. 2. Thermochromism of bow-shaped  $\pi$ -conjugated molecule.

## References

- 1) F.N. Lu, K. Jang, I. Osica, K. Hagiwara, M. Yoshizawa, M. Ishii, Y. Chino, K. Ohta, K. Ludwichowska, K.J. Kurzydowski, S. Ishihara, T. Nakanishi, *Chem. Sci.* **9**, 6774 (2018). Highlighted in *ChemSci Pick of the Week & Hot Article*.
- 2) S. Ishihara, J. Labuta, Z. Futera, S. Mori, H. Sato, K. Ariga, J. P. Hill, *J. Phys. Chem. B* **122**, 5114 (2018).
- 3) K. Tashiro, H. Ohtsu, M. Kawano, T. Kojima, T. Kato, *Inorg. Chem.* **57**, 13079 (2018).
- 4) K. Nagura *et al.*, *The 98<sup>th</sup> CSJ Annual Meeting*, 4F2-15.

## Nanoscale Multimaterials with Complex Anisotropies



Principal Investigator

Gero DECHER

(MANA Satellite at University of Strasbourg, CNRS, France)

## 1. Outline of Research

Our team has a longstanding research interest in the assembly of nanoorganized multimaterials. Whereas the number of components in most of the present nanocomposites is in the low single digit region, we have in the past developed the so-called Layer-by-Layer (LbL) assembly method<sup>1,2)</sup> which has the largest choice of deployable components (inorganic salts, organic molecules, polymers, DNA, nanoparticles or biological objects including cells) among all existing techniques for surface functionalization (Fig. 1). It allows to design and prepare nanoscale materials composed of hundreds of different components with adjustable multifunctionality, a task close to impossible for most other self-assembly methods. With more than three publications per day, LbL assembly has matured from a scientific oddity to a well respected tool for the preparation of nanoscale multimaterials.<sup>1)</sup> It has kindled research activities in hundreds of laboratories worldwide and it was a pleasure to see how the field has benefitted from the ideas of so many colleagues and how it developed in the almost 30 years of its existence.

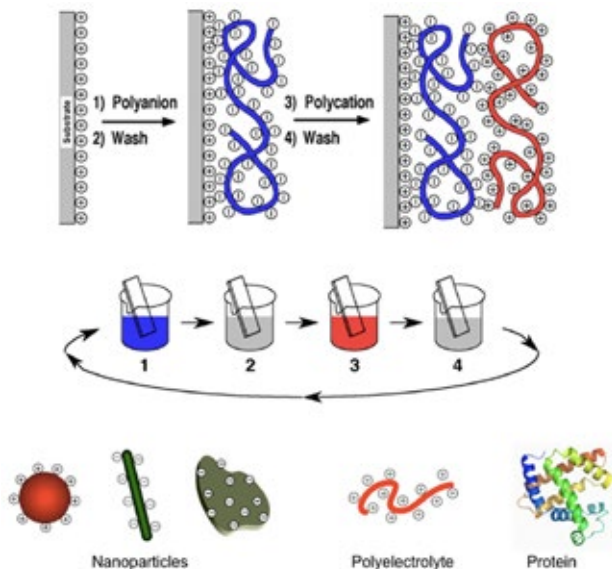


Fig. 1. Schematic depicting the LbL-assembly of multi-composite nanoscale films.

## 2. Research Activities

Most of the current materials are isotropic, materials with anisotropic properties are in general more difficult to prepare and more difficult to characterize. Our team has introduced grazing incidence spraying<sup>3,4)</sup> for aligning nano-wires, nano-rods and nano-fibers in-plane during the deposition of individual layers when building up LbL-assemblies (Fig. 2). With unidirectionally oriented multilayers one can for example fabricate multilayer films containing ultrathin polarizers.<sup>4)</sup> Grazing incidence spraying is, however, capable of producing more complex anisotropies even over large surface areas by changing the direction of alignment in each individual layer of a multilayer film.

The newly started partnership between MANA and the university of Strasbourg will allow us to continue to explore the assembly and properties of multifunctional multimaterial films and to compare nanocomposites with isotropic and anisotropic superstructures.

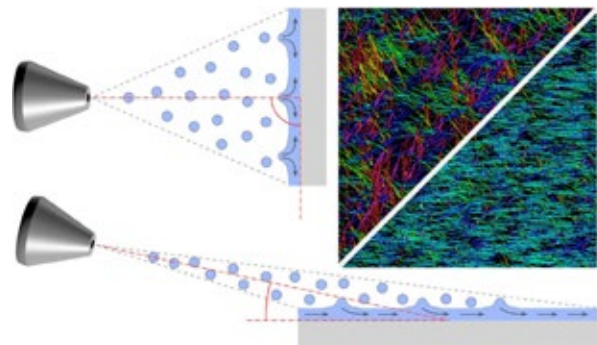


Fig. 2. Schematic depicting classic spray assisted LbL assembly which leads to isotropic films (top left) and grazing incidence spraying which produces films with in-plane anisotropy over large surface areas (bottom right).

## References

- 1) See for example: Layer-by-Layer Assembly of Multifunctional Hybrid Materials and Nanoscale Devices, Seyrek E and Decher G (2012). In: Polymer Science: A Comprehensive Reference, Vol 7, (2012) pp. 159–185, Matyjaszewski K. and Möller M. (eds.), Amsterdam: Elsevier BV.
- 2) G. Decher, *Science* **277**(5330), 1232 (1997).
- 3) R. Blell, X.F. Lin, T. Lindström, M. Ankerfors, M. Pauly, O. Felix, G. Decher, *ACS Nano* **11**, 84 (2016).
- 4) H. Hu, M. Pauly, O. Felix, G. Decher, *Nanoscale* **9**, 1307 (2016).

# Acoustic Propulsion of Autonomous Micromotors

**Principal Investigator**

**Thomas E. MALLOUK**

(MANA Satellite at Pennsylvania State University, USA)



## 1. Outline of Research

Engines and motors are everywhere in the modern world, but it is a challenge to make them work if they are very small. On the micron length scale, inertial forces are weak and conventional motor designs involving, e.g., pistons or flywheels cease to function. Biological motors work by a different principle and use catalysis to convert chemical to mechanical energy on the nanometer length scale. Together with Ayusman Sen and other colleagues at Penn State we have explored the concept of using catalysis to power synthetic nano- and micromotors. Bi- and trimetallic microwires are catalytically self-propelled in fuel-containing solutions at speeds that are comparable to those of flagellar bacteria. Detailed studies of the mechanism of chemically-driven motion on the micron length scale show that the propulsion of bimetallic motors derives from locally generated electric fields. The same principle can be used pump fluids using inorganic or enzymatic catalysts. Despite the difference in propulsion mechanisms, catalytic motors are subject to the same external forces as natural micromotors such as bacteria. Therefore they follow the same scaling laws and exhibit similar emergent behavior (e.g., magnetotaxis, chemotaxis, schooling, and predator-prey behavior). Interestingly, we find that a broad range of molecular catalysts (such as enzymes and polymerization catalysts) also move, transfer momentum to their surroundings, and are subject to chemotactic forces while carrying out their catalytic reactions.

In collaboration with Mauricio Hoyos at ESPCI (Paris) we have found that asymmetric nanoparticles also undergo autonomous motion and a range of interesting collective behaviors in fluids when they are excited by low power ultrasound. The acoustic propulsion mechanism, particularly when combined with magnetic, chemical, or photochemical propulsion for steering and assembly, is potentially useful for diagnostic and biomedical applications because it is salt-tolerant and does not involve toxic chemical fuels.<sup>1,2)</sup>

## 2. Research Activities

Rocket-shaped bimetallic micro-rods were made by electrodeposition of the appropriate metals in the pores of anodic aluminum oxide (AAO) membranes. In a MHz acoustic field these microrods undergo fast autonomous motion with the lighter end leading. Hydrogen peroxide, when added to the fluid, is decomposed by a bipolar electrochemical mechanism that creates local positive charge around the end of the rod (the anode) that preferentially oxidizes  $H_2O_2$  to  $O_2$ . This results in a catalytically generated electrostatic force that tilts the anode

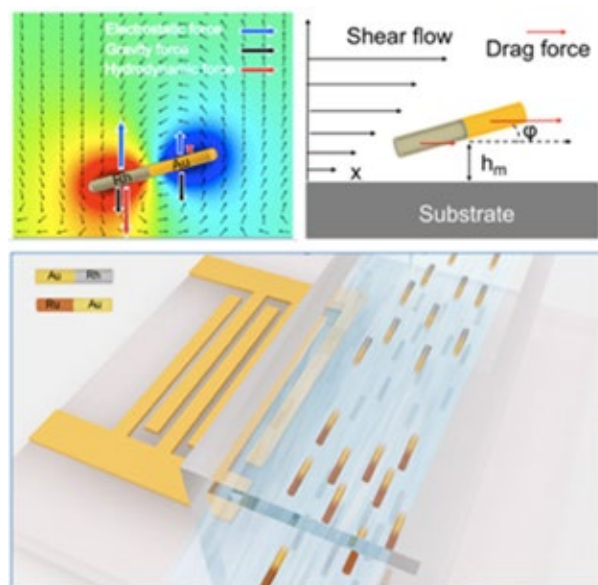


**Fig. 1. Combining chemical steering with acoustic propulsion.** Top left: Catalytically induced tilting of a bimetallic rod above a negatively charged surface in  $H_2O_2$  solution. Red and blue represent positive and negative potential. Top right: in a shear flow, the rod is oriented with its anode end facing into the flow. Bottom: Surface acoustic wave device propels the microrods upstream or downstream in a microfluidic device.

end of the micro-rod towards the floor of the chamber. When this experiment is done with a flowing liquid in a microfluidic channel, the resulting differential shear on the rod points the anode end upstream. Different bimetallic combinations (e.g., Rh-Au and Ru-Au) place the anode at the lighter or heavier end of the rod, resulting in strong rheotaxis (directional motion in a flow) in the upstream or downstream direction (Fig. 1).

Acoustic propulsion of bimetallic rods results from a local streaming effect and so far has required that the rods be situated at a pressure node of an acoustofluidic cell. This limits the distance between the micro-rods and the ultrasonic transducer to a few acoustic wavelengths, i.e., to sub-millimeter distances. An alternative motor geometry that does not require a resonant involves cup-shaped motors that contain a trapped air bubble. Preliminary experiments show that bubbles in the micron size range resonate at MHz frequency and enable fast propulsion of micromotors in three dimensions in fluids.

## References

- 1) L. Ren, D. Zhou, Z. Mao, P. Xu, T. J. Huang, T.E. Mallouk, *ACS Nano* **11**, 10591 (2017).
- 2) L. Ren, W. Wang, T.E. Mallouk, *Acc. Chem. Res.* **51**, 1948 (2018).



## Ultrathin Piezotronic Transistors with 2 nm Channel Lengths

**Principal Investigator**  
(MANA Satellite at Georgia Tech, USA)

**Zhong Lin WANG**

### 1. Outline of Research

A rapid development of high-performance and miniaturized electronic devices in nano-electromechanical systems (NEMS) calls for synthesis and discovery of low-dimensional piezoelectric materials. Many transition metal dichalcogenides (TMDs) are proposed theoretically as outstanding two-dimensional (2D) in-plane piezoelectric materials. Monolayer MoS<sub>2</sub>-based powering nanodevices and piezoelectric sensors have demonstrated possible applications of 2D nanomaterials in nanoscale electromechanical devices. We used the piezoelectric polarization charges presented on the surfaces within one to two atomic layer thickness, ultrathin piezotronic transistors were demonstrated with a physical channel length of ~2 nm.<sup>1)</sup> The stress-induced strong out-of-plane piezopotential can effectively modulate charge carrier transport. This study shows the effectiveness of the “gating” effect of the piezopotential within an ultrashort channel length in the 2D ZnO structures, with potential applications for energy harvesting, ultrasensitive sensors, and nanoscale electromechanical systems.

### 2. Research Activities

The single-crystalline ZnO ultrathin films were prepared at the water–air interface. In the synthesis process, oleylsulfate monolayer was used as a template to guide the growth of ZnO nanostructures, resulting in ZnO ultrathin films at the water–air interface with the c-axis perpendicular to the liquid level pointing to air. A typical morphology of the as obtained ZnO ultrathin films is a single triangular with edges from ~10 to 40 μm and a thickness of ~2 nm (Fig. 1a). Transmission electron microscopy (TEM) and high-resolution TEM (HRTEM) images reveal the single crystal structure of the ultrathin film in Fig. 1b. The electronic property of ZnO ultrathin film was investigated by fabricating field-effect transistors (FETs). The  $I_d-V_g$  curve presents a typical p-type semiconductor behavior (Fig. 1c).

We used piezoresponse force microscopy (PFM) to investigate the out-of-plane piezoelectricity of ZnO ultrathin film. Conductive PFM was applied to characterize the vertical piezoresponse of ZnO ultrathin film with the tip's voltages from 1.5 to 6.5 V. The amplitude images and corresponding topography and phase images under different tip voltages are presented in Figs. 1d–i. As expected, obvious amplitude changes were found as the tip voltage increased continuously, indicating a strong inverse piezoelectric effect. The insets are statistical distributions of amplitude values of the ZnO and the substrate. By deriving the slope of the amplitudes versus the voltages, the effective

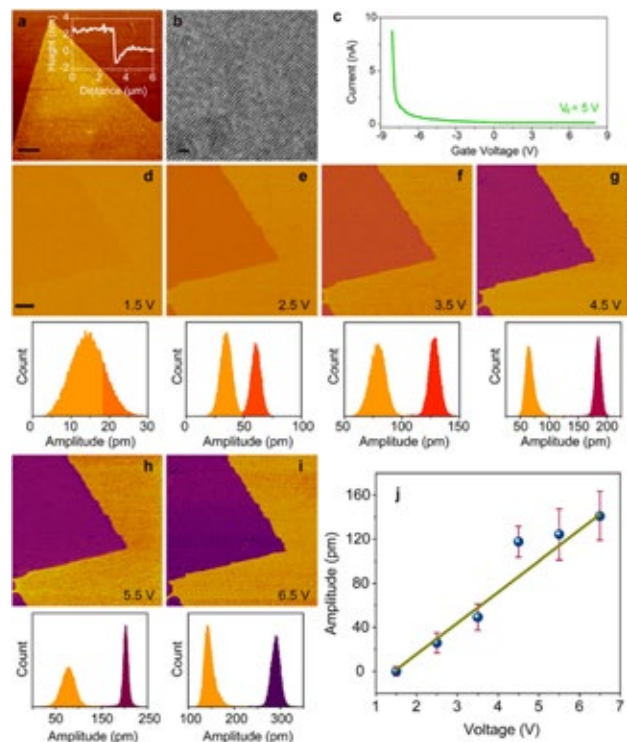


**Fig. 1. Materials characterization.** (a) Atomic force microscopy topography scans of typical ultrathin film. Scale bar, 3 μm. (b) HRTEM image of the ZnO ultrathin film. Scale bar, 1 nm. (c) Electronic property of ZnO ultrathin film demonstrates that the ZnO ultrathin film is p-type. (d–i) Amplitudes versus applied voltages (1.5–6.5 V) showing inverse piezoelectricity. The insets are statistical distribution of amplitude values of ZnO ultrathin film and substrate. Scale bars, 500 nm. (j) Average amplitude variations versus applied voltages derived from the statistical distributions of amplitude values of ZnO ultrathin film and substrate (d–i). Error bars indicate standard deviations. The piezoelectric coefficient ( $d_{eff}$ ) is evaluated to be ~23.7 pm·V<sup>-1</sup>.

piezoelectric coefficient ( $d_{eff}$ ) of ZnO ultrathin film is calculated to be ~23.7 pm·V<sup>-1</sup> (Fig. 1j). It is about two times larger than that of the bulk ZnO materials and even larger than that of some inorganic ferroelectric ceramics. The strong out-of-plane piezoelectricity of ZnO ultrathin film makes it an ideal candidate for ultrathin piezoelectric devices.

The atomic thickness of ZnO and the structure of a two-terminal piezotronic transistor enable the study of their physics at ultrashort channel by using the strong out-of-plane piezoelectricity, removing the need for an external gate electrode or any other patterning processes that are challenging at these scale lengths.

### Reference

- 1) L.F. Wang, S.H. Liu, G.Y. Gao, Y.K. Pang, X. Yin, X.L. Feng, L.P. Zhu, Y. Bai, L.B. Chen, T.X. Xiao, X.D. Wang, Y. Qin, Z.L. Wang, *ACS Nano* **12**, 4903 (2018).

## Multi-Responsive Porphyrin/Polymer Systems for Sensing Applications

Independent Scientist

Jan LABUTA



## 1. Outline of Research

Porphyrins are widely studied functional dyes that can coordinate a great variety of metal cations. In biological systems, porphyrins play essential roles as photosynthetic antenna and reaction center. In our previous research we use porphyrin derivatives for various sensing applications such as enantiopurity sensing,<sup>1-5)</sup> pH measurement<sup>6)</sup> or determination of trace water impurities in organic solvents.<sup>7,8)</sup> Most of these sensing features are realized by non-covalent interactions (H-bond, electrostatic,  $\pi$ - $\pi$ , etc.) between porphyrin and substrate (analyte). The sensing is unfortunately permitted only in organic solvents (CHCl<sub>3</sub>, THF, DMSO, etc.). Therefore, we have introduced water soluble moieties such as tetraethylene glycol (TEG) or poly(*N*-isopropylacrylamide) (PNIPAAm) at the periphery of porphyrin (TPP) functional unit (Fig. 1). These porphyrin/polymer systems exhibit response to whole range of stimuli (temperature, pH, solvent composition, etc.) and are potential candidates for various sensing applications.



Fig. 1. Structures of two examples of water soluble porphyrins.

## 2. Research Activities

## (1) Phase behavior.

The results show that upon heating above ca. 50 °C (TEG-TPP in H<sub>2</sub>O) the system undergoes reversible phase separation (Fig. 2a). This phenomenon is also known as lower critical solution temperature (LCST) behavior or cloud point transition (CPT). These porphyrins also exhibit reversible protonation depending on pH of solvent (Fig. 2b) which is accompanied by color change from purple-red to green and change in geometry of macrocyclic core from flat to saddle-like shape. Another interesting property is co-solvency (Fig. 2c). This is manifested as a phase separation dependent on composition of binary solvent (H<sub>2</sub>O/DMSO) mixture at constant temperature (i.e. the porphyrin derivatives are soluble in neat H<sub>2</sub>O or DMSO but insoluble in 50:50 H<sub>2</sub>O:DMSO mixture).

## (2) Sensing and potential applications.

There are only a few examples reported of phase-separable small molecules with well-defined structure and functionality.<sup>9)</sup> Our porphyrin derivatives combine rich field of porphyrin sensing properties with another large area of phase behavior (LCST) which is usually considered the

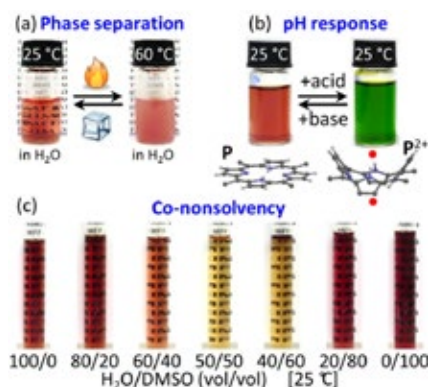


Fig. 2. (a) Temperature response of TEG-TPP/water system. (b) Reversible pH response accompanied with color and geometry change of porphyrin core. (c) Solvent composition response.

domain of polymers.<sup>10)</sup> Numerous applications of polymers are under current investigation in areas such as controlled drug release and delivery, bio-separation and others. The extension of the LCST phenomenon from polymeric to the non-polymeric supramolecular field will lead to the development of novel ‘smart’ materials for specific sensing, detection, separation and imaging purposes in aqueous media. For example, *in situ* monitoring of variation of enantiomeric excess (*ee*) in enantioenrichment reactions (Soai-type reactions), racemization reactions or conversion of pharmaceuticals during biological processes (Fig. 3). Also the possibility of pH variation or physical filtration based on LCST phenomenon may find interesting applications. In addition, these compounds can be potentially used in photodynamic therapy (PDT) or for heterogeneous catalysis when metal cation is introduced to porphyrin center.

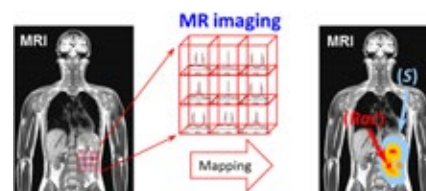


Fig. 3. Schematic visualization of *in vivo* enantiomeric excess (*ee*) mapping of chiral metabolites using MRI.

## References

- 1) S. Ishihara et al., *J. Phys. Chem. B* **122**, 5114 (2018).
- 2) J. Labuta et al., *Japanese Granted Patent*, No. **6128553** (2017).
- 3) J. Labuta et al., *Acc. Chem. Res.* **48**, 521 (2015).
- 4) J. Labuta et al., *J. Am. Chem. Soc.* **136**, 2112 (2014).
- 5) J. Labuta et al., *Nat. Commun.* **4**, 2188 (2013).
- 6) V. Brezina et al., *ChemistryOpen* **7**, 323 (2018).
- 7) S. Ishihara et al., *Chem. Commun.* **48**, 3933 (2012).
- 8) S. Ishihara et al., *Phys. Chem. Chem. Phys.* **16**, 9713 (2014).
- 9) G.J. Richards et al., *J. Phys. Chem. Lett.* **1**, 1336 (2010).
- 10) J. Spěváček et al., *Macromolecules* **44**, 2149 (2011).



## Semiconductor Nano-Interface Engineering for Power Device Application

Independent Scientist

Liwen SANG

### 1. Outline of Research

For the power electronic devices such as field effect transistors (FETs), the quality of metal-insulator-semiconductor (MIS) interface is crucial for the device reliability during high-voltage operations. However, for the wide-bandgap semiconductors, including GaN, SiC, or diamond electronic devices, the MIS interface is far from ideality due to the immature process and large surface states. The high-density traps and interfaces states exist and lead to threshold voltage instability and poor reliability at high temperatures.

Among the wide-bandgap semiconductors, III-V nitrides have much higher breakdown voltages, larger saturation velocity, higher carrier mobility and higher thermal stability compared to the conventional Si or GaAs, which enabled them promising for the high-power and high frequency electronic devices.<sup>1)</sup> Therefore, the investigation and engineering for the GaN-based interface becomes more and more important.

Following our research activity last year, our effort is still concentrated on the MIS interface modulation for the GaN and *p*-GaN materials in this year. We obtained nearly ideal n-GaN MOS structure without any trap charges grown on the GaN substrate by the effective surface pre and post treatments. For the *p*-GaN MOS structure, different gate dielectric layers were proposed, and it was found that, oxygen-free insulator, such as SiN<sub>x</sub>, CaF<sub>2</sub> are better to achieve a high reliability. we proposed a novel CaF<sub>2</sub> dielectric layer for the MIS capacitors, and successfully suppress the hysteresis in the capacitance- voltage (C-V) performance.

### 2. Research Activities

(1) *Nearly ideal MOS interface for GaN grown on GaN substrate.*<sup>1)</sup>

Although the rapid progress has been achieved in the vertical-type MIS or MOS field effect transistors (FETs), the quality of the MOS interface strongly affects the electrical properties of the devices. The threshold voltage is much lower and the on-resistance is still higher than the expected values due to the insufficient control of the GaN surface potential. To ultimately improve the performance of GaN-on-GaN vertical MOSFETs and realize real applications, a high-quality and stable MIS/MOS interface with low-density trap states not only at the interface but also close to the interface is required. We proposed a two-step surface treatment including surface cleaning and modification to reduce the trap states of the Al<sub>2</sub>O<sub>3</sub>/GaN MOS interface using epitaxial n-GaN layers grown on the free-standing GaN substrate. The two-step treatments inhibit the formation of disordered regions at the MOS interface,

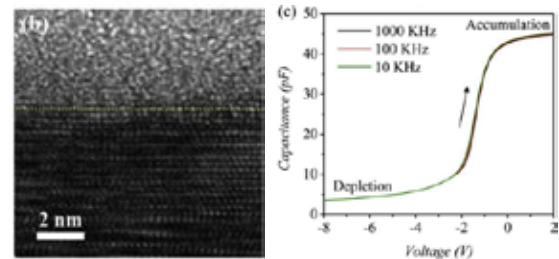


Fig. 1. (a) High-resolution TEM images for ALD-Al<sub>2</sub>O<sub>3</sub>/GaN interface. (b) Capacitance-voltage without frequency dispersion.

leading to an ultra-low interface state density in the range of  $10^{11} \text{ cm}^{-2}\text{eV}^{-1}$ . The oxide-trapped charges located at the transition layer between Al<sub>2</sub>O<sub>3</sub> and GaN are also suppressed. The MOS interface microstructure and electrical property can be seen in Fig. 1.

(2) *Approaching ideal p-GaN MIS interface on GaN substrate.*

We have successfully achieved the first *p*-channel MOSFETs which can be operated from cryogenic temperature to room temperature. It was found that, the quality of the dielectric/*p*-GaN interface is crucial to improve the stability of *p*-channel MOSFETs. Nevertheless, as a result of the Mg accumulation to the surface of *p*-GaN, the typically used ALD-Al<sub>2</sub>O<sub>3</sub>/*p*-GaN MOS capacitor displayed a serious electrical hysteresis in both the current-voltage and capacitance-voltage properties. The electrical hysteresis could lead to the threshold voltage instability, which is detrimental to MOSFETs.

Here, we deposit high-quality *p*-GaN on GaN substrate. To ultimately suppress the oxidized trap states, we propose the oxygen-free dielectric layer for the *p*-GaN FETs. A better interface quality with little electrical hysteresis and lowest interface traps were finally obtained, as shown in Fig. 2.

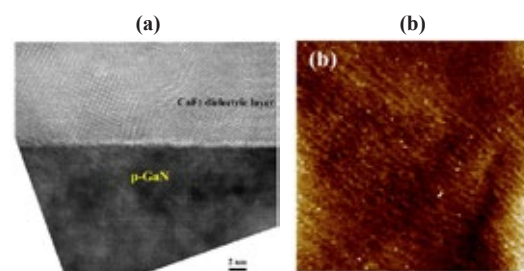


Fig. 2. *p*-GaN MIS interface by (a) TEM and (b) surface morphology by AFM.

### Reference

- 1) B. Ren, M. Sumiya, M. Liao, Y. Koide, X. Liu, Y. Shen, L. Sang, *J. Alloys Compd.* **67**, 600 (2018).

## Molecular Expansion of Layered Perovskites for Exotic Properties

Independent Scientist

Daiki UMEYAMA



## 1. Outline of Research

Means of controlling semiconductor bandgaps are of great importance in materials design. In particular, fabrication of layered heterostructures with controlled thickness and composition can be used to modulate the composites' electronic structures.<sup>1)</sup> In my recent research, I have focused on lead-iodide hybrid perovskites, and investigated the optical properties of a self-assembled layered perovskite functionalized with thiocyanate ions.<sup>2)</sup>

## 2. Research Activities

The three dimensional (3D) structure of lead-iodide hybrid perovskite  $(\text{CH}_3\text{NH}_3)[\text{PbI}_3]$  can be "sliced" with thiocyanate ions (SCN). By partially substituting the iodide ions with SCN ions, a two dimensional (2D) layered hybrid perovskite  $(\text{CH}_3\text{NH}_3)_2[\text{PbI}_2(\text{SCN})_2]$  (sample **1**) is obtained<sup>3)</sup> (Fig. 1). I characterized the effect of the substitution in terms of optical and mechanical properties to rationalize structure-properties relationships.

The ligand substitution to SCN ions reduces the dimensionality of the structure and enhances the effect of quantum confinement. This is clearly represented by the presence of exciton peak in the optical absorption spectrum of **1** even at room temperature. On the basis of the absorption spectrum at 6 K, I determined the exciton binding energy as 200 meV (Fig. 1). The binding energy is higher than that of the 3D perovskite  $(\text{CH}_3\text{NH}_3)[\text{PbI}_3]$  (~30 meV) owing to quantum confinement in **1**; however, it is smaller than that of conventional 2D perovskite such as  $(\text{C}_6\text{H}_{13}\text{NH}_3)_2[\text{PbI}_4]$  (~360 meV).<sup>4)</sup> This is most likely because the polarizable  $\pi$  electrons on SCN ions reduce dielectric confinement in **1**.<sup>5)</sup>

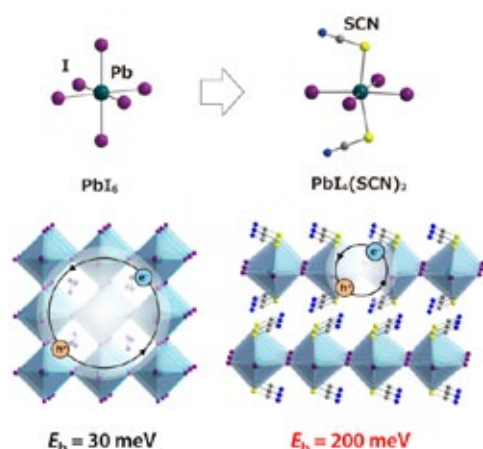


Fig. 1. Site-selective ligand substitution results in dimensional reduction of the lead-iodide perovskite. The 2D perovskite exhibits intermediate exciton binding energy ( $E_b$ ) owing to the competing effect between quantum and dielectric confinements.

The competing effect of quantum and dielectric confinements gives moderate exciton binding energy in **1**.

Another effect of the ligand substitution is observed in mechanical properties. When compressed in a diamond-anvil cell (DAC), **1** exhibits remarkable darkening of the crystal color at 2 GPa, suggestive of the bandgap reduction (Fig. 2a). In situ X-ray diffraction study indicates that the interlayer distance rapidly decreases upon compression, which is reasonable because compressible void space has been created between the layers due to the SCN substitution (Fig. 2b). Therefore, the striking piezochromism from red to black (corresponding the bandgap change from 2.3 to 2.0 eV) under relatively modest pressure is a direct effect of the ligand substitution.

In this work, I for the first time reported an accurate values of the bandgap and exciton binding energies of **1**, as well as its unique piezochromism. The fact that the bandgap closure occurs under mild pressure suggests potential utility of chemical pressures for this material. For a film on a substrate, there is a strain due to the mismatch in lattice parameters which can work as a source chemical pressure. Since bandgap tuning is demonstrated by film epitaxy, such highly compressible materials as **1** are of interest in term is bandgap engineering via epitaxy.

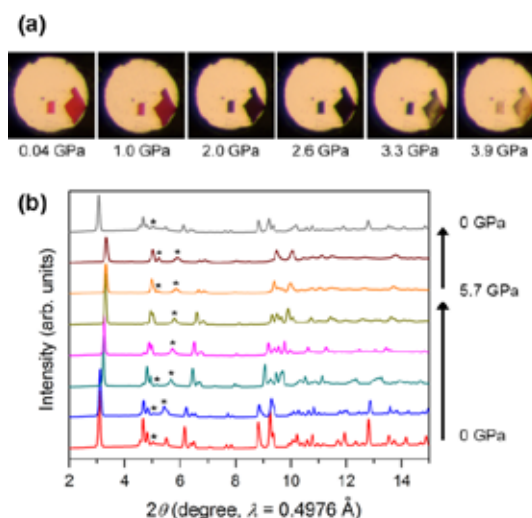


Fig. 2. (a) The crystals of **1** exhibit darkening upon compression in a DAC. (b) In situ X-ray diffraction study indicates that the interlayer distance rapidly decreases upon compression.

## References

- 1) L. Esaki, *IEEE J. Quantum Electron.* **22**, 1611 (1986).
- 2) D. Umeyama, Y. Lin, H.I. Karunadasa, *Chem. Mater.* **28**, 3241 (2016).
- 3) M. Daub, H. Hillebrecht, *Angew. Chem., Int. Ed.* **54**, 11016 (2015).
- 4) T. Kondo, K. Tanaka, *Sci. Technol. Adv. Mater.* **4**, 599 (2003).
- 5) T. Ishihara, *J. Lumin.* **60-61**, 269 (1994).



# Nano-Systems

**Kazuya Terabe**  
Field Coordinator

- 11 Research Groups**
- Nanoionic Devices Group
  - Nano Functionality Integration Group
  - Quantum Device Engineering Group
  - Nano-System Theoretical Physics Group
  - Photonics Nano-Engineering Group
  - Nano Frontier Superconducting Materials Group
  - Thin Film Electronics Group
  - Medical Soft Matter Group
  - Mechanobiology Group
  - Surface Quantum Phase Materials Group
  - Nanomechanical Sensing Group

**New nano-systems are changing the world:  
from artificial intelligence to energy and  
the environment, diagnosis and medicine**

This research field is searching for various nano-systems that will express novel functions by the interaction of nanostructures with unique characteristics, and is engaged in research to research to utilize those new nano-systems systematically. Concretely, based on basic research on nanoscale materials, such as atomic and molecular transport and chemical reaction processes, polarization and excitation of charge and spin and superconducting phenomena, we are conducting research on atomic switches, artificial synapses, molecular devices, new quantum bits, neural network-type network circuits, next-generation devices, high sensitivity integrated molecular sensors and other new applied technologies. Since the development of new nanoscale measurement methods is also a high priority, we are developing multi-probe scanning probe microscopes and other cutting-edge instruments. We also attach great importance to interdisciplinary fusion-type research with other research fields.

## Creation of Decision-Making Ionics Devices

**Principal Investigator**

(Field Coordinator, Group Leader)

**Kazuya TERABE**

**Yuji Okawa** (Chief Researcher), **Makoto Sakurai** (Principal Researcher),  
**Tohru Tsuruoka** (Principal Researcher), **Takashi Tsuchiya** (Senior Researcher)

**1. Outline of Research**

The importance of quickly recognizing and judging diversifying situations and acting appropriately is increasing in nowadays information society. Development of advanced artificial intelligence (AI) that makes it possible is attracting attention all over the world. Our group aims to build the basic technology of the new concept AI based on ionics technology.

We have succeeded to create a decision-making ionic device that can learn, memorize and make judgments properly.<sup>1)</sup> The decision-making device operates utilizing electrochemical phenomena caused by migration of hydrogen ions in the solid electrolyte. As an example, we addressed the multi-armed bandit problem in wireless communication. The decision-making device demonstrated the optimal choice to maximize communication traffic volume by adapting to changing situation of congested communication network. Creation of the decision-making ionics devices is expected to lead to the development of a new concept AI system operating with analog information processing, which is completely different from the conventional AI system operating with digital information processing using electronics devices and software.

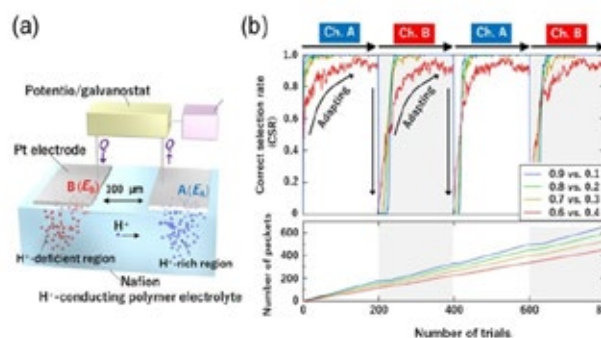
**2. Research Activities**

Fig. 1(a) shows a basic structure of the decision-making ionics device, where a platinum electrode is attached to a solid electrolyte called Nafion capable of transporting hydrogen ions. This device is connected to an electrical measuring unit that applies current and measures voltage and a computer for the measurement control and data processing. When pulsed current (2 Hz) is applied between two platinum (Pt) electrodes of the ionic device, electrochemical phenomena (charge of the electric double layer, oxidation-reduction reaction, etc.) accompanying movement of hydrogen ions in Nafion occurs at the electrode interface, which is caused concentration change of ions and molecules (hydrogen, oxygen, water etc.). As a result, the potential difference (voltage) between two Pt electrodes is generated by the action of the capacitor and the concentration cell when the circuit is opened. By utilizing these electrochemical phenomena occurring in the solid electrolyte, the ionics devices have a function to learn quickly and make an appropriate judgment.

Fig. 1(b) shows the experimental results of solving the multi-armed bandit problem using the decision-making device. The experiment was conducted under the various conditions of channel A and channel B with different

probability ( $P$ ) of successful communication. For example, in the case indicated by the blue line, the probabilities for the two channels A and B were assigned to  $P_A=0.9$  and  $P_B=0.1$ , respectively. Initially, the decision-making device did not learn any information about channels A and B and chooses A and B at random, so the correct selection rate (CSR) showed a value of about 0.5. Thereafter, as the number of learning was increased by repeating the selection trial, the CSR value gradually approached 1.0 of the complete correct answer. This result shows that the channel A with a high probability of success ( $P_A=0.9$ ) is judged correctly as the optimal choice by increasing the number of trials and learning many experiences of success and failure. After that, since the channel A continued to be selected, the amount of data (number of packets in lower part of Fig. 1(b)) transmitted increased steadily.

Suddenly the CSR value plummeted to 0 suddenly when the number of trials (learning) was 200 times. This is because the probability  $P$  assigned to channels A and B was intentionally reversed to  $P_A=0.1$  and  $P_B=0.9$  in order to simulate the congestion situation change of wireless communication. Thereafter, increasing the number of trials, it was quickly judged that channel B was the correct choice. The correct answer rate recovered rapidly to 1.0 which is the perfect correct answer rate. Even if inversion of these channel probabilities was repeated, quick adaptation could be repeated. Furthermore, similar adaptive behaviors were obtained when  $P_A$  and  $P_B$  were combined with other probabilities, as shown in upper part of Fig. 1(b).



**Fig. 1(a):** Decision-making ionics device achieved by using electrochemical phenomenon due to hydrogen ion migration. **(b):** Upper part: Relationship between the correct selection rate and number of trials. Lower part: Relationship between number of transmitted packets and number of trials.

**Reference**

- 1) T. Tsuchiya, T. Tsuruoka, S.J. Kim, K. Terabe, M. Aono, *Sci. Adv.* **4**, eaau2057 (2018).



## Integration of Nano Functionality

### Principal Investigator

(MANA Deputy Director, Administrative Director, Group Leader)

### Tomonobu NAKAYAMA

**Shigeki Kawai** (Principal Researcher), **Yoshitaka Shingaya** (Senior Researcher),  
**Takeo Minari** (Principal Researcher)

A. Diaz Alvarez (Postdoc), K. Sun (Postdoc), Q. Li (Graduate Student),  
K. Sasaya (Undergraduate Student), Y. Kato (Technical Assistant), K. Tanaka (Technical Assistant)

## 1. Outline of Research

We develop novel techniques and methodologies, based on scanning probe microscopy and related techniques. We aim to create nanomaterials and nanosystems that are realized by integration of appropriate nano parts. Multiple-probe scanning probe microscopes (MP-SPMs) are used to investigate electrical properties of nanomaterials and nanosystems. Nanocarbon integration is studied with high-resolution atomic force microscopy (AFM). A study on emergent dynamics of networks of unreliable elements has started.

## 2. Research Activities

### (1) Multiple-probe Scanning Probe Microscopes.<sup>1,2)</sup>

MP-SPM can simultaneously and independently control 2 to 4 scanning probes that are brought into electrical contact to a single nanostructure.<sup>1)</sup> This allows to study electrical properties of nanostructures.<sup>2)</sup> Our latest MP-SPM is operated using a home-built control system and software. As a result, complicated cooperative motions of four probes become possible. Kelvin-probe force microscopy (KPFM) measurement under current flow between two designated positions is one example of a complicated measurement. Cooperative control of probes is indispensable for the measurement. MP-AFM/KPFM measurements were conducted on a polyaniline (PANI) nanofiber network. Fig. 1 shows an AFM image of PANI nanofiber dispersed on SiO<sub>2</sub> substrate. Current flow was conducted with two probes at points A and B. Potential mapping under current flow was carried out with the third probe at area C using KPFM mode. The image on the right side shows the potential distribution during current flow. The current pathway can be deduced from the image. A change in the potential distribution has been observed after cutting a single nanofiber. Such information is important for network system where the current pathway can't be predicted simply from the structure.

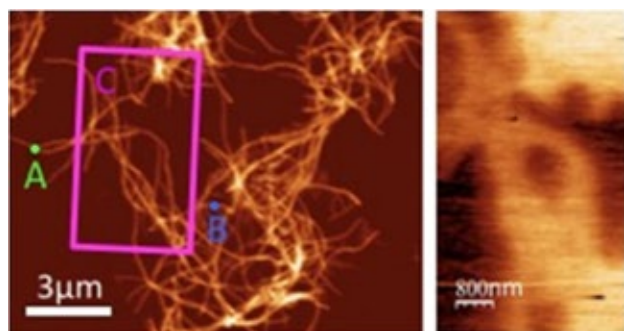


Fig. 1. AFM image of polyaniline nanofiber network and potential image under current flow with KPFM mode.

### (2) Nanocarbon integration.<sup>3-5)</sup>

In order to realize functionalized nano-carbon devices in a bottom-up manner, on-surface chemical reaction is of central importance. With a designed precursor molecule, multiple hetero-atom substituted graphene nanoribbon has successfully been synthesized by the Ullmann-type reaction.<sup>3)</sup> Furthermore, we demonstrated that high-resolution AFM with a CO terminated tip can discriminate boron, carbon and nitrogen atoms via the measured forces as well as the observed bond lengths (Fig. 2). To increase the variety of structures, exploring new reactions is mandatory. To this end, we have realized one-shot homo-coupling of trimethylsilyl.<sup>4)</sup> By annealing anthracene derivatives with trimethylsilyl groups on Cu(111) at 400K, the diacetylene linked anthracene oligomers were synthesized. This reaction is contamination free since the by-product trimethylsilane is highly volatile and doesn't remain on the surface. Besides on-surface syntheses, we also developed a technique to measure intermolecular forces directly. Setting the CO tip to the outermost hydrogen atom of three-dimensional hydrocarbon, a weak hydrogen bonding was quantitatively measured.<sup>5)</sup> This interaction is responsible for observation of hydrogen atom of the single molecule. To push forward the research of on-surface chemical reaction, a new low-temperature SPM system has been set up.

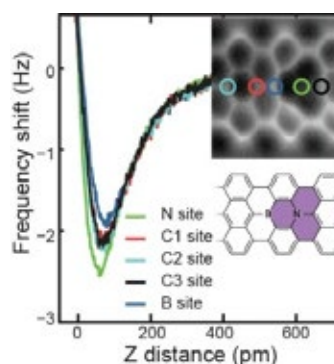


Fig. 2. Synthesis of multiple heteroatom substituted graphene nanoribbon and its analysis with high-resolution AFM.

## References

- 1) T. Nakayama, O. Kubo, Y. Shingaya, S. Higuchi, T. Hasegawa, C.S. Jiang, T. Okuda, Y. Kuwahara, K. Takami, M. Aono, *Adv. Mater.* **24**, 1675 (2012).
- 2) R. Higuchi, Y. Shingaya, T. Nakayama, *Jpn. J. Appl. Phys.* **55**, 08NB09 (2016).
- 3) S. Kawai, O. Krejčí, A.S. Foster, R. Pawlak, F. Xu, L. Peng, A. Orita, E. Meyer, *ACS Nano* **12**, 8791 (2018).
- 4) S. Kawai, S. Nakatsuka, T. Hatakeyama, R. Pawlak, T. Meier, J. Tracey, E. Meyer, A.S. Foster, *Sci. Adv.* **4**, eaar7181 (2018).
- 5) S. Kawai, T. Nishiuchi, T. Kodama, P. Spijker, R. Pawlak, T. Meier, J. Tracey, T. Kubo, E. Meyer, A.S. Foster, *Sci. Adv.* **3**, e1603258 (2017).

## Multi-Level Logic Circuits with Organic FET

## Group Leader

(MANA Deputy Director)

Yutaka WAKAYAMA

Shu Nakaharai (Principal Researcher), Ryoma Hayakawa (Senior Researcher), Satoshi Moriyama (Senior Researcher)



## 1. Outline of Research

Recently, wearable electronic devices have been developed for future flexible IoT devices, where organic electronics play key roles. However, the functions of these devices are still limited to simple data handling, e.g., for health condition monitoring. For further improvement, new device architectures for organic electronics are highly needed, in which both data processing capacity and mechanical flexibility must be satisfied at the same instant. To tackle this challenge, we developed a novel organic field-effect transistor (OFET), where a sharp increase and decrease in drain current was controllable by gate bias voltage.<sup>1)</sup> This unique property is pretty much upside down to that of an ambipolar transistor and, therefore, this is called “anti-ambipolar transistor (AAT)”. A uniqueness of the device configuration can be ascribed to a partially overlapped p-n heterojunction at the center of a transistor channel as illustrated in Fig. 1(a). The observed non-linear electrical transport (blue line in Fig. 1(b)) is analogous to that of a negative differential resistance and, therefore, this device has potential as a key element of multi-level logic circuits. In fact, we developed a ternary inverter by combining the AAT and n-type transistors (Fig. 1(c)).

## 2. Research Activities

Device configuration and molecular structures are

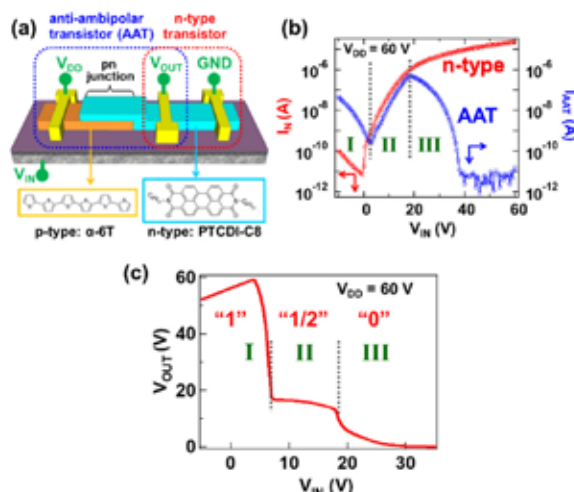


Fig. 1. (a) Schematic illustrations of device configuration and chemical structures of p- and n-type organic semiconductors. (b) Electrical current through anti-ambipolar ( $I_{AAT}$ ; blue) and n-type ( $I_N$ ; red) transistors. (c) Input ( $V_{IN}$ )-Output ( $V_{OUT}$ ) curve showing ternary logic states of (0, 1/2, 1).

shown in Fig. 1(a). The device is composed of sexithiophene ( $\alpha$ -6T) and a perylene derivative (PTCDI-C8) those work as p-type and n-type organic semiconductors, respectively. Here, three electrodes are connected with an AAT and an n-type organic transistor, and a gate bias voltage is applied from a highly doped Si substrate. This device was fabricated by vacuum deposition techniques.

Electrical currents are measured by sweeping gate bias voltage ( $V_{IN}$ ) at a constant drain voltage ( $V_{DD}$ ). Blue and red lines in Fig. 1(b) shows drain currents through the anti-ambipolar ( $I_{AAT}$ ) and n-type ( $I_N$ ) transistors, respectively. The non-linear current in the AAT is explained in terms of shoot-through current, which is commonly observable in a CMOS inverter.<sup>1)</sup> That is, electrical current is observable only when both p- and n-channels are on-states. In this figure, bias voltage range can be divided into three ranges: range I ( $I_{AAT} > I_N$ ), II ( $I_{AAT} = I_N$ ) and III ( $I_{AAT} < I_N$ ) depending on the magnitude relations of electrical current. In response to the balance of these electrical currents, an output voltage ( $V_{OUT}$ ) yields three distinct levels; ternary inverter operation was achieved as shown in Fig. 1(c).<sup>2)</sup>

In general, a conventional binary inverter shows two output levels (0,1). Then, integration density of  $N$ 's elements is proportional to  $2^N$ . Meanwhile, the ternary inverter yields three output levels (0, 1/2, 1), the integration density of which can be increased according to  $3^N$ .

It should be mentioned that the device performance demonstrated here has fatal bottleneck; extremely high operation voltage (ca. 60 V) are necessary. However, we found the operation voltages can be reduced by optimizing device geometries and by employing carrier injection layers together with a high-k dielectric layer.<sup>3,4)</sup> Consequently, we achieved two orders reduction of  $V_{IN}$  (< 1.0 V). Additionally, sharp switching and high on-off ratio are also simultaneously attained.

Specific emphasize is put on novelty of the device operation, which can overcome the limit of large-scale integration in conventional organic FETs to open up a new field of the flexible organic logic circuits.

## References

- 1) K. Kobashi, R. Hayakawa, T. Chikyow, Y. Wakayama, *Adv. Elect. Mater.* **3**, 1700106 (2017).
- 2) K. Kobashi, R. Hayakawa, T. Chikyow, Y. Wakayama, *Nano Lett.* **18**, 4355 (2018).
- 3) K. Kobashi, R. Hayakawa, T. Chikyow, Y. Wakayama, *ACS Appl. Mater. Interfaces* **10**, 2762 (2018).
- 4) K. Kobashi, R. Hayakawa, T. Chikyow, Y. Wakayama, *J. Phys. Chem. C* **122**, 6943 (2018).



## Topological Photonic States in Honeycomb Structures

**Principal Investigator**  
(Group Leader)

**Xiao HU**

**Toshikaze Kariyado** (Researcher)

X.C. Sun (Postdoc), Z.G. Chen (Postdoc),

H. Huang (Graduate Student), Y.C. Jiang (Graduate Student), X.X. Wang (Graduate Student)

### 1. Outline of Research

There has been a surge in searching for materials with topological features, whose transport properties are not influenced even the sample shapes are changed. Topological properties were first discovered in electron systems,<sup>1)</sup> and more recently the notion has been developed for light and electromagnetic waves, which is expected to be useful for building electromagnetic and optic waveguides immune to backscattering.

However, realization of topological properties in optic and electromagnetic waves often requires gyromagnetic materials under external magnetic field, and/or complex structures. In order to match with the existing electronics and photonics technologies, it is important to achieve topological properties based on conventional materials and simple structures.

We have revealed theoretically that topological properties in optic and electromagnetic waves can be achieved based on honeycomb-type photonic crystals made of conventional dielectric materials. The key feature of this approach is the Dirac dispersion relation supported by the honeycomb structure. When a band gap is opened upon deforming the honeycomb lattice with the  $C_{6v}$  symmetry preserved, a photonic topological insulator appears associated with the finite Berry phase induced by the geometry effect.

### 2. Research Activities

#### (1) Topological LC circuits and microstrip.<sup>2)</sup>

This time we succeed in fabricating topological microstrip, a typical transmission line, with honeycomb structure (Fig. 1), where electromagnetic waves can propagate without backscattering even when the interface between the topological and trivial regimes contains a sharp turn. The topological microstrips can work as electromagnetic waveguides, which would allow miniaturization and high integration in various electronics devices, such as mobile phones.

We first reveal theoretically that in a microstrip electromagnetic waves attain topological properties when the metallic strips form honeycomb structure and the strip widths inside and between hexagonal unit cells are set

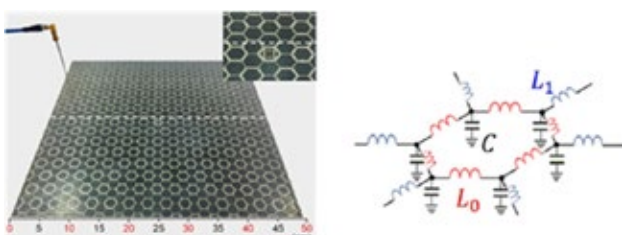


Fig. 1. Topological microstrips and effective LC circuit.

different. We then fabricate microstrips experimentally, and measure electric fields on their surfaces. As the result, we observe successfully the topological electromagnetic propagations along the interface, where local Poynting vectors are rotating in the directions locked with the interface propagating directions.

This work demonstrates that topological propagation of electromagnetic waves can be induced using conventional materials and simple structures. Because topological electromagnetic wave propagation is immune to backscatter even when interfaces turn sharply, design of compact electromagnetic circuits becomes possible, leading to miniaturization and high integration of electronics devices. In addition, the direction of vortex and the vorticity in the topological electromagnetic modes may be used as data carriers in high-density information communications. All these features can contribute to the development of advanced information society represented by IoT and autonomous vehicles.

#### (2) Topological photonic crystal made of dielectrics.<sup>3)</sup>

We demonstrate experimentally that a honeycomb-type photonic crystal made of  $Al_2O_3$  cylinders exhibits the topological electromagnetic property, similar to the quantum spin Hall effect in electronic systems. A pseudospin degree of freedom in the electromagnetic system associated with the orbital angular momentum arises due to a deformation of the photonic crystal from the ideal honeycomb lattice. It serves as the photonic analogue to the electronic Kramers pair.

We visualized qualitatively and measured quantitatively that microwaves of a specific pseudospin propagate only in one direction along the interface between a topological photonic crystal and a trivial one.

In order to show the robustness of the topological electromagnetic wave, we implant a sharp corner in the interface. We show explicitly that the intensity of interface electromagnetic wave before and after the corner does not change, indicating that the electromagnetic field cannot be scattered by the sharp corner, a property unexperienced in any conventional wave propagations.

Because only a conventional dielectric material is used and only local real-space manipulations are required, our scheme can be extended to visible light which will hopefully inspire many future photonic applications.

### References

- 1) T. Kariyado, Y. C. Jiang, H. X. Yang, X. Hu, *Phys. Rev. B* **98**, 195416 (2018).
- 2) Y. Li, Y. Sun, W. Zhu, Z. Guo, J. Jiang, T. Kariyado, H. Chen, X. Hu, *Nat. Commun.* **9**, 4598 (2018).
- 3) Y. Yang, Y. F. Xu, T. Xu, H. X. Wang, J. H. Jiang, X. Hu, Z. H. Hang, *Phys. Rev. Lett.* **120**, 217401 (2018).

## Materials and Devices for Nano-Scale Photo-Energy Transducers

### Principal Investigator

Tadaaki NAGAO

(Group Leader)

Satoshi Ishii (Senior Researcher)

T.D. Dao (Postdoc), S.L. Shinde (Postdoc),

H. Huang (Graduate Student), Y.C. Jiang (Graduate Student), X.X. Wang (Graduate Student)



### 1. Outline of Research

Since more than half of the solar radiation is composed of infrared light, harvesting infrared energy from sunlight as well as from thermal radiation associated with industry / human activity has become one of the important approaches towards the sustainable development goals (SDGs). The research on infrared (IR) nanophotonics, the science and technology for regulating the thermal radiation by amplifying, confining, or scattering the IR light with nano-materials has gained significant importance as one of the key technologies for small-scale energy harvesting. Nanophotonic materials, especially plasmonic materials and metamaterials are now accepted as useful paradigms for materials science which enable us to control the light in nanospace with great flexibility. In our laboratory, based on plasmonic/metamaterial approach, we are designing and developing energy-harvesting nano-systems, especially for highly-efficient photothermal applications and wavelength selective IR light emission and detection.<sup>1-4)</sup> Along with the device fabrications, we also explore various types of plasmonic compounds with appropriate optical properties, suitable for the high-temperature applications, efficient photothermal conversion, hot carrier generation, as well as high surface electromagnetic field enhancement.<sup>1-5)</sup>

### 2. Research Activities

#### (1) Photothermal heating by nanostructures and their applications.

Photothermal heating by nanostructures allows to locally heat their surrounding indirectly. Here we study liquids that are heated above their boiling points, known as superheating, by means of photothermal conversion (Fig. 1).<sup>1)</sup> In this metastable state, the liquid temperature keeps increasing as the liquid is being heated before the formation of bubbles. In contrast, we experimentally demonstrate that the temperature of superheated water can be kept constant even at elevated heating power. Water heating is done by irradiating the continuous wave laser to the plasmonic titanium nitride

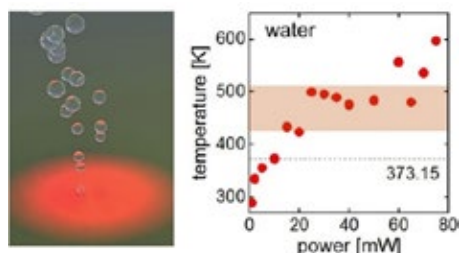


Fig. 1. Schematic diagram of water nano-heating based on TiN nanostructures.

nanostructures on a sapphire substrate. The temperature-constant superheating is also observed for ethylene glycol and 2-acetoxy-1-methoxypropane, and is attributed to high thermal conductivity of the substrate. This unique superheating yet achieved by a simple method can be useful in optical trapping and various optical heating applications.

#### (2) High-resolution spectroscopic mid-IR detector array.

Engineering light absorption at desired wavelengths using nanophotonic structures enables a wide variety of applications which do not exist in nature.<sup>5)</sup> In the past decades, plasmon-enhanced light absorptions for enhancing energy conversion efficiency have attracted many attentions owing to their potential applications in solar energy harvesting, light emitting devices, and infrared and heat transfer devices.<sup>1,2)</sup> In this work, we demonstrate an IR sensor array in which each resonant sensor exhibits four-wavelength detection with sub-100 nm wavelength resolution (Fig. 2). To realize high wavelength resolution as well as making them industry compatible, the structural design has been intended to efficiently absorb the thermal radiation at desired wavelengths with narrow window using Si nanofabrication techniques. The developed four-wavelength-selective IR sensor array exhibits a high performance with sub-100 nm bandwidth responsivity, which can be applied for non-dispersive IR spectroscopy, multicolor IR imaging, and remote sensing of absolute temperature.

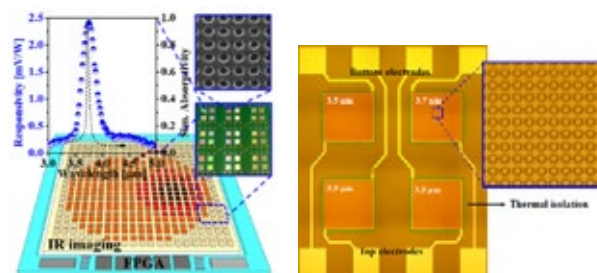


Fig. 2. (Left) Spectrum from a single IR detector with IR resonance designed at 3.7  $\mu\text{m}$ . (Right) A schematic diagram and SEM images of a multicolor (four-wavelength-selective) IR imaging device.

### References

- 1) S. Ishii, R. Kamakura, H. Sakamoto, T.D. Dao, S.L. Shinde, T. Nagao, K. Fujita, K. Namura, M. Suzuki, S. Murai, K. Tanaka, *Nanoscale* **10**, 18451 (2018).
- 2) M. Kaur, S. Ishii, S.L. Shinde, T. Nagao, *ACS Sustain. Chem. Eng.* **5**, 8523 (2017).
- 3) O. Anjaneyulu, K. Takeda, S. Ishii, S. Ueda, T. Nagao, P. Xiaobo, T. Fujita, M. Miyauchi, H. Abe, *Mater. Chem. Front.* **2**, 580 (2018).
- 4) R.P. Sugavaneshwar, S. Ishii, T.D. Dao, A. Ohi, T. Nabatame, T. Nagao, *ACS Photonics* **5**, 814 (2018).
- 5) K. Chen, P. Guo, T.D. Dao, S.Q. Li, S. Ishii, T. Nagao, R.P.H. Chang, *Adv. Opt. Mater.* **5**, 1700091 (2017).



## Data-Driven Approach for Discovery of New Pressure-Induced Superconductors

**Principal Investigator**  
(Group Leader)

**Yoshihiko TAKANO**

**Hiroyuki Takeya** (Chief Researcher)

### 1. Outline of Research

A data-driven approach based on high-throughput computation has recently been applied successfully to exploration of new functional materials such as battery materials, thermoelectric materials, superconductors, and so on. In this study, we have reported a case-study of the data-driven approach through a discovery of superior thermoelectric properties and pressure-induced superconductivity in selected compounds by the high-throughput screening.<sup>1,2)</sup>

### 2. Research Activities

1570 candidates were listed from the inorganic material database named AtomWork, based on the following restriction: abundant and nontoxic or less toxic constituent elements, and the number of atoms being less than 16 per primitive unit cell. The candidates were narrowed down by using the restriction of a narrow band gap and high density of state (DOS) near the Fermi level. By this screening, the number of candidate compounds was reduced to 45. Finally, we checked whether the band gap decreases (or even the metallic behavior appears) under pressure of 10 GPa, and screened out 27 promising compounds. The schematic image of the screening process is shown in Fig. 1.

Among the candidates,  $\text{SnBi}_2\text{Se}_4$  was successfully synthesized in single crystals. The band gap of  $\text{SnBi}_2\text{Se}_4$  is  $\sim 200$  meV and a metallization is suggested under 10 GPa by theoretical calculation. Fig. 2(a) shows temperature dependence of resistance of  $\text{SnBi}_2\text{Se}_4$  under various pressures measured by our originally designed diamond anvil cell with boron-doped diamond electrodes.<sup>3)</sup> The  $\text{SnBi}_2\text{Se}_4$  exhibited the insulating behavior at low pressure region. Under  $\sim 10$  GPa the sample showed insulator to metal transition with good correspondence to the theoretical prediction. Further pressure region at  $\sim 20$  GPa, the pressure-

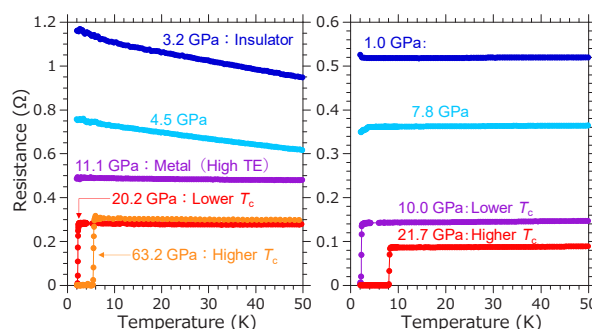


**Fig. 2.** Temperature dependences of (a)  $\text{SnBi}_2\text{Se}_4$  and (b)  $\text{PbBi}_2\text{Te}_4$  under various pressures.

induced superconductivity with clear zero-resistance was observed. Interestingly, the transition temperature suddenly increased like a phase transition.

The second target is  $\text{PbBi}_2\text{Te}_4$  which has the band gap of  $\sim 100$  meV under ambient pressure. The band gap is almost half of the first target of  $\text{SnBi}_2\text{Se}_4$ . Fig. 2(b) shows the high pressure property of  $\text{PbBi}_2\text{Te}_4$ . The sample exhibited as metal even at low pressure region. The pressure-induced superconductivity appeared under 10 GPa, which pressure is almost half of that of  $\text{SnBi}_2\text{Se}_4$ , reflecting their band gap difference. The  $\text{PbBi}_2\text{Te}_4$  also showed the sudden increase of the transition temperature like a phase transition. According to our data-driven approach, we have successfully discovered new superconductors in very short time.

### References

- 1) R. Matsumoto, Z. Hou, H. Hara, S. Adachi, H. Takeya, T. Irifune, K. Terakura, Y. Takano, *Appl. Phys. Express* **11**, 093101 (2018).
- 2) R. Matsumoto, Z. Hou, M. Nagao, S. Adachi, H. Hara, H. Tanaka, K. Nakamura, R. Murakami, S. Yamamoto, H. Takeya, T. Irifune, K. Terakura, Y. Takano, *Sci. Technol. Adv. Mater.* (2018), accepted for publication.
- 3) R. Matsumoto, A. Yamashita, H. Hara, T. Irifune, S. Adachi, H. Takeya, Y. Takano, *Appl. Phys. Express* **11**, 053101 (2018).

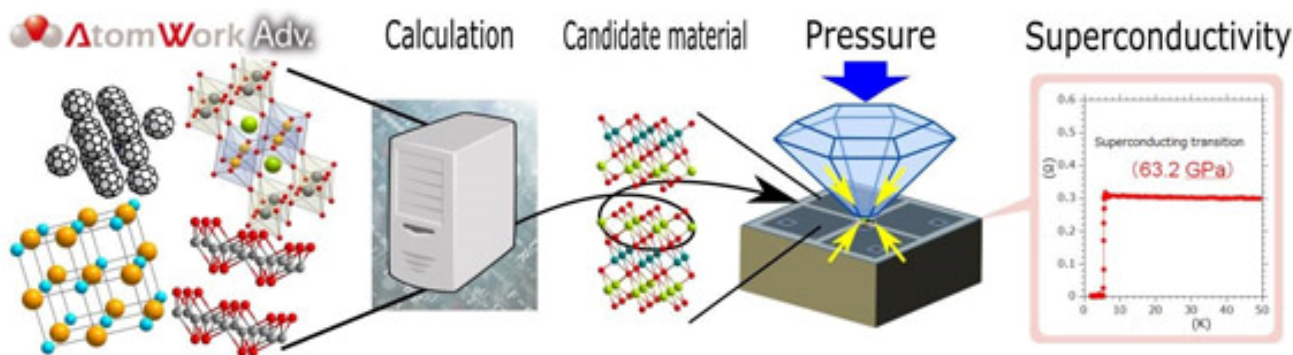


**Fig. 1.** Schematic image of the screening process in the data-driven exploration for pressure-induced superconducting materials.

# Pronounced Photogating Effect in Atomically Thin WSe<sub>2</sub> with a Self-Limiting Surface Oxide Layer

**Principal Investigator**

**Kazuhito TSUKAGOSHI**

(Group Leader)

Toshihide Nabatame (Chief Researcher), Seiichi Kato (Senior Researcher)



## 1. Outline of Research

Growing a high-quality oxide film with a tunable thickness on atomically thin transition metal dichalcogenides is of great importance for the electronic and optoelectronic applications.<sup>1)</sup> The photogating effect is a photocurrent generation mechanism that leads to marked responsivity in two-dimensional (2D) semiconductor-based devices. A key step to promote the photogating effect in a 2D semiconductor is to integrate it with a high density of charge traps. Here, we show that self-limiting surface oxides on atomically thin WSe<sub>2</sub> can serve as effective electron traps to facilitate *p*-type photogating.<sup>2)</sup>

## 2. Research Activities

We developed an original single layer oxidation process in which ozone (O<sub>3</sub>) exposure leads to homogeneous surface oxidation of atomically thin WSe<sub>2</sub> with a self-limiting thickness from single- to trilayers, depending on temperature. A single layer WSe<sub>2</sub> with WO<sub>x</sub> layer oxidized from single WSe<sub>2</sub> was electrically contacted by Au/Ti electrodes, and was characterized as a transistor (Fig. 1). By examining the gate-bias-induced threshold voltage shift of the *p*-type transistor, the electron trap density and the trap rate of the oxide are determined to be  $> 10^{12} \text{ cm}^{-2}$  and  $> 10^{10} \text{ cm}^{-2} \text{ s}^{-1}$ , respectively (Fig. 2). White-light illumination on an oxide-covered 4-layer WSe<sub>2</sub> transistor leads to the generation of photocurrent, the magnitude of which increases with the hole mobility. During illumination, the photocurrent evolves on a timescale of seconds, and a portion of the current persists even after illumination. These observations indicate that the photogenerated electrons are trapped deeply in the surface oxide and effectively gate the underlying WSe<sub>2</sub>. Owing to the pronounced photogating effect, the responsivity of the oxide-covered WSe<sub>2</sub> transistor is observed to exceed

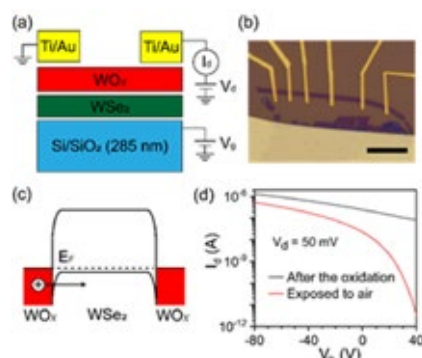


**Fig. 1.** (a) Schematic and (b) optical microscope images of a transistor based on single-layer WSe<sub>2</sub> with surface WO<sub>x</sub>. The scale bar in the optical image is 10 μm. (c) Quantitative band diagram showing a hole injection process from WO<sub>x</sub> into the heavily *p*-doped WSe<sub>2</sub>. EF indicates the Fermi level of the system. (d) Typical *I<sub>d</sub>*-*V<sub>g</sub>* characteristics of a WO<sub>x</sub>-covered single-layer WSe<sub>2</sub> transistor immediately after oxide growth (black line) and after exposure to air for 1 h (red line). The drain bias is 50 mV.

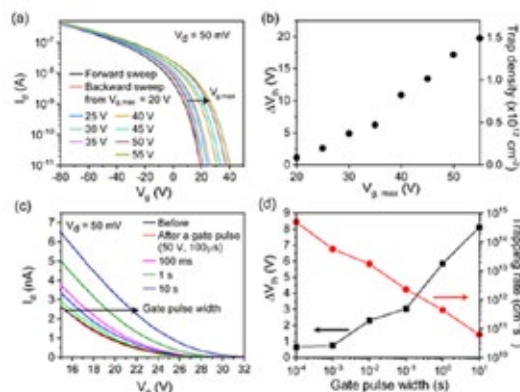


**Fig. 2.** (a) *I<sub>d</sub>*-*V<sub>g</sub>* characteristics of a WO<sub>x</sub>-covered single-layer WSe<sub>2</sub> transistor (*V<sub>d</sub>* = 50 mV). The black curve shows the initial sweep from -80 V to *V<sub>g,max</sub>*, while the other curves show backward sweeps from different *V<sub>g,max</sub>* to -80 V. (b) Threshold voltage shift and trap density as functions of *V<sub>g,max</sub>*. (c) Backward *I<sub>d</sub>*-*V<sub>g</sub>* characteristics of the WO<sub>x</sub>-covered single-layer WSe<sub>2</sub> transistor (*V<sub>d</sub>* = 50 mV). The gate voltages are swept from 32 V to 15 V. The black curve is the initial sweep, while the other curves show sweeps after applying gate pulses with a height of 50 V and different widths. (d) Threshold voltage shift and trapping rate as functions of the gate pulse width.

3000 A/W at an incident optical power of 1.1 nW. The observed responsivity is four times higher than a typical commercial Si-photodiode, suggesting the effectiveness of surface oxidation in facilitating the photogating effect in 2D semiconductors (Fig. 3). This research was developed with Dr. Mahito Yamamoto (Previous group member. Current: Osaka University).

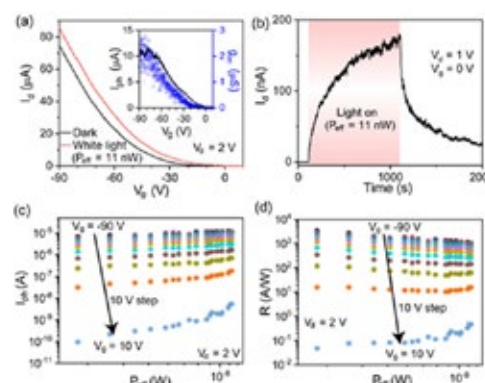


**Fig. 3.** (a) Backward (from 10 to -90 V) *I<sub>d</sub>*-*V<sub>g</sub>* characteristics of a WO<sub>x</sub>-covered 4-layer WSe<sub>2</sub> transistor under dark (black curve) and white-light illumination with an incident power of 11 nW (red curve). The drain bias is 2 V. The inset shows the generated photocurrent and the transconductance of the transistor as functions of the gate voltage. (b) Time evolution of the drain current under illumination with an incident power of 11 nW. The drain and gate biases are 1 V and 0 V. (c) Photocurrents and (d) extracted responsivities as functions of the incident power for various gate voltages (*V<sub>d</sub>* = 2 V).

## References

- 1) M. Yamamoto, S. Dutta, S. Aikawa, S. Nakaharai, K. Wakabayashi, M.S. Fuhrer, K. Ueno, K. Tsukagoshi, *Nano Lett.* **15**, 2067 (2015).
- 2) M. Yamamoto, K. Ueno, K. Tsukagoshi, *Appl. Phys. Lett.* **112**, 181902 (2018).



## Non-Equilibrium Dynamics of Pharmaceutical Glass

Group Leader

Kohsaku KAWAKAMI

Chiho Kataoka (Senior Researcher), Yoko Shirai (Principal Engineer)

### 1. Outline of Research

Amorphous solids can offer higher solubility and dissolution rates in aqueous media relative to crystals; thus it can be used for improving oral absorption of poorly soluble drugs.<sup>1)</sup> However, the number of marketed oral amorphous formulations is still small, in part due to the difficulty in predicting their dynamic behaviors including crystallization and dissolution. We are investigating non-equilibrium dynamic behaviors of pharmaceutical glasses both in solid and suspended state to provide deeper understanding on their solid-state stability and supersaturation behavior after their dissolution.

### 2. Research Activities

Isothermal crystallization of nine pharmaceutical compounds was investigated under carefully controlled conditions.<sup>2-4)</sup> Despite large variations of data in literature, we could explain their initiation time for crystallization in a very simple manner; those for most compounds fell onto one line, as shown as universal line in Fig. 1, which means that crystallization is totally governed by a ratio of glass transition temperature ( $T_g$ ) to storage temperature ( $T$ ). Some compounds exhibited slower crystallization, which was explained by strong interactions between molecules. However, crystallization of those compounds can be accelerated by increasing surface area which was proved by using freeze-dried glass as shown for ritonavir in Fig. 1,<sup>3)</sup> because crystallization of those compounds is initiated by heterogeneous nucleation. As a result, crystallization of ritonavir was also explained by the universal line. Thus, this line is likely to be regarded as the worst case for the compounds which apparently exhibit better stability. Also found was that such compounds can be stabilized by sub- $T_g$  annealing, which was explained by reorganization of hydrogen bonding pattern and reduction in packing volume.<sup>5)</sup>

Practical amorphous formulations utilize hydrophilic polymers to improve stability and dissolution behavior. It is

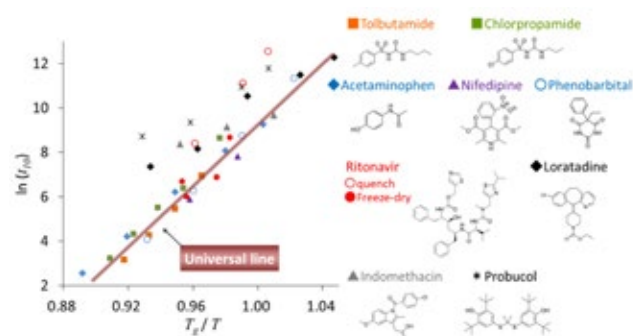


Fig.1. Initiation time for crystallization of nine pharmaceutical glasses as a function of  $T_g/T$  and chemical structures of compounds.

favorable to have the drug and polymers mixed in a molecular level. We have investigated their time-dependent phase separation behaviors.<sup>6)</sup> The phase separation of some mixtures was faster under high-temperature conditions, whereas the opposite trend was observed with the others. The phase behaviors of former appeared to be dominated by molecular mobility due to the low  $T_g$ , whereas departure from equilibrium was a dominating factor for the latter.

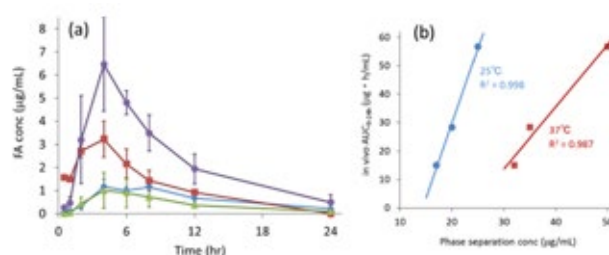


Fig. 2. (a) Plasma concentration of fenofibric acid, an active metabolite of FEN, after administration of three types of amorphous solid dispersions and crystalline FEN (blue) to rats. (b) Correlation between AUC (area under concentration curve) of the plasma concentration profile (a) and phase separation concentration for each formulation. One solid dispersion which exhibited dissolution rate-limited absorption was excluded from the analysis.

Dissolution of amorphous solids is a complicated process, which may involve phase separation from the supersaturated state based on spinodal decomposition and formation of a colloidal phase. However, relevance of the phase separation behavior to oral absorption is not well understood. We investigated phase separation behavior of a supersaturated fenofibrate (FEN) solution in the presence of polymers and the in vivo absorption in the form of amorphous solid dispersions which utilized the same polymer.<sup>7)</sup> As shown in Fig. 2, the phase separation concentration was found to be a good and simple indicator to estimate the absorption-enhancing ability of the polymeric excipients for amorphous formulations, if the absorption is limited by solubility. This result indicated that the dispersed phase after the phase separation did not contribute to the absorption, which must be comprehended well for predicting oral absorption from solid dispersions.

### References

- 1) K. Kawakami, *Adv. Drug Delivery Rev.* **64**, 480 (2012).
- 2) K. Kawakami, T. Harada, K. Miura, Y. Yoshihashi, E. Yonemochi, K. Terada, H. Moriyama, *Mol. Pharmaceutics* **11**, 1835 (2014).
- 3) K. Kawakami, *J. Pharm. Sci.* **104**, 276 (2015).
- 4) K. Kawakami, C. Ohba, *Int. J. Pharm.* **517**, 322 (2017).
- 5) S. Tominaka, K. Kawakami, M. Fukushima, A. Miyazaki, *Mol. Pharmaceutics* **14**, 264 (2017).
- 6) K. Kawakami, Y. Bi, Y. Yoshihashi, K. Sugano, K. Terada, *J. Drug Delivery Sci. Technol.* **46**, 197 (2018).
- 7) K. Kawakami, K. Sato, M. Fukushima, A. Miyazaki, Y. Yamaura, S. Sakuma, *Eur. J. Pharm. Biopharm.* **132**, 146 (2018).

## Materials for Cellular Mechanobiology

## Group Leader

Jun NAKANISHI

Mitsuhiro Ebara (Associate PI), Takeshi Ueki (Senior Researcher),  
Chiaki Yoshikawa (Senior Researcher)



## 1. Outline of Research

Mechanobiology is a discipline that studies the role of physical force in life phenomena. Recent studies in this field shed light on the significance of force, comparable to chemical and biochemical cues, in the regulation of various biological and pathological processes. We are developing new materials and methodologies, based on the concept of nanoarchitectonics, not only to study basic principle in mechanobiology, but also to develop drug screening platforms for “mechanomedicine” and medical devices based on mechanobiology.<sup>1-3)</sup>

## 2. Research Activities

(1) Photoactivatable hydrogels to decouple chemical and mechanical regulation of collective migration.<sup>4)</sup>

Collective migration is the mechanobiological interplay within migrating cell clusters and against underneath extracellular matrices, mediating various physiological and pathological processes. Therefore, it is crucial to develop a robust platform, where collective migration can be studied in standardized conditions, to understand how cells migrate differently between normal and disease states. We have developed photoactivatable hydrogel interfaces composed of poly(acrylamide) hydrogel, whose surface was sequentially functionalized with poly-D-lysine and photocleavable poly(ethylene glycol) (Fig. 1). On the surface of the gel substrates, cell clusters with any given geometries can be prepared by controlling the irradiation patterns (geometrical cue), and their collective migration can be induced by the following irradiation of the surrounding regions. Moreover, the substrate mechanical property can be controlled by changing the composition of the poly(acrylamide) hydrogel (mechanical cue), and the chemical properties were controlled by changing the amount of immobilized poly-D-lysine, thereby altering the adsorption amount of extracellular matrix proteins (chemical cue). Through the study of the interplay of these

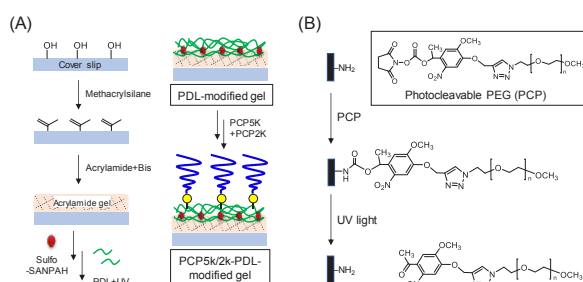


Fig. 1. Photoactivatable hydrogel. Schematic representation of (A) preparation procedure and (B) its chemical reaction.

environmental cues in the regulation of collective characteristics, we found additive effects of chemical and mechanical cues on the suppression of circular expansion by up-regulating the epithelial morphology. Also, the impact of geometrical cues became more significant by decreasing the chemical cue.

(2) A drug screening platform for mechanically-induced epithelial-mesenchymal transition.<sup>5)</sup>

Epithelial-mesenchymal transition (EMT), phenotypic changes in cell adhesion and migration, is involved cancer invasion and metastasis, hence becoming a target for anti-cancer drugs. In this study, we report a method for the evaluation of EMT inhibitors by using a photoactivatable gold substrate, which changes from non-cell-adhesive to cell-adhesive in response to light. The method is based on the geometrical confinement of cell clusters and the subsequent migration induction by controlled photoirradiation of the substrate. As a proof-of-concept experiment, a known EMT inhibitor was successfully evaluated in terms of the changes in cluster area or leader cell appearance, in response to biochemically and mechanically induced EMT. Furthermore, an application of the present method for microbial secondary metabolites identified nanaomycin H as an EMT inhibitor, potentially killing EMTed cells in disseminated conditions (Fig. 2). These results demonstrate the potential of the present method for screening new EMT inhibitors.

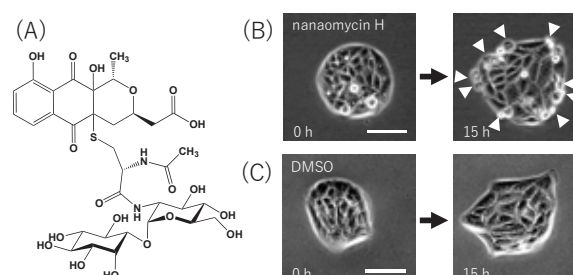


Fig. 2. Selective cytotoxic effect of nanaomycin H (A) on cells undergoing mechanically-induced EMT. (B, C) Cluster expansion behaviors in the presence of (B) nanaomycin H and (C) DMSO.

## References

- 1) J. Nakanishi, *Chem. Rec.* **17**, 611 (2017).
- 2) S.A. Abdellatif, J. Nakanishi, *Biomaterials* **169**, 72 (2018).
- 3) S. Yamamoto, H. Ikegami, K. Yamaguchi, J. Nakanishi, *ChemPhotoChem* **2**, 786 (2018).
- 4) S. Yamamoto, K. Okada, N. Sasaki, A. Chang, K. Yamaguchi, J. Nakanishi, *Langmuir*, in press.
- 5) J. Nakanishi, K. Sugiyama, H. Matsuo, Y. Takahashi, S. Ōmura, T. Nakashima, *Anal. Sci.*, in press.



## Tunable 2D Superconducting Heterostructures with Organic Molecules

Group Leader

Takashi UCHIHASHI

Ryuichi Arafune (Senior Researcher), Katsumi Nagaoka (Senior Researcher),  
Takahide Yamaguchi (Senior Researcher)

### 1. Outline of Research

Recent advancement in nanotechnology has led to realization of two-dimensional (2D) superconductors with truly atomic-scale thicknesses.<sup>1)</sup> Since this is against the general belief that 2D superconductivity cannot exist or should be at least very fragile, the finding is surprising and has attracted much attention. Particularly, we successfully demonstrated the existence of ideal 2D superconductivity, by growing epitaxial indium atomic layers on a silicon surface and by directly measuring macroscopic superconducting currents for the first time.<sup>2)</sup>

For future applications, precise control of the superconducting properties is highly desirable. For this purpose, we have proposed that the self-assembly of organic molecules on 2D superconductors may be employed based on the concept of Material Nanoarchitectonics. As widely recognized, usage of organic molecules is advantageous in terms of flexible and rational designing, which allows a fine tuning of the local interactions at the interface. Furthermore, organic molecules should allow us to add to the system new functionalities such as optical detection. Fig. 1(a) shows a schematic illustration of the concept. Here the metal atomic layer on a semiconductor surface plays the role of a host 2D material. The adsorbed organic molecules can be a source of charges and spins.

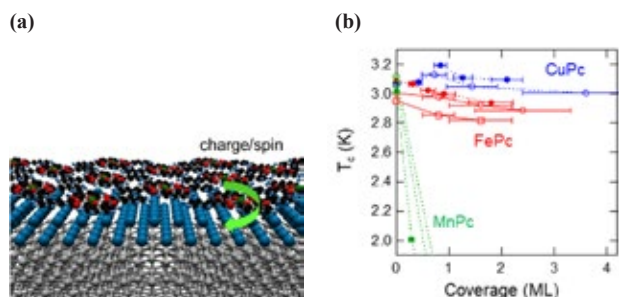


Fig. 1. (a) Concept of a 2D hybrid superconductor consisting of the metal atomic layer (blue spheres) on a semiconductor (grey spheres) and self-assembled organic molecules (on top). (b) Molecular coverage dependences of superconducting transition temperature ( $T_c$ ) for CuPc, MnPc, and FePc. FePc can coexist with superconductivity while slightly suppress it.

Non-trivial phenomena such as field-induced superconductivity may occur under such conditions. The coexistence and competition of molecular magnetism, superconductivity, and the Rashba effect on the surface may also lead to rich physics such as topological superconductivity and Majorana fermions.

### 2. Research Activities

We have successfully materialized the above concept

using indium atomic layers on silicon and metal-phthalocyanine (MPc, M = Mn, Cu) molecules.<sup>3)</sup> Our electron transport measurements revealed that CuPc enhanced the superconducting transition temperature ( $T_c$ ) of the indium layer slightly while MnPc easily destroys it. The origin of these distinctive behaviors was attributed to a competition of two effects; molecule-induced surface doping and exchange interaction between the spin magnetic moments of the molecules and the conduction electrons in the indium layers. Particularly, the strength of the latter was determined by the orientations of spin-related molecular orbitals.

To have a deeper insight into this system, we used FePc molecule in place of MnPc to study its effect on superconductivity.<sup>4)</sup> Unexpectedly, FePc was found to coexist with superconductivity only with a slight suppression of  $T_c$  although FePc has electronic and spin states very similar to those of MnPc; when adsorbed on the Indium atomic layers, both retain sizable spin magnetic moments that couples to the conduction electrons. This result suggests that the exchange interaction is not solely responsible for the destruction of superconductivity observed for MnPc. Rather, the manifestation of the Kondo effect should play an important role. The Kondo effect competes with superconductivity and suppresses it because the two quantum many-body states have incompatible ground states. Indeed, a clear signature of the Kondo effect, the resistance minimum, was found through our transport measurements.

We also used  $F_{16}$ CuPc molecule in place of CuPc to utilize its strong hole-doping character.<sup>5)</sup> In this case, the fluorination caused the molecule to tilt from the in-plane orientation and to substantially redistribute charge and spin. This allows the spin magnetic moment of  $F_{16}$ CuPc to couple with the conduction electrons through exchange interaction. Consequently,  $T_c$  was suppressed moderately.

The present work indicates that the subtle balance of electronic and spin states within the molecule is crucial in terms of the influence on superconductivity. It also suggests a possibility of manipulating superconducting properties through rational design of appropriate molecules.

### References

- 1) T. Uchihashi, *Supercond. Sci. Technol.* **30**, 013002 (2017). Topical Review.
- 2) T. Uchihashi, P. Mishra, M. Aono, T. Nakayama, *Phys. Rev. Lett.* **107**, 207001 (2011). Editor's Suggestion and featured in *Physics*.
- 3) S. Yoshizawa, E. Minamitani, S. Vijayaraghavan, P. Mishra, Y. Takagi, T. Yokoyama, S. Watanabe, T. Nakayama, T. Uchihashi, *Nano Lett.* **17**, 2287 (2017).
- 4) T. Uchihashi, S. Yoshizawa, P. Mishra, E. Minamitani, S. Watanabe, Y. Takagi, T. Yokoyama, in preparation.
- 5) N. Sumi, Y. Yamada, M. Sasaki, R. Arafune, N. Takagi, S. Yoshizawa, T. Uchihashi, *J. Phys. Chem. C*, submitted.

## Nanomechanical Sensing towards Mobile Olfaction

Group Leader

Genki YOSHIKAWA

Kota Shiba (Senior Researcher)



### 1. Outline of Research

Demands for new sensors to detect or identify target molecules are rapidly growing in various fields; agriculture, food, medicine, security, environment, cosmetics, *etc.* Although nanomechanical sensors have potential to contribute to these challenges, it is still required to improve their performance in both hardware and software aspects to achieve robust and reliable sensing in actual applications.

### 2. Research Activities

(1) *Discrimination of structurally similar odorous molecules based on chemical properties.*<sup>1)</sup>

In this study, we have demonstrated the discrimination of odorous molecules in a series of similar physical structures by the appropriate selection of signal features based on the mechanism of a nanomechanical sensor using Membrane-type Surface stress Sensor (MSS).<sup>2)</sup> Fig. 1 shows the sensing signals and the corresponding score plots of principal component analysis (PCA). Such diverse identification of physical/chemical properties will enhance the potential of nanomechanical sensors for various applications.

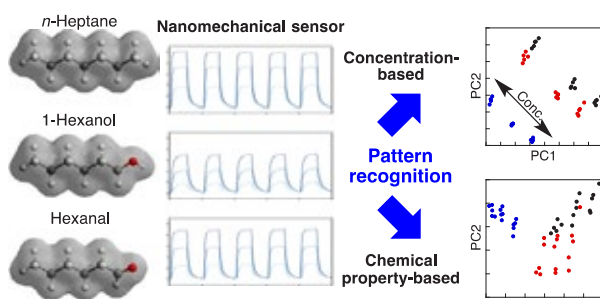


Fig. 1. Target molecules and corresponding MSS signals. Different signal features can provide various information.

(2) *Functional receptor materials for robust sensing in humid conditions.*<sup>3)</sup>

Porphyrin is one of the most promising materials for realizing a practical artificial olfactory sensor system. In this study, we focus on non-substituted porphyrins — porphines — as receptor materials of MSS to investigate the effect of center metals on gas sensing. It is revealed that iron insertion enhances sensitivity to various gases, while zinc and nickel insertion leads to equivalent or less sensitivity than free-base porphine. We also demonstrated the high robustness of the iron porphine to humidity, showing the high feasibility of porphine-based nanomechanical sensor devices for practical applications in ambient conditions (Fig. 2).

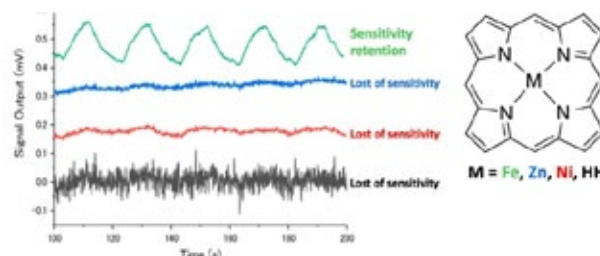


Fig. 2. Demonstration of the sensitivity control at atomic scale using Porphine as a base material. Robust sensing against humidity with superior sensitivity was achieved using iron porphine.

(3) *Functional nanoparticles-coated nanomechanical sensor arrays for machine learning-based quantitative odor analysis.*<sup>4)</sup>

In this study, we demonstrated that quantitative odor analysis can be achieved through systematic material design-based nanomechanical sensing combined with machine learning. A ternary mixture consisting of water, ethanol, and methanol was selected as a model system where a target molecule coexists with structurally similar species in a humidified condition (Fig. 3). Combination of various types of functional nanoparticles with machine learning model based on Gaussian process regression achieved the simultaneous quantification of the concentrations of each gas in the ternary mixture with high accuracy. The feedback obtained by the machine learning was effectively utilized to optimize material design for better performance.

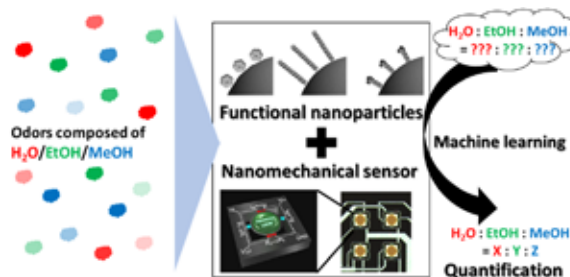


Fig. 3. Simultaneous quantification of gases in the ternary mixture through the combination of advanced sensing and machine learning.

### References

- 1) K. Minami, K. Shiba, G. Yoshikawa, *Anal. Methods* **10**, 3720 (2018).
- 2) G. Yoshikawa, T. Akiyama, S. Gautsch, P. Vettiger, H. Rohrer, *Nano Lett.* **11**, 1044 (2011).
- 3) H. T. Ngo, K. Minami, G. Imamura, K. Shiba, G. Yoshikawa, *Sensors* **18**, 1640 (2018).
- 4) K. Shiba, R. Tamura, T. Sugiyama, Y. Kameyama, K. Koda, E. Sakon, K. Minami, H. T. Ngo, G. Imamura, K. Tsuda, G. Yoshikawa, *ACS Sensors* **3**, 1592 (2018).



## MANA Brain: Neuromorphic Atomic Switch Networks

### Principal Investigator

(MANA Satellite at CNSI, UCLA, USA)

Adam Z. Stieg (Satellite Vice Director), S. Lilak (Student Researcher)

**James K. GIMZEWSKI**

### 1. Outline of Research

The limits of traditional complementary metal-oxide-semiconductor (CMOS) technology have become increasingly apparent alongside society's increasing demands for efficient processing of massive, complex datasets in fields ranging from the modeling financial markets to autonomous navigation. Traditional computing architectures are inefficient for processing information in real-time and lack the autonomy to handle such large, complex datasets efficiently. By contrast, natural systems such as the mammalian brain, are highly energy efficient (operating around 20 W) and are autonomous by design.

Inspiration from the mammalian brain has led to the development of atomic switch networks (ASN) as a nanoarchitectonic platform for such complex computing applications.<sup>1)</sup> The ASN consists of a highly interconnected, randomly oriented array of individual atomic switch junctions on the order of  $10^8$  junctions/cm<sup>2</sup>. These switching elements exhibit a non-linear, dynamic current voltage response and are capable of demonstrating both short- and long-term memory dependent on the network's stimulation.<sup>2)</sup> This research aims to expand upon the ASN framework through the development of new switching materials and their subsequent implementation into emerging computing paradigms.

### 2. Research Activities

The ASNs neuromorphic inspiration is realized through the self-organization of interconnected, interacting non-linear elements which yield both spatial and temporal dynamics within the functionalized system. The spatiotemporal dynamics of the ASN implicate it as an optimal architecture for the implantation of neural network learning techniques, most notably as a material substrate for reservoir computing (RC).<sup>3)</sup> The utilization of RC provides potential advantages in both flexibility and efficiency. Employing the ASN as a physical reservoir, its ability to discern spoken digits from the free spoken digit dataset (FSDD) has been demonstrated.

#### (1) Self-organized non-linear dynamics.

The fabrication of ASNs hybridizes conventional top-down microfabrication techniques with bottom-up synthetic methods, ultimately enabling its potential for integration with existing CMOS processes. The self-organized, bottom-up fabrication of nanowires results in a randomly oriented complex network, which upon functionalization yields dense atomic switch connections bearing a visual resemblance to mammalian neocortex. These individual atomic switch elements exhibit a non-linear current-voltage response, which is amplified by the tightly packed, random distribution of interconnected switches. Their operational properties can be further tuned through the selection of

different insulating mediums.<sup>4)</sup> Controlled stimulation of the network realizes a complex, non-linear transformation of the stimulus and demonstrates a significant potential for applications in complex computation.

#### (2) Reservoir computing.

Reservoir computing is an extension of traditional recurrent neural networks (RNN), both of which operate through the utilization of dynamic memory from input signal transformations, enabling the processing of temporal information (Fig. 1). RC offers many benefits over RNNs by only weighting the synaptic connections between the reservoir and output layer, greatly minimizing training costs and also enables scaling-up while being less resource intensive. The inherent spatiotemporal dynamics of the ASN implicate it as a prime candidate for in-materio RC applications.<sup>4,5)</sup>

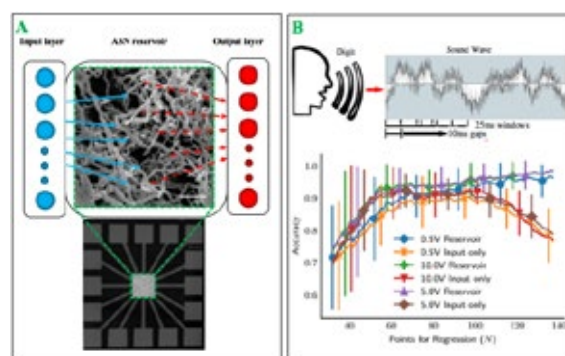


**Fig. 1. A) Schematic of reservoir computing on an ASN (SEM scale bar 5  $\mu$ m), only the dashed arrows are weighted. B) FSDD accuracy at different operating voltages through linear regression of the inputs or a combination of the inputs and outputs (reservoir).**

#### (3) Spoken digit recognition.

The FSDD is a free, publicly available dataset of various individuals vocalizing single digits. Through the conversion of the raw audio data into Mel-Frequency Cepstrum Coefficients (MFCC), a common technique for speech recognition, the resulting array of MFCCs is then sequentially fed into the ASN at specific time intervals, acting as a temporal sequence of inputs for RC. Individual digits were then discerned through linear regression of the target function with up to 100% accuracy.<sup>5)</sup> These results represent the first speech recognition with ASN devices.

### References

- 1) A.Z. Stieg, A.V. Avizienis, H.O. Sillin, C. Martin-Olmos, M. Aono, J.K. Gimzewski, *Adv. Mater.* **24**, 286 (2012).
- 2) E. Demis, R.C. Aguilera, K. Scharnhorst, M. Aono, A.Z. Stieg, J.K. Gimzewski, *Jpn. J. Appl. Phys.* **55**, 11 (2016).
- 3) K. Scharnhorst, J. Carbajal, R. Aguilera, E. Sandouk, M. Aono, A.Z. Stieg, J.K. Gimzewski, *Jpn. J. Appl. Phys.* **57**, 03ED02 (2018).
- 4) E. Demis, R.C. Aguilera, H.O. Sillin, K. Scharnhorst, E.J. Sandouk, M. Aono, A.Z. Stieg, J.K. Gimzewski, *Nanotechnology* **26**, 204003 (2015).
- 5) S. Lilak, A.Z. Stieg, J.K. Gimzewski, (2019), in preparation.

Surface Atomic Scale Logic Gate

**Principal Investigator** Christian JOACHIM

(MANA Satellite at CEMES, CNRS, France)

W.H. Soe, (Senior Researcher), O. Faizy (Postdoc), S. Srivastava (Postdoc)



**1. Outline of Research**

The Pico-Lab CEMES-CNRS Toulouse MANA satellite is working on the experimental and theory of QHC logic gates design, their current intensity drive, their mechanical inputs and by extension on single molecule machinery like molecule-motors and nano-cars. The atomic scale logic gate complexity roadmap is explored to master the emergence of a maximum quantum calculation power inside a single molecule or at the surface of a passivated semi-conductor.

**2. Research Activities**

(1) *The first NAND QHC molecule logic gate.*

After the QHC NOR-molecule, the Toulouse MANA satellite had now succeeded to design, on-surface synthesized and tested experimentally the functioning of a Boolean QHC NAND-molecule. Its QHC quantum graph was first established (Fig. 1b) leading (using the topological Hückel theory) to the Fig. 1a molecular structure which was on-surface synthesized on Au(111). Its functioning was certified using STS dI/dV tunneling spectroscopy technique.<sup>1)</sup>

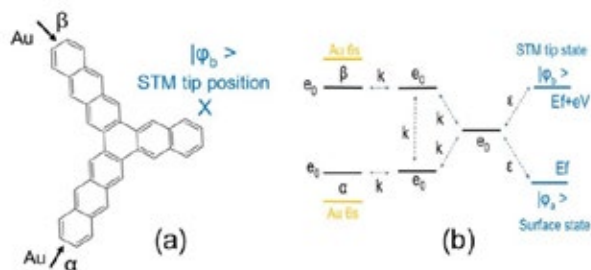


Fig. 1. (a) The NAND QHC molecule logic gate molecular structure after (b) its QHC quantum graph.<sup>1)</sup>

(2) *Qubits and QHC Performances comparison.*

After the design of all the Boolean 2 inputs-1 output QHC logic gates, the minimal QHC 1/2-adder quantum graph was established comparing its performances with the well-know 3 qubits (8 states) 1/2-adder. As presented in Fig. 2, QHC is more robust to noise, required less energy per calculation step but the duration of a logical calculation is a bit larger than with the qubit approach.<sup>2)</sup>

(3) *The Toulouse molecule-car.*

The Toulouse molecular-car which had participated to Nanocar Race I was revisited to understand why its wheels have not rotated during the race. After a detail STS dI/dV tunneling spectroscopy recorded on the Toulouse LT-UHV 4-STM (Fig. 3a), it was shown that there is a too large energy barrier to switch each of the wheel in a rotatable up conformation relative to the surface. Furthermore and at high pulsed bias voltage, the inelastic energy provided by

	Classical 1/2 adder	Qubit 1/2 adder	QHC 1/2 adder
Number of States/Transistors	4 transistors	8 quantum states	4 quantum states
Robustness to noise	Robust	Less robust	More robust
Energy Cost $\Delta E$	$\gg 4kT \log 2$	Minimum $3\delta$ Maximum $5\delta$	Minimum $0.48\delta$ Maximum $0.73\delta$
Calculation time	$\Delta t \gg 1 \text{ ps}$	$\Delta t = 3 \text{ h}/(8\delta)$	$\Delta t = 5 \text{ h}/(3\delta)$
$\Delta E \Delta t$	$\gg 1000 \text{ h}$	1,125 h	1,25 h

Fig. 2. Performances comparison between the 3 different designs of a Boolean 1/2 logic gate with  $h$  the Plank constant and  $\delta$  the characteristic energy for the quantum system, about 1 eV for the Fig. 1a molecule.<sup>2)</sup>

the tunneling current passing through the molecule is not well localized to favor a rotation as presented in Fig. 3b, a very unique molecular state dI/dV mapping (4 hours of constant current dI/dV maps on the LT-UHV 4-STM). A tentative molecular orbital interpretation is presented Fig. 3c indicating that each Fig. 3a resonance is not a molecular orbital resonance but a molecular electronic state resonance.

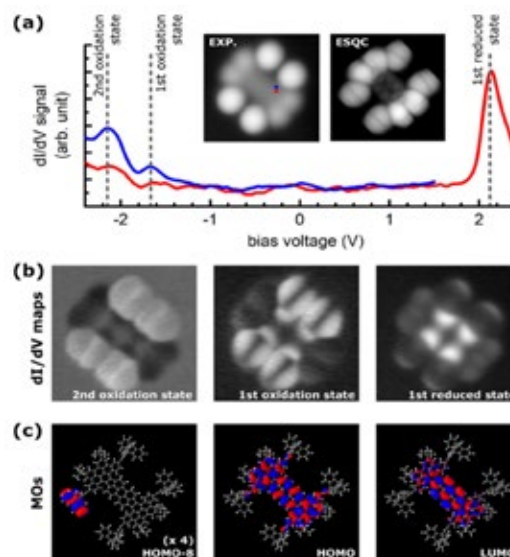


Fig. 3. (a) Typical scanning tunneling dI/dV spectra recorded using the Toulouse LT-UHV 4-STM on the molecule chassis but near the wheel. (b) The corresponding dI/dV maps and (c) the calculated PM6 molecular orbital location on the Toulouse molecule car skeleton.<sup>3)</sup>

**References**

- 1) D. Skidin, O. Faizy, J. Krüger, F. Eisenhut, A. Jancarik, K.H. Nguyen, G. Cuniberti, A. Gourdon, F. Moresco, C. Joachim, *ACS Nano* **12**, 1139 (2018).
- 2) G. Dridi, O. Faizy, C. Joachim, *Quantum Science and Technology* **3**, 025005 (2018).
- 3) W.H. Soe, C. Durand, O. Guillermet, S. Gauthier, H.P. Jacquot deRouville, S. Srivastava, C. Kammerer, G. Rapenne, C. Joachim, *Nanotechnology* **7**, 495401 (2018).



## Nanoarchitectonics-Driven Functional Nanoparticles and Interfaces

**Principal Investigator**

**Françoise M. WINNIK**

(MANA Satellite at University of Helsinki, Finland)

F. Pooch (Student Researcher), B. Qi (Postdoc), G. Beaune (Postdoc), A. Moquin (Researcher)

### 1. Outline of Research

Our research aims to design and fabricate functional nanoparticles and interfaces of controlled chemistry and morphology for possible applications as therapeutic delivery agents and diagnostic tools.

### 2. Research Activities

(1) *Effective and relevant test of the fouling properties of surfaces.*

Cell aggregates consist of thousands of cells assembled into spheroids via interactions between cadherin receptors on the cells surface. The statics and dynamics of their spreading on a surface can be analyzed in the framework of wetting.<sup>1)</sup> The regimes of wetting are characterized by a spreading parameter,  $S$ , defined as  $S = W_{cs} - W_{cc}$ , where  $W_{cs}$  is the cell/substrate adhesion energy per unit area and  $W_{cc}$  is the cell/cell adhesion energy per unit area. If the cell/cell adhesion energy is larger than the cell/substrate adhesion energy ( $S < 0$ , partial wetting), the aggregate at equilibrium forms a spherical cup with a finite contact angle (partial wetting). If  $S > 0$  the aggregate spreads on the substrate by expanding outwards a cell monolayer (complete wetting). We applied this method to rate the non-fouling characteristics of materials used as coatings for medical implants and nanoparticles, such as poly(sulfobetains) (SB) and polymers bearing phosphorycholine moieties (Fig. 1).<sup>2)</sup>



**Fig. 1. Spreading of cell aggregates on chitosan (fouling) and chitosan-SB (non-fouling).<sup>2)</sup>**

(2) *Polymersomes for the delivery of proteins and hydrophobic molecules.*

The wound-healing properties of vesicles consisting of a poly(2-methyl-2-oxazoline)-based membrane were loaded with trophic factors, such as neurotrophin-3 and insulin-like growth factors, in combination with small biologically active agents, such as curcumin. The loaded vesicles were

assessed in 2D biological models (“wound in the dish assay”) and in 3D explanted ganglia consisting of several different cell populations. The study established that the combined encapsulation in the polymersomes of trophic factors and curcumin, is an effective delivery method of wound healing agents readily degraded in biological media (Fig. 2).<sup>3)</sup>

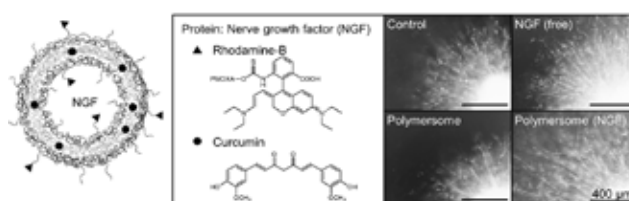


**Fig. 2. Morphology and loading of polymersomes labeled with rhodamine-B and bright-field photomicrographs of dorsal root ganglia explants after 4 days in culture.<sup>3)</sup>**

(3) *Copolymers of poly(lactide) and poly(2-isopropyl-2-oxazoline) for drug delivery.*

We prepared di-block copolymers consisting of poly(lactide) (PLA), an FDA-approved hydrophobic biodegradable polymer and poly(2-isopropyl-2-oxazoline) (PiPOx), a water-soluble, non-toxic polymer. We discovered that PLA and (PiPO<sub>x</sub>) are miscible in the bulk, a rare occurrence for a pair of hydrophobic and hydrophilic polymers.<sup>4)</sup> The self-assembly of these polymers is determined by the balance of two opposing interactions: the attraction of the two miscible blocks and the hydration of the hydrophilic PiPOx block, which can lead to unusual morphologies under current investigation.

(4) *Synthesis and photophysics of coumarin-caged luciferin.*

In collaboration with H. Akiyama (ISSP, Tokyo University), we reported the synthesis and photophysics of a new coumarin-caged D-luciferin, useful to track fast dynamical properties of luciferin *in vivo*. It also provides new opportunities as an actuator in ultrafast devices.<sup>5)</sup>

### References

- 1) G. Beaune, U. Nagarajan, F. Brochard-Wiart, F. Winnik, *Langmuir* (2018), published online. doi: 10.1021/acs.langmuir.8b01736
- 2) B. Qi, H. Feng, X.P. Qiu, G. Beaune, X. Guo, F. Brochard-Wyart, F. Winnik, *Langmuir* (2018), published online. doi: 10.1021/acs.langmuir.8b02461
- 3) A. Moquin, J. Ji, K. Neibert, F.M. Winnik, D. Maysinger, *ACS Omega* **3**, 13882 (2018).
- 4) F. Pooch, M. Sliepen, K.J. Svedstrom, A. Korpi, F.M. Winnik, H. Tenhu, *Polym Chem.* **9**, 1848 (2018).
- 5) M. Kurata, M. Hiyama, T. Narimatsu, Y. Hazama, T. Ito, Y. Hayamizu, X. Qiu, F.M. Winnik, H. Akiyama, *J. Photochem. Photobiol. B* **189**, 81 (2018).

## Materials for Functional Nanomedicine

Managing Researcher

Hisatoshi KOBAYASHI



### 1. Outline of Research

In general, organism selected quite limited molecules such as amino acids, lipids, sugar moieties, and limited metals and inorganics, and combined the limited molecules and finally constructed such highly functionalized complex systems.

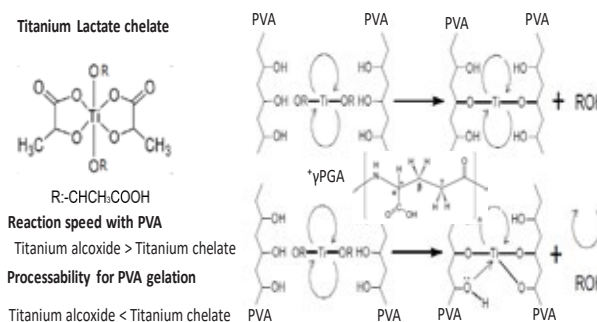
### 2. Research Activities

(1) *Poly(vinyl alcohol)-Poly( gamma-glutamate) blend hydrogel crosslinked with Ti derivative for the application of bio-lubrication and non-biofouling surface.*<sup>1)</sup>

Biolubrication and non-biofouling against the implanted medical devices are very important for the biocompatibility in many cases such as contact lens as well as articular surface of joint implant and adhesion prevention devices, etc. Many trials have been attempted to give very low friction and non-biofouling on the surfaces, for example, introduction of the water-soluble polymer brush on the surface, polysaccharide adsorption on the surfaces, hydrogel usage, etc. These are works very well in many cases, but there is still need to improve the characteristics of durability, production cost, etc. In this study, we aim to develop cheaper and process friendly coating technology to give low friction and non-biofouling properties on the surface of medical devices.

Poly(vinyl alcohol) (PVA, Ave. Mw=77000, % Saponification= 99.9, Kuraray Co Ltd.) and Poly(gamma-glutamate)(PGA, Ave. Mw=200,000-500,000, Wako chemical Co. Ltd.) were used as the base materials. And Titanium lactate (Ti-lac, TC-315, Matsumoto fine chemical Co. Ltd.) was used as crosslinker. Silicone lenses (kindly donated from SEED Co. Ltd.) were used as model substrate for the coating. The characterization of the coatings was carried out by contact angle and FT-IR spectroscopy measurement. And content of the Titanium in the coated layer was analyzed by SEM-EDX. And the cytotoxicity assay was done using L-929 cells following usual procedure.

0.3 ml of 10%PVA aqueous solution and 0.1 ml of 1%PGA aqueous solution were gently mixed. Then 0.1ml of 40%Ti-Lac aqueous solution and 3.6 ml of double distilled water were added and the solution was placed in ultrasonic bath for 10 min to make the homogeneous coating solution and was kept under 4 degrees C until coating process. Coating process was carried out at room temperature. Silicone lenses were dipped into the coating solution for 10 second and the wet samples were placed in 80 degrees C Oven for 24 hours to pre-curing the coating, then the samples were autoclaved at 121 degrees C for 30 min to complete the crosslinking reaction (Fig. 1).



Reaction schema for PVA gelation with Ti derivative

Fig. 1. Synthesis of PVA-γPGA Blend hydrogel crosslinked with Ti derivatives .

In the contact angle measurement (Fig. 2), contact angle of non-treated lens was about 130 degrees. On the contrary, that of the coated samples was about 75, the wettability was dramatically improved. And the contact angle value was not changed even after two days immersion in pure water. The results suggested that very stable coating layer was created just under the simple process. This is a benefit for the manufacturing process. SEM-EDX data showed that about 6wt % of titanium was included in the coating layer. It would react with the OH group of PVA and improve the coating stability. Moreover, very little cytotoxicity (96 % of viability after one day) was observed in this condition.

All the results suggested that the Poly(vinyl alcohol)-Poly(gamma-glutamate) blend hydrogel coating stabilized with Ti-Lac have a potential to apply as coating materials for medical devices.

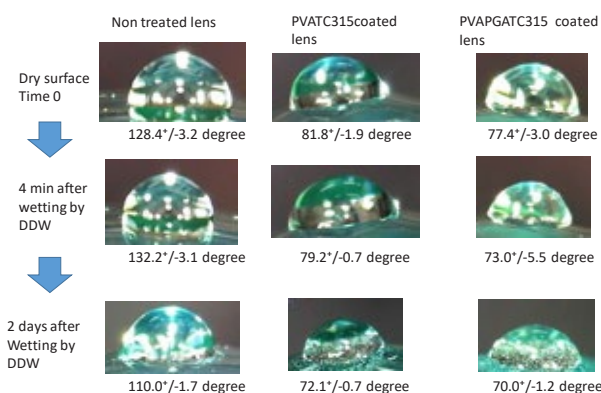


Fig. 2. Water contact angle measurement on the treated lens.

### Reference

- 1) H. Kobayashi, Abstract book of Bordeaux Polymer Conference – May 28-31, 2018 - Bordeaux (France).



## Data Analysis Methods for Sensor Systems

Independent Scientist

Gaku IMAMURA

## 1. Outline of Research

Development of signal processing methods for gas sensor systems is essential for realizing practical artificial olfaction. By applying a data-scientific approach to the sensing signals obtained with gas sensors, I develop new analysis methods that can identify odors—complex mixtures of gases. In addition to such data-scientific approach, I also investigate sensor signals on the basis of the working principle of sensors.

## 2. Research Activities

## (1) Machine learning models based on transfer functions.

To identify gas species from sensor responses, signal features which are intrinsic to gas species are extracted from the signals. In a conventional measurement procedure, gas input patterns need to be fixed for every measurement in order to obtain comparable signal features because the signal features depend on gas input patterns. To overcome this issue, we developed an analysis method based on transfer functions—a mathematical representation that describes the relationship between inputs and outputs. Transfer functions of a sensor are determined by the interaction between the sensor and gas species; hence, gas species can be identified by the transfer functions. Moreover, arbitrary gas input patterns can be utilized in measurements as transfer functions are independent of gas input patterns.

To demonstrate the gas identification based on transfer

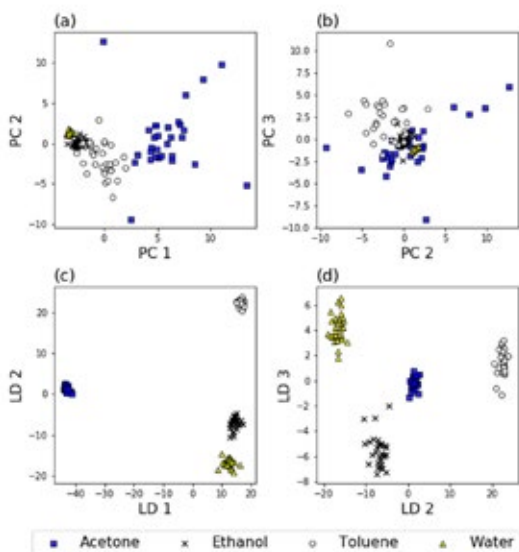


Fig. 1. Scatter plots of the results of (a) PCA and (b) LDA performed on the dataset of transfer functions.

functions, four solvent vapors were measured with Membrane-type Surface stress Sensors (MSS). Unlike a typical measurement procedure, the solvent vapors were injected randomly in this study. Transfer functions are calculated from the sensing signals obtained with the measurements. Fig. 1 shows the results of principal component analysis (PCA) and linear discriminant analysis (LDA). Data points from each vapor form a cluster and are separated from each other, reflecting different interactions between sensors and gas species. We then developed machine learning models for gas identification. Using support vector machines (SVMs) as a classifier, we achieved classification accuracy of  $0.93 \pm 0.03$ .

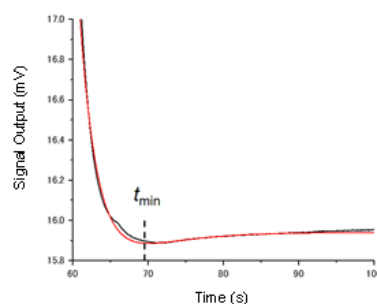


Fig. 2. A sensing signal for water vapor measured with a polymer-coated MSS (black line) and the theoretical curve (red line).

(2) Parameter estimation from sensing signals obtained with nanomechanical sensors.<sup>1,2)</sup>

A nanomechanical sensor is a chemical sensor that detects changes in mechanical properties such as stress, deformation, and mass. To investigate transient responses of a nanomechanical sensor operated in the static mode, we developed an analytical model that includes gas sorption behaviors and viscoelastic properties of the receptor layer. As shown in Fig. 2, the theoretical model successfully reproduces the sensing signal experimentally obtained with a polymer-coated MSS. Moreover, the comparison between experimental results with the analytical model leads to the estimation of physical parameters, which can be used for gas identification.

## References

- 1) G. Imamura, G. Yoshikawa, T. Washio, *17th International Meeting on Chemical Sensors - IMCS 2018*, (2018). doi: 10.5162/IMCS2018/AR1.1
- 2) G. Imamura, K. Shiba, G. Yoshikawa, T. Washio, *AIP Advances* **8**, 075007 (2018).

## Magnetic Susceptibility in Organic Dirac Fermion System

Independent Scientist

Takako KONOIKE



## 1. Outline of Research

Since the discovery of graphene, it has been attracting a great deal of interest because the electrons in graphene behave like massless Dirac fermions. In contrast with normal electrons with parabolic energy band structure, Dirac fermions show anomalous behaviors resulting from the peculiar linear dispersion, so-called Dirac cone. It is now become evident that such a linear dispersion is realized not only in graphene, but also in various materials. In particular, organic conductor  $\alpha$ -(BEDT-TTF)<sub>2</sub>I<sub>3</sub> is known to be a first bulk crystal of Dirac fermion system. By taking advantage of its bulk nature, we experimentally study the physical properties of Dirac fermions in this organic compound.<sup>1,2)</sup>

## 2. Research Activities

Organic conductor  $\alpha$ -(BEDT-TTF)<sub>2</sub>I<sub>3</sub> is composed of organic molecule BEDT-TTF and inorganic anions I<sub>3</sub>. These molecules are stacked alternatively and forming a multi-layered structure of conducting and insulating layer, respectively. At ambient pressure, this compound is semimetallic and undergoes semimetal-insulator transition at 135 K accompanied by charge ordering. By pressurizing the sample above 15 kbar, the charge ordering state is suppressed and then the Dirac cone dispersion appears in the energy band structure.

## (1) Orbital diamagnetism in Dirac fermion system.

The anomalously large diamagnetism in bismuth has been clarified that the orbital diamagnetism due to the inter-band effects of magnetic field plays an essential role in Dirac fermion systems.<sup>3)</sup> Theoretically, graphene is also expected to show a large orbital diamagnetism in low temperature,<sup>4,5)</sup> though the clean single crystal is too small to detect the intrinsic nature of massless Dirac fermions. Here, we study the magnetic properties in organic Dirac fermion system.

## (2) Magnetic susceptibility of Organic Dirac fermion system.

The magnetic properties of organic conductor under pressure are generally investigated by using SQUID magnetometer. However, this method needs large amount of samples to detect the sample signal superimposed on large background from the pressure cell. Here, we tried to apply the field modulation technique to measure the ac susceptibility of one piece of single crystal.

Fig. 1 shows the pickup coil for ac susceptibility measurements. The dimensions of the coil are determined by the sample space in the pressure cell. The pickup coil consists of inner and outer coils. These coils are wound

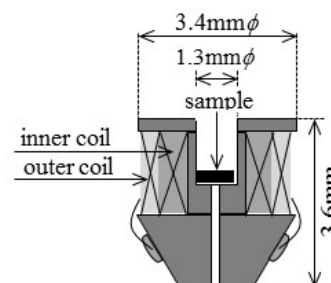


Fig.1. Pickup coil.

inversely, and the number of turns is adjusted not to detect the electromotive force induced by the uniform modulation field and external magnetic field sweep. Single crystal sample is set into this coil as shown in Fig. 1. These are capped by a Teflon capsule filled with an oil and then set to the clamp type pressure cell. The measurements were performed in a dilution refrigerator and superconducting magnet. The external magnetic field is modulated by a small ac field generated by the field modulation coil.

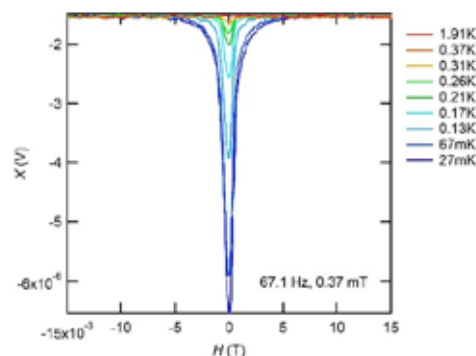


Fig. 2. Field dependence of magnetic susceptibility.

Then, we measured the magnetic susceptibility of  $\alpha$ -(BEDT-TTF)<sub>2</sub>I<sub>3</sub> at 12 kbar. We observed diamagnetic signal at low temperatures below 0.3 K and in very limited region up to 5 mT (Fig. 2). We will examine the reproducibility of the measurements, and consider the origin of this diamagnetism. And we also should exclude the possibility of the superconductivity under uniaxial pressures in this compound reported previously.

## References

- 1) T. Konoike, K. Uchida, T. Osada, *J. Phys. Soc. Jpn.* **81**, 043601 (2012).
- 2) T. Konoike, M. Sato, K. Uchida, T. Osada, *J. Phys. Soc. Jpn.* **82**, 073601 (2013).
- 3) H. Fukuyama, *Prog. Theor. Phys.* **45**, 704 (1971).
- 4) H. Fukuyama, *J. Phys. Soc. Jpn.* **76**, 043711 (2007).
- 5) M. Koshino, Y. Arimura, T. Ando, *Phys. Rev. Lett.* **102**, 177203 (2009).



## Microbial Transmembrane Nano Electric Conduit

Independent Scientist

Akihiro OKAMOTO

## 1. Outline of Research

Transmembrane multi-heme *c*-type cytochrome (OM *c*-Cyt) complexes function in unison as a biological “electron conduit” to transport electrons 20 nm or more across the outer membrane to the cell exterior in several genera of iron-reducing or -oxidizing bacteria (Fig. 1). The ability of the multi-heme alignment and interaction to promote highly efficient long-range electron transport under non-equilibrium conditions has been a focal point for nanoscale electronic applications. Also, the kinetics of this microbial electron transport, referred as extracellular electron transport (EET), has implications for controlling the rate of microbial reactions during bioenergy or biochemical production, iron corrosion, and natural mineral cycling. To these ends, we study electron transport mechanisms through the transmembrane biological electric conduit by pioneering whole-cell physico-chemical methodology combined with molecular-biological approaches.

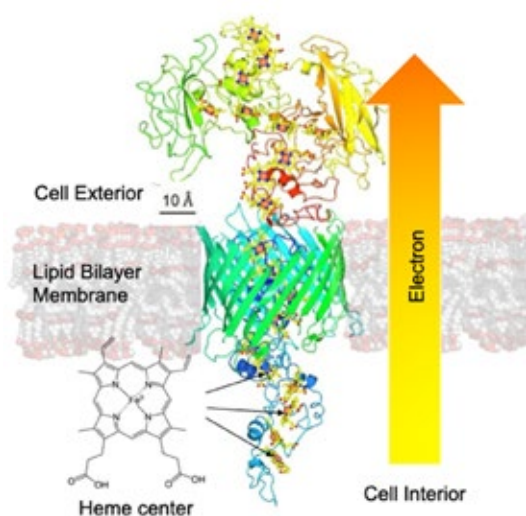


Fig. 1. Transmembrane multi-heme *c*-type cytochrome (OM *c*-Cyt) complex with 20 heme redox centers in *Shewanella oneidensis* MR-1.

## 2. Research Activities

(1) Proton Transfer Dictates EET Kinetics.<sup>1)</sup>

Although the pathways and kinetics of electron flow during EET have been studied over the past three decades, little attention has been given to the alternative roles of counter cations, other than that of a proton motive force (PMF). We examined the kinetics of proton transport associated with EET via an OM *c*-Cyt complex by solvent kinetic isotope effect, and PMF generation during the EET using whole-cell electrochemical measurements in wild-

type (WT) and mutant strains of iron-reducing bacteria, *Shewanella oneidensis* MR-1. Our data revealed that the role of the proton is not to promote the formation of chemiosmotic force but to regulate the rate of electron transport via the OM *c*-Cyt.

(2) Whole-cell Spectroscopy to Monitor Heme Alignment in OM *c*-Cyts.<sup>2)</sup>

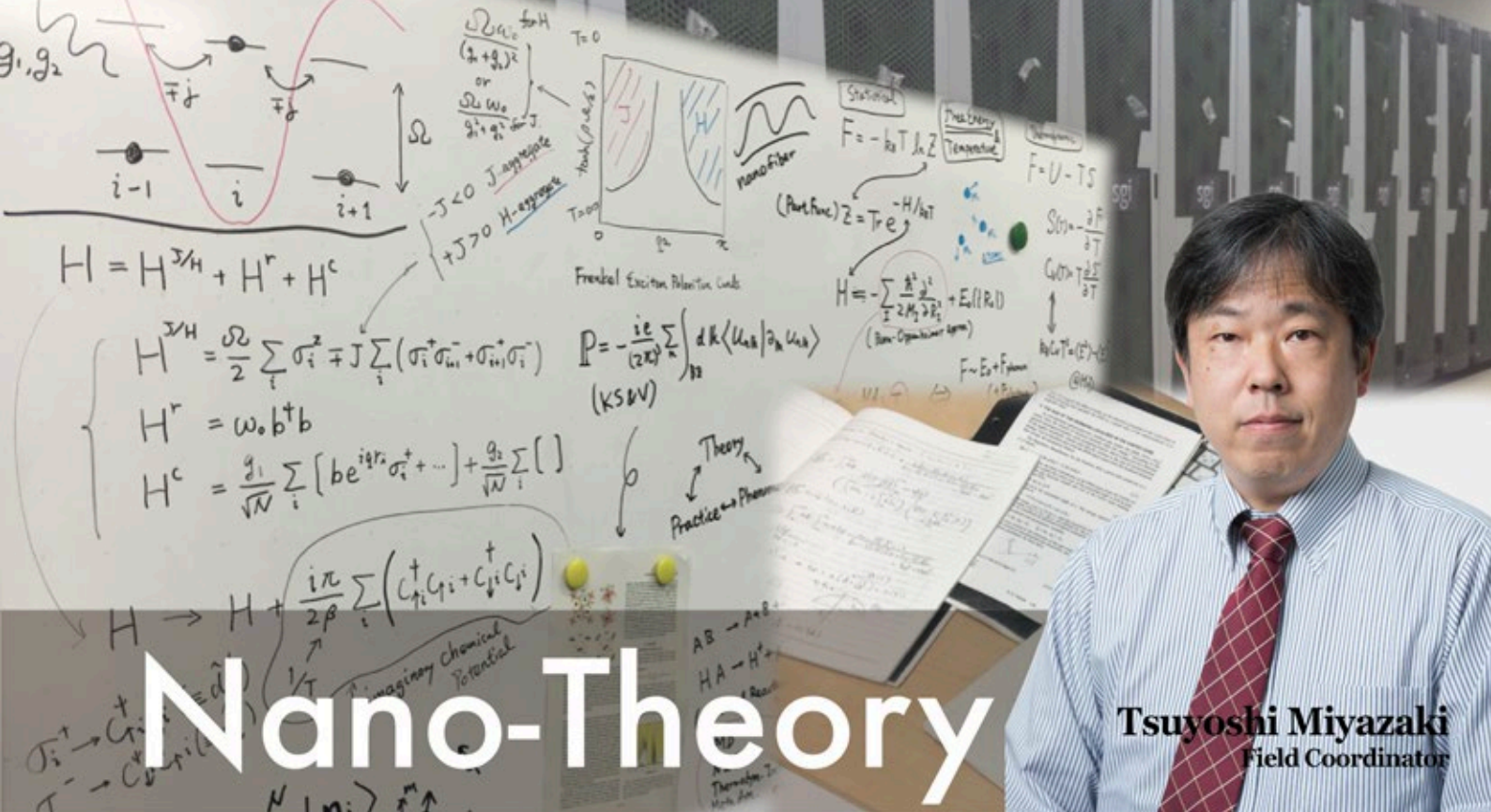
The ten hemes with a minimal distance of 4 Å in OM *c*-Cyts would provide a large amplitude in circular dichroism (CD) signal according to their exciton coupling between  $\pi$ -conjugated systems, which is inversely proportional to cube of the distance. However, direct observation of heme protein encoded by single gene in an intact cell remains a challenge, often due to the presence of other heme proteins, especially for *S. oneidensis* MR-1 cells with 39 genomes encoding heme proteins. Therefore, we established the whole-cell CD difference spectroscopy using *S. oneidensis* MR-1 WT and mutant strain lacking MtrC to acquire the CD signal of MtrC under native conditions. Our data revealed that MtrC in intact cells exhibits a distinct heme alignment, which most likely affects the rate of electron transport.

(3) Novel Clade of OM *c*-Cyts in iron-corrosion bacteria.<sup>3)</sup>

We have discovered that iron-oxidizing and sulfate-reducing bacteria responsible for anaerobic iron corrosion in petroleum pipelines, etc. possess a group of OM *c*-Cyts which enable them to directly extract electrons from extracellular solids. Our whole-cell electrochemical assay confirmed that electrons were removed from an indium-tin doped oxide electrode only when these OM *c*-Cyts were expressed. These results provide strong evidence supporting that this sulfate reducing bacterium can accelerate iron corrosion by direct electron uptake from iron. In addition, we searched the ubiquity of the newly discovered enzymes in the protein databases and found that the amino acid sequences were widely conserved by various sulfur-metabolizing bacteria inhabiting deep-sea sediments, and distinct from those previously identified in iron-reducing bacteria, therefore likely formed a new clade of OM *c*-Cyts. Our discovery will enable us to compare the electron conduction mechanisms in two distinct biological nano electric conduits.

## References

- 1) A. Okamoto, Y. Tokunou, S. Kalathil, K. Hashimoto, *Angew. Chem. Int. Ed.* **56**, 9082 (2017).
- 2) Y. Tokunou, P. Chinotaikul, S. Hattori, T. A. Clarke, L. Shi, K. Hashimoto, K. Ishii, A. Okamoto, *Chem. Commun.* **54**, 13933 (2018). Selected as Front Back Cover.
- 3) X. Deng, N. Dohmae, K.H. Nealon, K. Hashimoto, A. Okamoto, *Sci. Adv.* **4**, eaao5682 (2018).



**Tsuyoshi Miyazaki**  
Field Coordinator

### 3 Research Groups

- First-Principles Simulation Group
- Computational Nanoscience Group
- Emergent Materials Property Theory Group

## Understanding phenomena in the nanospace region, predicting new phenomena and creating novel nanostructured materials

Nanospace is a world in which common sense does not apply, where extremely small atoms are in motion, and electrons fly about in an even smaller space. Moreover, when huge numbers of these atoms and electrons act in coordination, they come to display behavior markedly different from those of single electrons and atoms. Ways of thinking and methods that are not bound by everyday common sense—namely, quantum mechanics and statistical mechanics—are essential for a proper understanding of the phenomena that occur there, and further, for devising new materials. Key activities in the field of nanotheory, which help achieve an understanding of the myriad phenomena emerging in nanospace, include building fundamental theories behind these novel behaviors by incorporating quantum mechanics and statistical mechanics, using our supercomputing facilities to obtain quantitative numerical predictions and develop new and efficient calculation methods. Besides providing interpretations of results obtained in other nanofield areas, we aim at invoking the outcomes of our research to predict as yet unearthed phenomena and to propose new materials featuring novel properties.



## Theoretical Study of Nano-Scale Materials using Large-Scale DFT and Machine Learning Techniques

**Principal Investigator**

**Tsuyoshi MIYAZAKI**

(Field Coordinator, Group Leader)

Ayako Nakata (Senior Researcher), Jun Nara (Senior Researcher),  
Ryo Tamura (Senior Researcher)

### 1. Outline of Research

We develop new theoretical methods to calculate physical properties of complex nano-structured materials, including future electronic devices. Using the various developed theoretical methods, we clarify the dynamical processes in the formation of nano-scale structures and their exotic properties, in collaboration with the experimental groups in MANA. We mainly use first-principles calculation methods based on the density functional theory (DFT), but machine-learning techniques are also used to search new materials having given or preferable functions.

### 2. Research Activities

(1) *Development of large-scale DFT methods and its applications on complex systems.*

We have been developing a large scale DFT code CONQUEST, jointly with the group of Prof. David Bowler. One of the important techniques with the code is called multisite (MS) support function method, which enables us to express the electronic structures of large systems accurately and efficiently with the local orbital basis sets. This method can be used for various materials, including metallic systems. The advantages of the method in the study of graphene on Rh (111) surfaces (Fig. 1) are reported recently.<sup>1)</sup> We have also developed a constant pressure dynamics method with a linear-scaling DFT method. The code was also used in the study of structural properties of Si/Ge or Ge/Si core-shell nanowires.<sup>2)</sup>

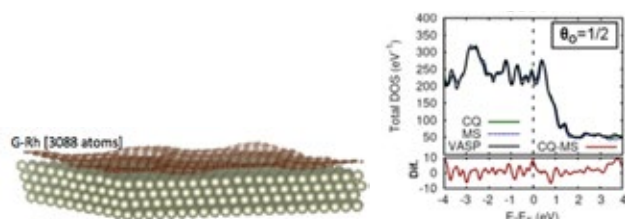


Fig. 1. Atomic structure of graphene on Rh (111) system, and comparison of the density of states using a planewave DFT code VASP and those obtained by CONQUEST with primitive PAO basis sets (CQ) and multisite (MS) methods.

(2) *Graphen growth on SiC(0001).*

We constructed the interatomic potential based on the first-principles calculation and performed long-time and large-scale simulation on the graphene growth on SiC(0001) substrate.<sup>3)</sup> Not single atoms but atomic wires contribute to the growth of graphene. The formed C-atom two-dimensional structures are made of a mixture of five, six, and seven membered rings and gradually transform to a so-called honeycomb structure with only six-member rings (Fig. 2).

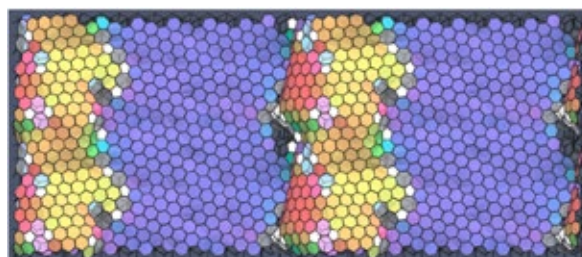


Fig. 2. Top view of a graphene grown on SiC(0001) substrate. Colores mean directions of six-member ring. Many of the rings have the same orientation.

(3) *De novo molecule generation by machine learning.*

By collaborating with Frontier Molecules Group in MANA, we studied the de novo molecule generation by machine learning.<sup>4)</sup> We prepared AI-assisted chemistry platform for discovering new photo-functional molecules (Fig. 3). It consists of ChemTS (molecule generator) and GAUSSIAN (DFT simulator) and was configured to generate molecules whose first excited state is at desired wavelength. Among the molecules discovered, six were synthesized and five were confirmed to reproduce DFT predictions. This result shows the potential of AI-assisted chemistry to discover ready-to-synthesize novel molecules with modest computational resources.

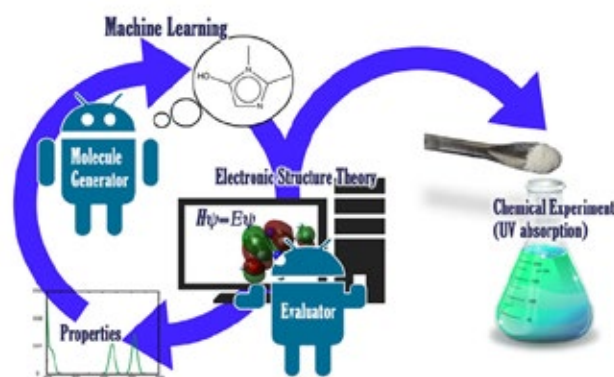


Fig. 3. AI-assisted chemistry platform for discovering new functional molecules.<sup>3)</sup>

### References

- 1) C. Romero-Muñiz, A. Nakata, P. Pou, D. R. Bowler, T. Miyazaki, R. Pérez, *J. Phys.: Condens. Matter* **30**, 505901 (2018).
- 2) C. O'Rourke, S.Y. Mujahed, C. Kumarasinghe, T. Miyazaki, D. R. Bowler, *J. Phys.: Condens. Matter* **30**, 465303 (2018).
- 3) S. Takamoto, T. Yamasaki, J. Nara, T. Ohno, C. Kaneta, A. Hatano, S. Izumi, *Phys. Rev. B* **97**, 125411 (2018).
- 4) M. Sumita, X. Yang, S. Ishihara, R. Tamura, K. Tsuda, *ACS Cent. Sci.* **4**, 1126 (2018).

## Theoretical Studies of Low Dimensional System

## Group Leader

Masao ARAI



Takahisa Ohno (Senior Scientist with Special Missions),  
 Wataru Hayami (Principal Researcher), Jun-ichi Inoue (Principal Researcher),  
 Kazuaki Kobayashi (Principal Researcher), Shigeru Suehara (Principal Researcher),  
 Junya Shimizu (Principal Engineer)

## 1. Outline of Research

Our group investigate electronic structures and physical properties of bulk and nanostructured materials with theoretical and computational methods. Ultimate goal of our research is to understand exotic properties and predict nanomaterials with novel properties. This year, we studied nanostructures on surface and various two-dimensional sheets with theoretical methods including topological analysis and first-principles calculations based on the density-functional theory (DFT).

## 2. Research Activities

## (1) Artificial TiN nanostructure on MgO surface.

We have been investigating nanostructured TiN/MgO superlattices from first-principles calculations. Two types of TiN dots on MgO substrate are considered: rectangular (*r*-TiN) and rectangular parallelepiped (*rp*-TiN) ones. The dots with 2x1, 2x2, and 3x3 superlattices have been studied previously. We focus on those with 4x4 and 5x5 superlattices. Structurally relaxed *r*-TiN/MgO and *rp*-TiN/MgO with 4x4 and 5x5 superlattices become semiconductor although relaxed *rp*-TiN/MgO with 2x2 and 3x3 superlattices are metallic. The band gap of *r*-TiN/MgO increases with the size of the MgO substrate although the difference of the band gap between 4x4 and 5x5 is small with approximately 0.01 eV. The electronic properties of these nanostructures depend on the shape of the TiN dot and the size of the MgO substrate. Therefore, the TiN dot shape and MgO substrate size are important to control the band gap value.

(2) Siliborophene on ZrB<sub>2</sub>(0001) surface.

A new two-dimensional silicon boride phase ‘siliborophene’ was synthesized on the ZrB<sub>2</sub>(0001) surface. High-resolution electron energy loss spectroscopy, reflection high-energy electron diffraction, Auger electron spectroscopy and the first-principles density-functional theory (DFT) were employed to elucidate the atomic and electronic structures of this phase. Among many theoretically derived surface models, only one structure made of Si<sub>3</sub>B<sub>6</sub> can reproduce details of the experimental measurements. The identified new structure ‘siliborophene’ consists of a cyclic boron ring (cB<sub>6</sub>) capped by a Si atom, SiB<sub>6</sub> group, and sp<sup>2</sup>-like Si atoms connecting them. The Si<sub>3</sub>B<sub>6</sub> phase is much more robust compared than that of silicene: it shows no order-disorder transition until 1300 K (cf. 1000 K for silicene); above that temperature, Si is desorbed gradually. The electronic band structure calculation for the isolated film of Si<sub>3</sub>B<sub>6</sub> exhibits a band crossing at the K point, which

makes this material promising for use with Fermi level engineering.

(3) Graphite-like BC<sub>2</sub> sheet.

Graphite-like BC<sub>2</sub> has yet to be synthesized; however, it stably exists in the Sc<sub>2</sub>B<sub>1.1</sub>C<sub>3.2</sub> compound, where the boron atoms are arranged as far apart from each other as possible. Recently, a theoretical study on monolayer BC<sub>2</sub> reported that the most stable structure has B atoms positioned adjacent to each other, which disagrees with the former result. From extensive first-principles calculations, we found that this discrepancy originates from the difference in their electric charges. The most stable structure among the six possible structures changes with the increase in the negative electric charge, which well explain both the previous results without contradiction.<sup>1)</sup>

The Li intercalation potential for BC<sub>2</sub> was calculated to investigate its applicability as an anode for a lithium-ion battery. Our results revealed that Li atoms can be intercalated into BC<sub>2</sub> to yield Li<sub>1.5</sub>BC<sub>2</sub>, whose gravimetric capacity is approximately 2.6 times higher than that of LiC<sub>6</sub>.<sup>2)</sup> However, the most stable structure with intercalated Li atoms became unstable when all the Li atoms were extracted. This feature may hinder the repetitive charge-discharge cycle of the anode and hence needs to be carefully considered.

## (4) Topological characterization of novel 2D system.

A topological characterization was proposed and performed for a two-dimensional system that is intrinsically incompatible with conventional schemes. The novelty of the system, a quadripartite-lattice system taken as an example, lies in both point- and line-degeneracies in tight-binding energy bands. The latter survives even after time reversal symmetry is broken by, e.g. irradiation of circularly polarized light, which, in turn, prevents from application of the conventional methods. Here, we introduced a topological number for a bunch of energy bands and demonstrated its effectiveness by confirming consistency with well-established three knowledges. On the basis of this effort, we constructed a phase diagram summarizing topological nature of the system. This work also has a facet as a natural extension of the seminal work by Nobel laureate, Haldane. The idea and concept provided in this work would be helpful for exploring future topological materials.

## References

- 1) W. Hayami, T. Tanaka, *J. Solid State Chem.* **254**, 144 (2017).
- 2) W. Hayami, T. Tanaka, *J. Solid State Chem.* **269**, 113 (2019).



Theoretical Quest for Emergent Materials Function

Group Leader

Akihiro TANAKA

Yoshihiko Nonomura (Principal Researcher), Igor Solovyev (Principal Researcher)

1. Outline of Research

Predicting materials functions can be a formidable task, since they generally emerge “bottom-up” out of collective interactions among electrons, which vary in a complex way depending on energy/length scale. Thus, as the scientific community continues to seek increasingly exotic quantum functions, they tend to become difficult to foresee “top-down” solely from the handful of basic rules available to the traditional solid-state physicist. To confront with this situation, we develop and integrate an assortment of theoretical methods powerful enough to zoom in on the behavior of the many-body system: first principle calculations, numerical schemes based on statistical mechanics, and nonperturbative (analytical) quantum field theory methods. Our primary aim is to extract from such studies novel material properties which can lead to resourceful quantum mechanical functions.

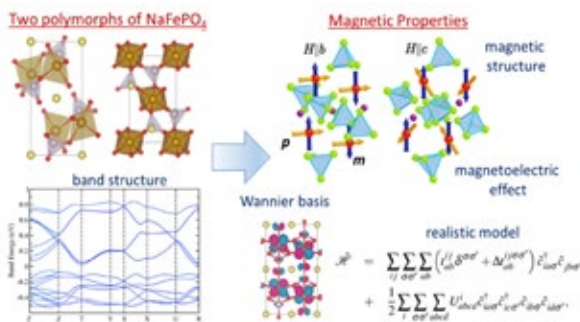


Fig. 1. Schematic view of the realistic modeling approach which was used for the analysis of magneto-electric effect and other magnetic properties of NaFePO<sub>4</sub>, and related polyanionic compounds.

2. Research Activities

(1) Rechargeable battery materials.<sup>1)</sup>

The magnetic properties of NaFePO<sub>4</sub>, an important cathode material for Na-ion batteries, are investigated at the molecular level, by constructing and solving a realistic model Hamiltonian, extracted from first-principles electronic structure calculations (Fig. 1). The study implies, among other findings, that in addition to its already established electrochemical properties, this material also should exhibit interesting magnetoelectric effects which may be of practical value to applications. Unlike some earlier investigations into related problems, the results are highly reliable in that our model Hamiltonian derives directly from accurate *ab initio* density functional theory.

(2) Spin-orbit coupled systems.<sup>2)</sup>

We proposed that the magnetic properties of the

3d-electron based material, CuAl<sub>2</sub>O<sub>4</sub>, due to peculiarities of its spinel structure and effects of Coulomb correlations, are largely controlled by spin-orbit interactions (Fig. 2). As such search had typically been made among materials containing heavy and expensive 5d elements, our finding opens a new strategy for amplifying the effects of the spin-orbit coupling in materials science.

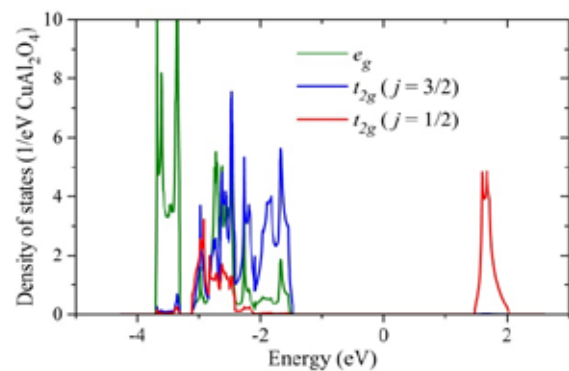


Fig. 2. Electronic density of Cu 3d states in CuAl<sub>2</sub>O<sub>4</sub>, showing that unoccupied states are of pure *j*=1/2 character, split off by the spin-orbit interaction. This feature controls the material properties. The Fermi level is at zero energy.

(3) Topological states of matter.<sup>3)</sup>

Using our realistic modelling approach, we investigated how multiferroicity arises in the lacunar spinel GaV<sub>4</sub>S<sub>8</sub>, and verified e.g. that the skyrmion excitations which are induced by an external magnetic field are electrically polarized. On another front we developed theoretical schemes enabling researchers to diagnose the quantum entanglement properties peculiar to topological states in terms of the widely-used Ginzburg-Landau effective description of phases of matter.

(4) Study of relaxational dynamics in spin systems.<sup>4)</sup>

We continue to develop numerical algorithms which are powerful enough to deal with complex statistical mechanical problems which are otherwise difficult to access. We carried out a detailed demonstration that shows that our methods can be employed to analyze the critical relaxational dynamics of spin systems reliably.

References

- 1) O. Arcelus, S. Nikolaev, J. Carrasco, I. Solovyev, *Phys. Chem. Chem. Phys.* **20**, 13497 (2018).
- 2) S.A. Nikolaev, I.V. Solovyev, A.N. Ignatenko, V.Yu. Irkhin, S.V. Streltsov, *Phys. Rev. B* **98**, 201106(R) (2018).
- 3) A. Tanaka, *Mathematical Sciences* **667**, 47 (2018), in Japanese.
- 4) Y. Tomita, Y. Nonomura, *Phys. Rev. E* **98** 052110 (2018).

## Nano-System Computational Science

Principal Investigator

Yoshitaka TATEYAMA



## 1. Outline of Research

We are working on (1) developments of theoretical, computational and data-driven techniques as well as (2) understanding and design of materials and reactions, essential in the energy and environmental technologies such as battery, catalyst and solar cell. For the former issue, we're exploring the techniques for redox reactions, electron & proton transfer with high-performance computing. In addition to the density functional theory (DFT) calculations, we're interested in multi-scale and data-driven AI techniques as well. Regarding the application studies, our goal is to provide novel understanding of the microscopic mechanisms of the batteries, catalysts and cells, and suggest promising candidates for the next-generation technology. In particular, we focus on electrolytes as well as electrolyte-electrode interfaces, which play crucial roles in the energy storage and conversion.

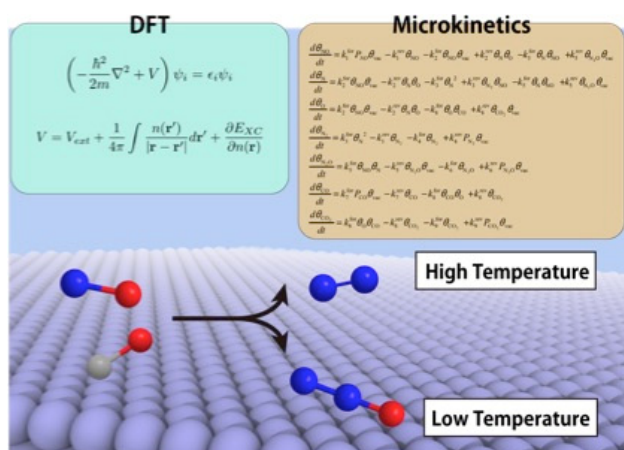


Fig. 1. A schematic picture of first-principles surface microkinetics simulations where we combine DFT electronic states calculations and microkinetics equations. This allows us to analyze and design more realistic reactions with multiple pathways.<sup>1)</sup>

## 2. Research Activities

For the fundamental science projects, we have developed program / protocol of first-principles surface microkinetics calculation, which is almost the first approach in the world. This method allows temperature dependent reactor simulations with multiples reaction pathways, leading to more accurate prediction and design of catalytic and battery reactions under realistic conditions (Fig. 1).<sup>1)</sup> We have also demonstrated the novel data-driven AI techniques with the explorations of electrolyte materials for the next-generation batteries.<sup>2,3)</sup>

On the application studies, we have carried out several DFT calculation studies to understand the microscopic mechanisms and explore the promising materials for the

development of battery materials (Fig. 2).<sup>4,5)</sup> For the catalysis field, DFT-MD sampling analysis of CeO<sub>2</sub> / Pt cluster / water interface systems were extensively investigated (Fig. 3).<sup>6)</sup> We then provide the interfacial water dynamics as well as electron transfer. These findings will give useful aspects for the energy and environmental technologies as well as fundamental interface science.

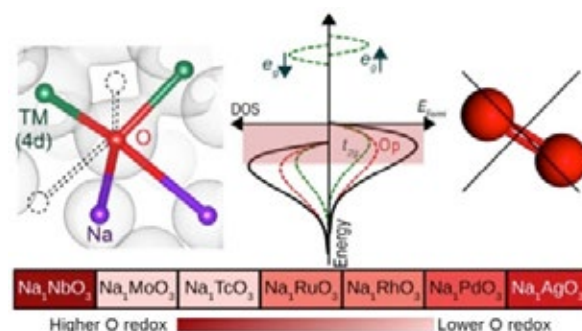


Fig. 2. A schematic picture of exploration of Na-excess ilmenite-type cathode materials containing 3d and 4d transition metals. NaNbO<sub>3</sub> and NaVO<sub>3</sub> were found to be promising systems for stable use in Na-ion battery.<sup>4)</sup>

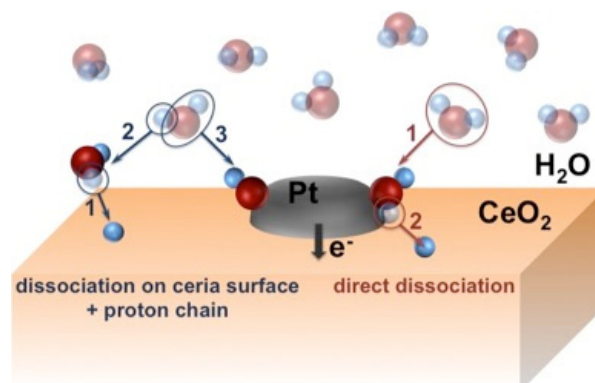


Fig. 3. A schematic picture of water dynamics and dissociation behavior in the interface region of CeO<sub>2</sub> (111) / Pt cluster / bulk H<sub>2</sub>O, which is a promising system for various types of catalytic reactions, deduced from the comprehensive DFT molecular dynamics samplings.<sup>6)</sup>

## References

- 1) A. Ishikawa, Y. Tateyama, *J. Phys. Chem. C* **122**, 17378 (2018).
- 2) R. Jalem, M. Nakayama, Y. Noda, T. Le, I. Takeuchi, Y. Tateyama, H. Yamazaki, *Sci. Tech. Adv. Mater.* **19**, 231 (2018).
- 3) K. Sodeyama, Y. Igarashi, T. Nakayama, Y. Tateyama, M. Okada, *Phys. Chem. Chem. Phys.* **20**, 22585 (2018).
- 4) M.H.N. Assadi, M. Okubo, A. Yamada, Y. Tateyama, *J. Mater. Chem. A* **6**, 3747 (2018).
- 5) M. Hattori, K. Yamamoto, M. Matsui, K. Nakanishi, T. Mandai, A. Choudhary, Y. Tateyama, K. Sodeyama, T. Uchiyama, Y. Orikasa, Y. Tamenori, T. Takeguchi, K. Kanamura, Y. Uchimoto, *J. Phys. Chem. C* **122**, 25204 (2018).
- 6) L. Szabová, M.F. Camellone, F.N. Ribeiro, V. Matolin, Y. Tateyama, S. Fabris, *J. Phys. Chem. C* **122**, 27507 (2018).



## Development and Application of O(N) DFT, and Studies of Strain and Doping on Nanomaterials

**Principal Investigator**

**David BOWLER**

(MANA Satellite at University College London, UK)

### 1. Outline of Research

Our ultimate aim is to understand advanced nano-structured materials for applications in photovoltaic devices, as well as future electronic devices. Our research combines close collaboration with experiment and theoretical modeling to give a detailed insight into the properties of the materials. In our first satellite project, we investigated how to combine biological inspiration with electronics to give high efficiency materials and solar cells with applications to energy and sustainability. In our present project, we are studying the growth and properties of silicon-germanium nanostructures, both nanowires and clusters formed on surfaces, to optimize their characteristics, particularly concentrating on the mobility and location of dopants. We are also continuing to study biological systems, to seek inspiration for hybrid solid-state/biological nano-architectures, and branching out into the new area of perovskites.

We are leading the development of *ab initio* methods that can be applied to large systems. Much of our research involves development of the CONQUEST linear scaling DFT code, which has been developed through a long-term collaboration between UCL and NIMS, and is now expanding to include other sites around the world.

We have a long-established network of collaboration between MANA in NIMS, and the London Centre for Nanotechnology in University College London. In this year, we have arranged collaborative research visits to MANA for the PI and the MANA UCL student, as well as visits to UCL from researchers in NIMS.

We are also expanding our international links, collaborating with the Institute for Molecular Science in University of Bordeaux and Osaka University, in a four-way exchange of personnel and expertise.

### 2. Research Activities

#### (1) Application of CONQUEST to large-scale problems.

We have continued our work on the growth and properties of silicon nanowires and germanium-silicon core-shell nanowires, in collaboration with Dr. N. Fukata in MANA, who grows the nanowires. We have studied the distribution of strain in the core and the shell of the nanowire.<sup>1)</sup> In Fig. 1 we show the strain in a silicon core, germanium shell nanowire, demonstrating that the distribution is highly non-uniform, and requires accurate quantum mechanical modelling. These simulations used the linear-scaling approach in CONQUEST to model several thousand atoms.

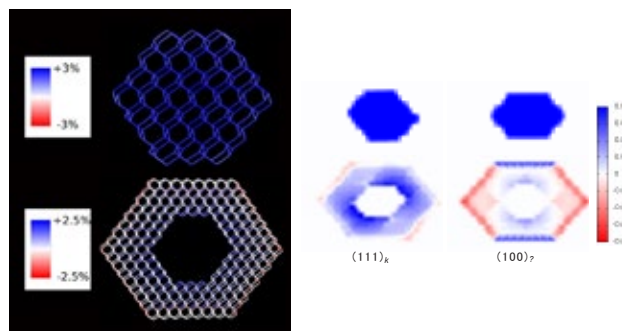


**Fig. 1. Properties of core-shell nanowire calculated with CONQUEST. Left: Percentage variation in bond length, relative to bulk bond lengths for the Si-Si bonds in the core (top), and Ge-Ge bonds in the shell (bottom) for SiGe-NWs with a 3-layer core and 5-layer Ge shell thickness. Right: Average bond strain map for the cross-section of the Si core (top) and Ge shell (bottom) of the same 3 5 SiGe-NW.<sup>1)</sup>**

We have also used the recently developed multi-site approach to apply exact diagonalisation to the problem of graphene on Rh(111), showing that this approach is accurate enough to reproduce plane-wave results<sup>2)</sup> and can be extended to several thousand atoms.

#### (2) Doping of semiconductors.

We continue to study dopants in semiconductors, recently showing with a joint experimental-theoretical study that delta-doping layers of Mn can be grown in silicon and at germanium/silicon interfaces.<sup>3)</sup> We have also studied AlH<sub>3</sub> as a source for deterministic doping with acceptors<sup>4)</sup> (by analogy to PH<sub>3</sub>, which is used for donors).

#### (3) New directions: perovskites.

We are starting new projects in the area of perovskites, which have important properties including ferroelectricity. We are investigating BiFeO<sub>3</sub> for its potential applications as a photovoltaic material, specifically concentrating on how we can accurately model this complex material system with relatively low computational cost.<sup>5)</sup> We will expand our studies of perovskites and ferroelectricity in the future.

### References

- 1) C. O'Rourke, S.Y. Mujahed, C. Kumarasinghe, T. Miyazaki, D.R. Bowler, *J. Phys.: Condens. Matter* **30**, 465303 (2018).
- 2) C. Romero-Muñiz, A. Nakata, P. Pou, D.R. Bowler, T. Miyazaki, R. Pérez, *J. Phys.: Condens. Matter* **30**, 505901 (2018).
- 3) K. Murata, C. Kirkham, S. Tsubomatsu, T. Kanazawa, K. Nitta, Y. Terada, T. Uruga, K. Nittoh, D.R. Bowler, K. Miki, *Nanoscale* **10**, 295 (2018).
- 4) R. Smith, D.R. Bowler, *J. Phys.: Condens. Matter* **30**, 105002 (2018).
- 5) K. Shenton, W.L. Cheah, D.R. Bowler, R. Bowler, *J. Phys.: Condens. Matter* **29**, 445501 (2018).



February 2019

Cover art by Dr. Rintaro Higuchi and  
Prof. Tomonobu Nakayama (MANA)

I-I Namiki Tsukuba,  
Ibaraki 305-0044 JAPAN

Email: [mana-pr@ml.nims.go.jp](mailto:mana-pr@ml.nims.go.jp)  
URL: <http://www.nims.go.jp/mana/>

TEL: +81-29-860-4709  
FAX: +81-29-860-4706



World Premier International  
Research Center Initiative  
(WPI)



International Center for  
Materials Nanoarchitectonics  
(WPI-MANA)



National Institute for  
Materials Sciences  
(NIMS)